8-2011

LENTIVIRAL-MEDIATED RNAi KNOCKDOWN YIELDS A NOVEL MOUSE MODEL FOR STUDYING CYP2B FUNCTION

Basma Damiri
Clemson University, bdamiri@clemson.edu

LENTIVIRAL-MEDIATED RNAi KNOCKDOWN YIELDS A NOVEL MOUSE MODEL FOR STUDYING CYP2B FUNCTION

A Dissertation
Presented to
the Graduate School of
Clemson University

In Partial Fulfillment
of the Requirements for the Degree
Doctor of Philosophy
Environmental Toxicology

---

by
Basma R. Damiri
August 2011

Accepted by
Dr. William Baldwin, Committee Chair
Dr. Lisa Bain
Dr. Charles Rice
Dr. Xianzhong Yu

ABSTRACT

The Cyp2b subfamily contains five members (Cyp2b9, Cyp2b10, Cyp2b13, Cyp2b19, and Cyp2b23) of which three (Cyp2b9, Cyp2b10, Cyp2b13) are hepatic enzymes involved in xenobiotic detoxification. In this study, we made a Cyp2b-knockdown mouse using lentiviral-promoted shRNA homologous to all five Cyp2b subfamily members in FVB/NJ mouse to characterize Cyp2b's role in xenobiotic detoxification. We assessed the *in vivo* function of Cyp2bs in the toxicity from pesticides (i.e. parathion) and drugs (i.e. zoxazolamine). We demonstrated that Cyp2b isoforms play a key role in parathion and Zoxazolamine metabolism and toxicity. In addition, we in partially phenotyped and characterized Cyp2b-KD model and assessed changes associated with the lack of Cyp2bs. We focused on role that Cyp2bs play in lipid metabolism. Changes in Cyp2b expression led to perturbation in lipid metabolism in Cyp2b-KD mice. Both young and old Cyp2b-KD male and female mice showed significant changes in some organ weights, especially an increase in abdominal, inguinal, and renal adipose. Interestingly, associated with changes in fat to body ratios was changes in non-fasting triglycerides levels. Our data suggest that Cyp2b is more than a detoxification enzyme, but is also involved in the metabolism of unsaturated fatty acids as Cyp2b-KD mice have increased fat deposition and show increased serum and liver lipid levels.

DEDICATION

This dissertation is dedicated to my parents who kept praying for me all the time and have given me all their love and support. Your prayers and love become the catalyst to my desire to finish this dissertation. I am just a lucky daughter. Along the way are my sisters and my brothers who are my source of strength and had a dream of seeing me in a graduation gown. Your understanding support and interest encouraged me throughout my journey and made this academic accomplishment possible. Without your efforts, I cannot continue.

ACKNOWLEDGMENTS

My deepest gratitude is to my advisor Dr. William Baldwin who gave me the freedom and the guidance to do my work. Dr Baldwin taught me how to question thoughts and express ideas throughout the time it took me to complete this research and write the dissertation. Without his advice throughout the entire process, I cannot do this work. I'm grateful as well to my committee, Dr Lisa Bain, Charles Rice, and Xianzhong Yu. Special thanks go to Dr Bain, Dr Rice, Dr van den Hurk, Dr Yu, and their students who helped me and allowed me to use their labs. Dr Bain kindness made me feel that I'm a part of her lab. Many thanks go to Eric Holle and Gia-Ming Hong for all the support and the help you provided for me. I would like to thank also my lab group: Gautum, Yang, and Omaima. I have been lucky to work with you in the same lab. I'm lucky also to meet Elina in our lab and have a wonderful time with her. The acknowledgements would not be complete without a heartfelt thanks to my friend Dr Linda Mota for her help and support and for the wonderful things she did to me and the nice time we spent together. Finally, I would like to thank Ford Foundation in New York and America-Mideast Educational and Training Services (AMIDEAST) in Palestine for giving me the chance to come and study in the USA and meet all the these wonderful people.

TABLE OF CONTENTS

Page

LIST OF TABLES

LIST OF FIGURES

CHAPTER ONE

INTRODUCTION

The mouse has become the dominant experimental model in the study of human cytochrome P450-mediated processes. The mouse genome contains 105 cytochrome P450 (Cyp) genes while the human genome contains 58 Cyp genes. The CYP superfamily is one of the most ancient, widespread and diverse enzyme systems found in animals, plants, and microorganisms. A superfamily of mammalian CYP genes encodes a multitude of CYP enzymes that play a pivotal role in the metabolism and detoxification or bioactivation of a variety of xenobiotics (e.g. drugs, carcinogens, environmental toxicants, plant products) as well as functioning in the biotransformation of numerous endobiotics (e.g. steroid hormones, bile acids, fatty acids, eicosanoids) (Nelson et al., 1996). CYPs enzymes play a central role in the metabolic conversion of these xenobiotic and endobiotics to more polar derivatives that can be conjugated by phase II enzymes to be removed rapidly (Danielson, 2002). The CYPs are also involved in the formation of toxic intermediates and may cause adverse drug reactions (ADRs).

CYPs are separated into families, subfamilies, and isoforms. For example, CYP2B6 is the human isoforms (gene) in family 2 (CYP2), subfamily B, isoforms 6. CYP2B6 was first described in 1989 (Yamano et al., 1989) as the human ortholog to the phenobarbital-inducible CYP2B in rodents. The functional CYP2B6 gene and the pseudogene CYP2B7P are located in the middle of the chromosome-19 cluster, which also contains the CYP2A and CYP2F subfamilies (Rodriguuez-Antona and Ingleman

2006). CYP2B6, initially thought to consist of a small fraction of hepatic P450 and expressed at low levels, has gained more attention in recent studies because of its role in xenobiotic detoxification and its inducibility (Wang and Tompkings, 2008). It was estimated that CYP2B6 encompasses 2-10% of the total microsomal P450 pool in liver (Gervot et al., 1999; Lang et al., 2001), but lower levels of CYP2B6 are found in several other tissues, including the brain, kidney, trachea, lung, small intestine, uterus, endometrius, bronchoalveolar macrophages, peripheral blood and lymphocytes (Gervot et al., 1999; Lang et al., 2001; Ding and Kaminsky, 2003; Miksys et al., 2003; Bernauer et al., 2006; Yengi et al., 2003).

Although CYP2B6 has been thought to constitute only a small percentage of total hepatic P450, it has a wide range of xenobiotic and endobiotic substrates such as bile acids, steroid hormones, and bilirubin (Wei et al., 2000; Hodgson and Rose, 2007). Initially underestimated, the number of drugs recognized as CYP2B6 substrates has been constantly increasing, and several clinically important substrates are known to be preferred substrates of this enzyme. It is involved in the metabolic activation and inactivation of a growing number (25-30%) of clinically important drugs ([a]Ekins and Wrighton 1999; Lang et al., 2001; Guana et al, 2006), such as the HIV-1 reverse transcriptase inhibitors nevirapine and efavirenz (Erickson et al., 1999; Ward et al., 2003). Recently, efavirenz was described as a potentially important phenotyping tool for CYP2B6-mediated metabolic activity (Haas et al., 2004).

Table 1.1: Some of Cyp2b6 substrates

Classification	Substrate	References
Antidepressant	Bupropion	Faucette et al., 2000; Hesse et al., 2000
Chemotherapeutics	Cyclophosphamide Tamoxifen Ifosfamide	Chang et al., 1993; Roy et al., 1999 White et al., 1995 Granvil et al., 1999
Anti retrovirals	Efavirenz Nevirapine	Erickson et al., 1999 Ward et al., 2003
Anti malarial	Artemisinin	Svensson and Ashton, 1999
Opioids	Methadone	Gerber et al., 2004
	Nicotine	McCracken et al., 1992; Yamazaki et al., 1999
Steroids	Estrogen Testosterone	[b]Ekins et al., 1999

Five CYP2B isoforms have been identified in mouse (Cyp2b9, 2b10, 2b13, 2b19, and 2b23) that are expressed in different tissues and putatively perform specific and redundant functions. Cyp2b isoforms are primarily expressed in the liver with Cyp2b9, Cyp2b10, and to a lesser extent Cyp2b13 being the major hepatic CYP2b isoforms (Honkakoski et al., 1998; Wei et al., 2000; Hernandez et al., 2009; Mota et al., 2010). The hepatic Cyp2bs also show sexual dimorphism as female mice express more Cyp2b9 and Cyp2b13 than males (Jarukamjorn et al., 2002; Wiwi et al., 2004; Hernandez et al., 2006; Mota et al., 2010). Cyp2bs are also expressed in other tissues such as small intestine (Zhang et al., 2003), kidney (Jarukamjorn et al., 2001), brain (Albores et al., 2001; Rosenbrock et al., 2001), lungs (Forkert et al., 1986), testes, (Omiecinski, 1986) skeletal muscles (Finger et al., 2011), skin (Keeney et al., 1998, Du et al., 2005) adipose (Yoshinari et al., 2004), and prostate (Kumagai et al., 2007).

Cyp2bs (mainly Cyp2b9 and Cyp2b10) are involved in the metabolism of several exogenous chemicals such as parathion, chlorpyrifos, phenobarbital, nonylphenol, some

PCBs, and DDT (Lee et al., 1998; Foxenberg et al., 2007) and endogenous compounds such steroid hormones, prostaglandins, and fatty acids (Waxman, 1988; Keeney et al., 1998; Kawamoto et al., 2000; Ladd et al., 2003; Du et al., 2005). Cyp2b19 is considered a novel specific cellular marker of late differentiation in skin keratinocytes (Keeney et al., 1998; Du et al., 2005). It is involved in arachadonic acid metabolism, a normal constituent of cellular membranes and the precursor of biologically active lipids such as epoxyeicosatrienoic (EET) acids, hydroxyeicosatetraenoic (HETE) acids, leukotrienes, thromboxanes, and prostaglandins (Keeney et al., 1998).

Several transcription factors regulate the basal and the inducible expression of CYP2B. Importantly, expression of CYP2B is strongly inducible by different drugs and potentially toxic chemicals, thereby allowing for enhanced detoxification following exposure (Denison and Whitlock, 1995). Induction of hepatic Cyp2b family members in mice (Cyp2b10) and humans (CYP2B6) is regulated by the constitutive androstane receptor (CAR) and the pregnane X receptor (PXR) (Honkakoski et al., 1998; Tzameli et al., 2000; Wei et al., 2000). However, CAR is of special interest because of the identification of a phenobarbital response element (PBREM) in the 5' region of Cyp2b10 and the elucidation of CAR as the receptor that is activated following phenobarbital exposure (Honkakoski et al 1996; Wang et al., 2004). Several CAR activators such as phenobarbital, 1,4-bis[2-(3,5-dichloropyridyloxy)]benzene (TCPOBOP), phenytoin, nonylphenol, and O-(3,4-dichlorobenzyl) oxime (CITCO) are potent Cyp2b inducers and therefore Cyp2b is an excellent biomarker for CAR activation (Maglich et al., 2003;

Wang et al., 2004; Hernandez et al., 2007). However, as evidence mounts that CAR is also a nutrient sensor (Masson et al., 2008; Dong et al., 2009; Kono et al., 2009; Gao et al., 2009; Maglich et al., 2009), Cyp2b10's function may need to be re-evaluated.

It has been demonstrated that Cyp2b9 regulated by the forkhead box protein A2 (FOXA2) (Hashita et al., 2008). FoxA2 is activated by fasting and fatty acids, and inhibited by insulin (Wolfrum et al., 2004). Therefore; it must be considered that Cyp2b9 is an important energy metabolism enzymes.

The importance of CYP2B6 as an effective monooxygenase for environmental chemicals is illustrated by the fact that the use of phenotyped human microsomes shows a correlation between CYP2B6 content and increased production of metabolites of known CYP2B6 substrates (Hodgson and Rose, 2007). For example, using human hepatocytes, CYP2B6 was involved in the activation of chlorpyrifos to chlorpyrifos oxon. Also, endosulfan sulfate was determined to be the major product from human microsomes and CYP2B6 was the primary CYP responsible for α-endosulfan metabolism (Hodgson and Rose, 2007). Although the relative importance of CYP2B6 in drug and pesticide metabolism is apparent from *in vitro* (microsomal) and recombinant studies; its function *in vivo* is not clear. Most studies were done *in vitro* with microsomes or recombinant enzymes, or *in vivo* using nuclear receptor-null mice such as CAR- null mice (Ramírez et al., 2004, Hernandez et al., 2007). There is no null (Cyp2b knockout) mouse to study the physiological, pharmacological and toxicological functions of Cyp2b *in vivo*, and the role

of CYP2B-produced intermediates in causing adverse effects. In fact, few of the detoxifying P450s with multiple isoforms have been knocked out. If not for the recent production of the Cyp3a-null mouse by in part chromosomal deletion (van Herwaarden et al. 2007), there would be no CYP-null mice for P450 subfamilies with multiple isoforms.

The problem is that there are more P450 isoforms in each subfamily of the mouse genome than there are in the human genome. For instance, there is one isoform in the human CYP2B subfamily (CYP2B6) while the murine Cyp2b subfamily has five individual isoforms (Cyp2b9, Cyp2b10, Cyp2b13, Cyp2b19, and Cyp2b23) with most likely redundant functions. Knocking down one isoform will have presumably little to no effect as other Cyp2b isoforms with redundant functions will still be available to metabolize the chemical of interest. Therefore, the redundancy in CYP subfamily members has made the typical P450 gene knockout ineffective, or extremely difficult to produce. The cost of knocking down all the isoforms is impractical. Modern technologies such as siRNA under the control of lentiviral promoters may alleviate such obstacles and produce efficient knockdown mice.

Small Interfering RNAs (siRNAs) are short, double-stranded RNA molecules (21-25 nucleotides) that can form complementary sequences with single-stranded mRNAs, and in turn target them for degradation in a process called RNA interference (RNAi) (Elbashir, 2001). This leads to a decrease (but not the absence) of the expression of the corresponding protein. The siRNA-mediating gene silencing is likely a self-defense

mechanism against viral invasion. RNAi has emerged as a powerful tool to downregulate the expression of specific genes. The gene silencing effect of dsRNA is mediated in a two-step process: 1) the dsRNA is recognized by Dicer, an RNase III family of nucleases that processes the dsRNA into small double-stranded molecules called siRNA (Nykanen et al., 2001); 2). Following the cleavage of dsRNA into siRNAs by Dicer, the second important stage of mRNA degradation occurs. This is mediated by a protein complex with nuclease activity known as RNA-induced silencing complex (RISC) which is guided to its target RNA by siRNA (Martinez et al., 2002; Tijsterman et al., 2002). Functional RISC is believed to contain at least four different subunits, an endonuclease, an exonuclease, a helicase, and "homology searching" component (Nykanen et al., 2001, Martinez et al., 2004). The most successful application of the discovery of RNAi has been to study the gene function in cultured human and mouse cells. However, the knockdown effect of siRNA is transient. To achieve a more sustained gene silencing effect, shRNA (small hairpin RNA) expressed from a vector is preferred (Gao and Zhang, 2007).

Viral vectors carrying siRNA expression cassettes have been developed in an attempt to achieve delivery to a range of cell types (including neurons) and longer-term expression, leading to a more persistent silencing effect **(**Bantounas et al., 2004). Lentiviral vectors are becoming the vectors of choice for short-interfering RNA (siRNA) (Sachdeva et al., 2007). They have been successfully used to knock down the expression of specific genes *in vivo* and *in vitro.* The control of the shRNA under a lentiviral

promoter allows the incorporation of the construct into the hosts DNA and therefore, provides stable expression, and germline transmission (Lois et al., 2002). The cytomegalovirus (CMV) promoter was considered to drive a robust transgene expression (Park, 2007) and lentivirus vectors containing the U6 promoter have been used to generate transgenic animals at high efficiency (100%) in F0 mice and 50% in F1 mice (Punzon et al., 2004; Okada et al., 2007). Recently, short hairpin RNA (shRNA) molecule overexpression has become popular using lentiviral transgenesis, with low-to moderate transgenic efficiencies (13-53%) observed in founder mice harboring a shRNA construct (Tiscorina et al., 2003; Dann et al., 2006; Kissler et al., 2006; Rubinson et al., 2007). However, RNAi was not used to knockdown whole subfamilies. There are conserved areas between the Cyp2b murine subfamily members that show high homology and therefore are potential targets for shRNA that could knockdown all of the Cyp2b subfamily members (see next Chapter). Therefore, we can potentially knockdown all five isoforms with one siRNA.

A Cyp2b knockdown (Cyp2b-KD) mouse model will be an important tool in toxicological and pharmacological studies. This model will enable us to perform many studies *in vivo,* currently too expensive or impractical and provides a model to build on for the future. We proposed to use siRNA to knockdown the expression of the whole Cyp2b subfamily in mice using lentiviral driven shRNA. The loss of Cyp2b function caused changes in susceptibility to toxicants, and potentially changes in basic physiology (lipid metabolism). This genetic model (Cyp2b - knockdown mouse) will provide

powerful tools for further study Cyp2b-mediated xenobiotics metabolism, as well as the physiological and toxicological functions of Cyp2b complex.

1.1 Research Objectives

The Cytochrome P450s (CYPs) are important enzymes in protecting us from xenobiotics (e.g. drugs, pesticides, industrial chemicals) and endobiotics (e.g. steroid hormones, bilirubin, arachadonic acid, fatty acids, bile acids) chemicals. However, few *in vivo* models are available to study the function of CYPs in metabolizing, detoxifying, and eliminating drugs and environmental toxicants. Knockout mice are important animal models for studying the role of genes *in vivo*. There are very few P450-null (P450 knockout) mice and there are no Cyp2b null-mice because the murine Cyp2b subfamily has five members with redundant functions. Knocking out one isoform in the subfamily will have little effect of the physiology of the mouse as other redundant isoforms are still available to metabolize the chemical of interest. Therefore, we need to knockout all the isoforms at once. The redundancy has made typical Cyp2b knockout worthless. Further, the cost of knocking down the five isoforms has made Cyp2b knockout impractical. Small interference RNA (siRNA) technology under the control of lentiviral promoter may alleviate this obstacle and produce efficient knockdown mice. Because there is no model of Cyp2b function, the exact physiological roles that Cyp2b subfamily plays have not been thoroughly studied using proven, substantiated techniques, *in vivo*. To systematically assess the *in vivo* impact of Cyp2b on the physiology, and the relative contributions of the liver to first-past metabolism of many drug substrates and other

chemicals, we made and characterized a Cyp2b-knockout mouse. This research has the following objectives:

Objective 1: Make siRNA constructs for Cyp2b and a scrambled construct within a lentiviral promoted vector, and test these constructs *in vitro*.

A. Design, produce, concentrate, and titer lentivirus expressing Cyp2b-specific siRNA and scrambled siRNA (*in vivo* control).

B. Determine the construct that consistently represses (knock's down) Cyp2b mRNA and protein levels the greatest in mouse primary hepatocytes.

Objective 2: Produce RNAi transgenic mice that overexpress the Cyp2b-siRNA (a Cyp2b knockdown mouse, repress Cyp2b function, and determine the efficacy of the Knockdown.

A. Produce Cyp2b siRNA knockdown mice. The mice were genotyped and the founders were used for breeding studies. Test whether Cyp2b-knockdown (Cyp2b-KD) mice shown reduced Cyp2b expression.

B. Determine if TCPOBO the potent Cyp2b-inducer (TCPOBOP), can out-compete shRNA-mediated repression, or if the knockdown is powerful enough to continue reducing Cyp2b expression.

Objective 3: Test whether the loss of Cyp2b alters the phenotype of the mouse.

A. Determine the role of Cyp2b in the metabolism of a variety xenobiotics and endobiotics such as parathion.

B. Test whether Cyp2b-KD mice are sensitive to the effects of drugs such as zoxazolamine.

C. Determine if the Cyp2b-knockdown mouse shows any histological, pathological, or clinical abnormalities.

1.2 Summary

Cytochrome P450s, including the Cyp2b subfamily, are important in the metabolism and elimination of drugs and environmental toxicants; however, few *in vivo* models are available for their study. Cyp2b is a key enzyme in our chemical sensitivity to a number of drugs, and occupational and environmental chemicals and Cyp2b is instrumental in steroid hormone homeostasis and bile acid metabolism.

There is no Cyp2b knockdown mouse model due to the fact that Cyp2b has several isoforms with redundant functions and knocking down one isoform will have little to no effect on the metabolism rate. RNA interference (RNAi, siRNA, shRNA) under the control of lentiviral promoters may alleviate such obstacles and is an efficient toll to produce efficient knockdown mice.

The main objective of this study is to produce efficient Cyp2b knockdown mice to study their function *in vivo*. We were able to produce the knockdown mice for Cyp2b-

KD2 mice. The next step is to perform *in vivo* studies to determine the Cyp2b function. These studies will increase our knowledge of the human sensitivity to toxicant and drugs and will aid to the understanding of the xenobiotic metabolism.

1.3 Organization of the Dissertation

This dissertation is organized into chapters intended for publications in peer-reviewed journals. Therefore, some of the introductory material and methods are repeated. Chapter 1 introduces the importance of cytochrome P450 (CYP2B6) and the uses of siRNA in knocking down Cyp2bs in mice. Chapter 2, titled "Lentiviral-mediated RNAi knockdown yields a novel mouse model for studying Cyp2b function" will be submitted for publication in Toxicological Sciences. Chapter 3, titled "*In vivo* RNAi Repression of Cyp2b Expression Increases Adipose Deposition and Serum Lipids" has been submitted for publication in American Journal of Physiology: Gastrointestinal and Liver Physiology. Chapter 4 summarized the overall results and purpose of this research, its importance in toxicology and physiology, and future considerations.

1.4 References

Albores A, Ortega-Mantilla G, Sierra-Santoyo A, Cebrián ME, Muñoz-Sánchez JL, Calderón-Salinas JV, Manno M. Cytochrome P450 2B (CYP2B)-mediated activation of methyl-parathion in rat brain extracts. Toxicol Lett. 2001 Oct 15;124(1-3):1-10.

Baldwin WS, LeBlanc GA. The anti-carcinogenic plant compound indole-3-carbinoldifferentially modulates P450-mediated steroid hydroxylase activities in mice.Chem Biol Interact. 1992 Aug 14;83(2):155-69.

Bantounas I, Phylactou LA, Uney JB. RNA interference and the use of small interfering RNA to study gene function in mammalian systems. J Mol Endocrinol. 2004 Dec;33(3):545-57. Review.

Bernauer U, Heinrich-Hirsch B, Tönnies M, Peter-Matthias W, Gundert-Remy U. Characterisation of the xenobiotic-metabolizing Cytochrome P450 expression pattern in human lung tissue by immunochemical and activity determination. Toxicol Lett. 2006 Jul 14;164(3):278-88.

Chang TK, Weber GF, Crespi CL, Waxman DJ. Differential activation of cyclophosphamide and ifosphamide by cytochromes P-450 2B and 3A in human liver microsomes. Cancer Res. 1993 Dec 1;53(23):5629-37.

Danielson PB. The cytochrome P450 superfamily: biochemistry, evolution and drug metabolism in humans. Curr Drug Metab. 2002 Dec;3(6):561-97. Review.

Dann CT, Alvarado AL, Hammer RE, Garbers DL. Heritable and stable gene knockdown in rats. Proc Natl Acad Sci U S A. 2006 Jul 25;103(30):11246-51.

Denison MS, Whitlock JP Jr. Xenobiotic-inducible transcription of cytochrome P450 genes. J Biol Chem. 1995 Aug 4;270(31):18175-8. Review.

Ding X, Kaminsky LS. Human extrahepatic cytochromes P450: function in xenobiotic metabolism and tissue-selective chemical toxicity in the respiratory and gastrointestinal tracts. Annu Rev Pharmacol Toxicol. 2003;43:149-73. Review.

Dong B, Saha PK, Huang W, Chen W, Abu-Elheiga LA, Wakil SJ, Stevens RD, Ilkayeva O, Newgard CB, Chan L, Moore DD. Activation of nuclear receptor CAR ameliorates diabetes and fatty liver disease. Proc Natl Acad Sci U S A. 2009 Nov 3;106(44):18831-6.

Du L, Yermalitsky V, Ladd PA, Capdevila JH, Mernaugh R, Keeney DS. Evidence that cytochrome P450 CYP2B19 is the major source of epoxyeicosatrienoic acids in mouse skin. Arch Biochem Biophys. 2005 Mar 1;435(1):125-33.

[a]Ekins S, Wrighton SA. The role of CYP2B6 in human xenobiotic metabolism. Drug Metab Rev. 1999 Aug;31(3):719-54. Review.

[b]Ekins S, Bravi G, Ring BJ, Gillespie TA, Gillespie JS, Vandenbranden M, Wrighton SA, Wikel JH. Three-dimensional quantitative structure activity relationship analyses of substrates for CYP2B6. J Pharmacol Exp Ther. 1999 Jan;288(1):21-9.

Elbashir SM, Lendeckel W, Tuschl T. RNA interference is mediated by 21- and 22-nucleotide RNAs. Genes Dev. 2001 Jan 15;15(2):188-200.

Erickson DA, Mather G, Trager WF, Levy RH, Keirns JJ. Characterization of the *in vivo* biotransformation of the HIV-1 reverse transcriptase inhibitor nevirapine by human hepatic cytochromes P-450. Drug Metab Dispos. 1999 Dec;27(12):1488-95.

Faucette SR, Hawke RL, Lecluyse EL, Shord SS, Yan B, Laethem RM, Lindley CM. Validation of bupropion hydroxylation as a selective marker of human cytochrome P450 2B6 catalytic activity. Drug Metab Dispos. 2000 Oct;28(10):1222-30.

Finger JH, Smith CM, Hayamizu TF, McCright IJ, Eppig JT, Kadin JA, Richardson JE, Ringwald M. The mouse Gene Expression Database (GXD): 2011 update. Nucleic Acids Res. 2011 Jan;39(Database issue):D835-41.

Finn RD, Henderson CJ, Scott CL, Wolf CR. Unsaturated fatty acid regulation of cytochrome P450 expression via a CAR-dependent pathway. Biochem J. 2009 Jan 1;417(1):43-54.

Forkert PG, Vessey ML, Elce JS, Park SS, Gelboin HV, Cole SP. Localization of phenobarbital- and 3-methylcholanthrene-inducible cytochromes P-450 in mouse lung with monoclonal antibodies. Res Commun Chem Pathol Pharmacol. 1986 Aug;53(2):147-57.

Foxenberg RJ, McGarrigle BP, Knaak JB, Kostyniak PJ, Olson JR. Human hepatic cytochrome p450-specific metabolism of parathion and chlorpyrifos. Drug Metab Dispos. 2007 Feb;35(2):189-93.

Gao J, He J, Zhai Y, Wada T, Xie W. The constitutive androstane receptor is an anti-obesity nuclear receptor that improves insulin sensitivity. J Biol Chem. 2009 Sep 18;284(38):25984-92.

Gao X, Zhang P. Transgenic RNA interference in mice. Physiology (Bethesda). 2007 Jun;22:161-6. Review.

Gerber JG, Rhodes RJ, Gal J. Stereoselective metabolism of methadone N-demethylation by cytochrome P4502B6 and 2C19. Chirality. 2004 Jan;16(1):36-44.

Gervot L, Rochat B, Gautier JC, Bohnenstengel F, Kroemer H, de Berardinis V,Martin H, Beaune P, de Waziers I. Human CYP2B6: expression, inducibility and catalytic activities. Pharmacogenetics. 1999 Jun;9(3):295-306.

Granvil CP, Madan A, Sharkawi M, Parkinson A, Wainer IW. Role of CYP2B6 and CYP3A4 in the *in vivo* N-dechloroethylation of (R)- and (S)-ifosfamide in human liver microsomes. Drug Metab Dispos. 1999 Apr;27(4):533-41.

Guan S, Huang M, Chan E, Chen X, Duan W, Zhou SF. Genetic polymorphisms of cytochrome P450 2B6 gene in Han Chinese. Eur J Pharm Sci. 2006 Sep;29(1):14-21.

Haas DW, Ribaudo HJ, Kim RB, Tierney C, Wilkinson GR, Gulick RM, Clifford DB, Hulgan T, Marzolini C, Acosta EP. Pharmacogenetics of efavirenz and central nervous system side effects: an Adult AIDS Clinical Trials Group study. AIDS. 2004 Dec 3;18(18):2391-400.

Hashita T, Sakuma T, Akada M, Nakajima A, Yamahara H, Ito S, Takesako H, Nemoto N. Forkhead box A2-mediated regulation of female-predominant expression of the mouse Cyp2b9 gene. Drug Metab Dispos. 2008 Jun;36(6):1080-7.

Hernandez JP, Chapman LM, Kretschmer XC, Baldwin WS. Gender-specific induction of cytochrome P450s in nonylphenol-treated FVB/NJ mice. Toxicol Appl Pharmacol. 2006 Oct 15;216(2):186-96. Epub 2006 May 25.

Hernandez JP, Huang W, Chapman LM, Chua S, Moore DD, Baldwin WS. The environmental estrogen, nonylphenol, activates the constitutive androstane receptor. Toxicol Sci. 2007 Aug;98(2):416-26.

Hernandez JP, Mota LC, Huang W, Moore DD, Baldwin WS. Sexually dimorphic regulation and induction of P450s by the constitutive androstane receptor (CAR). Toxicology. 2009 Feb 4;256(1-2):53-64.

Hesse LM, Venkatakrishnan K, Court MH, von Moltke LL, Duan SX, Shader RI, Greenblatt DJ. CYP2B6 mediates the *in vivo* hydroxylation of bupropion: potential drug interactions with other antidepressants. Drug Metab Dispos. 2000 Oct;28(10):1176-83.

Hodgson E, Rose RL. The importance of cytochrome P450 2B6 in the human metabolism of environmental chemicals. Pharmacol Ther. 2007 Feb;113(2):420-8. Epub 2006 Oct 24. Review.

Honkakoski P, Moore R, Gynther J, Negishi M. Characterization of phenobarbital-inducible mouse Cyp2b10 gene transcription in primary hepatocytes. J Biol Chem. 1996 Apr 19;271(16):9746-53.

Honkakoski P, Zelko I, Sueyoshi T, Negishi M. The nuclear orphan receptor CAR-retinoid X receptor heterodimer activates the phenobarbital-responsive enhancer module of the CYP2B gene. Mol Cell Biol. 1998 Oct;18(10):5652-8.

Jarukamjorn K, Sakuma T, Nemoto N. Sexual dimorphic expression of mouse hepatic CYP2B: alterations during development or after hypophysectomy. Biochem Pharmacol. 2002 Jun 1;63(11):2037-41.

Kawamoto T, Kakizaki S, Yoshinari K, Negishi M. Estrogen activation of the nuclear orphan receptor CAR (constitutive active receptor) in induction of the mouse Cyp2b10 gene. Mol Endocrinol. 2000 Nov;14(11):1897-905.

Keeney DS, Skinner C, Wei S, Friedberg T, Waterman MR. A keratinocyte-specific epoxygenase, CYP2B12, metabolizes arachidonic acid with unusual selectivity, producing a single major epoxyeicosatrienoic acid. J Biol Chem. 1998 Apr 10;273(15):9279-84.

Kissler S, Stern P, Takahashi K, Hunter K, Peterson LB, Wicker LS. *In vivo* RNA interference demonstrates a role for Nramp1 in modifying susceptibility to type 1 diabetes. Nat Genet. 2006 Apr;38(4):479-83.

Konno Y, Kodama S, Moore R, Kamiya N, Negishi M. Nuclear xenobiotic receptor pregnane X receptor locks corepressor silencing mediator for retinoid and thyroid hormone receptors (SMRT) onto the CYP24A1 promoter to attenuate vitamin D3 activation. Mol Pharmacol. 2009 Feb;75(2):265-71.

Kumagai J, Fujimura T, Takahashi S, Urano T, Ogushi T, Horie-Inoue K, Ouchi Y,Kitamura T, Muramatsu M, Blumberg B, Inoue S. Cytochrome P450 2B6 is a growth-inhibitory and prognostic factor for prostate cancer. Prostate. 2007 Jul 1;67(10):1029-37.

Ladd PA, Du L, Capdevila JH, Mernaugh R, Keeney DS. Epoxyeicosatrienoic acids activate transglutaminases in situ and induce cornification of epidermal keratinocytes. J Biol Chem. 2003 Sep 12;278(37):35184-92.

Lang T, Klein K, Fischer J, Nüssler AK, Neuhaus P, Hofmann U, Eichelbaum M, Schwab M, Zanger UM. Extensive genetic polymorphism in the human CYP2B6 gene with impact on expression and function in human liver. Pharmacogenetics. 2001 Jul;11(5):399-415.

Lee PC, Marquardt M, Lech JJ. Metabolism of nonylphenol by rat and human microsomes. Toxicol Lett. 1998 Oct 15;99(2):117-26.

Li-Masters T, Morgan ET. Effects of bacterial lipopolysaccharide on phenobarbital-induced CYP2B expression in mice. Drug Metab Dispos. 2001 Mar;29(3):252-7.

Lois C, Hong EJ, Pease S, Brown EJ, Baltimore D. Germline transmission and tissue-specific expression of transgenes delivered by lentiviral vectors. Science. 2002 Feb 1;295(5556):868-72.

Martinez J, Patkaniowska A, Urlaub H, Lührmann R, Tuschl T. Single-stranded antisense siRNAs guide target RNA cleavage in RNAi. Cell. 2002 Sep 6;110(5):563-74.

Martinez J, Tuschl T. RISC is a 5' phosphomonoester-producing RNA endonuclease. Genes Dev. 2004 May 1;18(9):975-80.

Masson D, Qatanani M, Sberna AL, Xiao R, Pais de Barros JP, Grober J, Deckert V, Athias A, Gambert P, Lagrost L, Moore DD, Assem M. Activation of the constitutive androstane receptor decreases HDL in wild-type and human apoA-I transgenic mice. J Lipid Res. 2008 Aug;49(8):1682-91.

Maglich JM, Parks DJ, Moore LB, Collins JL, Goodwin B, Billin AN, Stoltz CA, Kliewer SA, Lambert MH, Willson TM, Moore JT. Identification of a novel human constitutive androstane receptor (CAR) agonist and its use in the identification of CAR target genes. J Biol Chem. 2003 May 9;278(19):17277-83.

Maglich JM, Lobe DC, Moore JT. The nuclear receptor CAR (NR1I3) regulates serum triglyceride levels under conditions of metabolic stress. J Lipid Res. 2009 Mar;50(3):439-45.

McCracken NW, Cholerton S, Idle JR. Cotinine formation by cDNA-expressed human cytochromes P 450. Med. Sci Res. 1992 20; 877-878.

Miksys S, Lerman C, Shields PG, Mash DC, Tyndale RF. Smoking, alcoholism and genetic polymorphisms alter CYP2B6 levels in human brain. Neuropharmacology. 2003 Jul;45(1):122-32.

Mota LC, Hernandez JP, Baldwin WS. Constitutive androgen receptor-null mice are sensitive to the toxic effects of parathion: association with reduced cytochrome p450-mediated parathion metabolism. Drug Metab Dispos. 2010 Sep;38(9):1582-8.

Nelson DR, Koymans L, Kamataki T, Stegeman JJ, Feyereisen R, Waxman DJ, Waterman MR, Gotoh O, Coon MJ, Estabrook RW, Gunsalus IC, Nebert DW. P450 superfamily: update on new sequences, gene mapping, accession numbers and nomenclature. Pharmacogenetics. 1996 Feb;6(1):1-42. Review.

Nykänen A, Haley B, Zamore PD. ATP requirements and small interfering RNA structure in the RNA interference pathway. Cell. 2001 Nov 2;107(3):309-21.

Okada H, Suh WK, Jin J, Woo M, Du C, Elia A, Duncan GS, Wakeham A, Itie A, Lowe SW, Wang X, Mak TW. Generation and characterization of Smac/DIABLO-deficient mice. Mol Cell Biol. 2002 May;22(10):3509-17.

Omiecinski CJ. Tissue-specific expression of rat mRNAs homologous to cytochromes P-450b and P-450e. Nucleic Acids Res. 1986 Feb 11;14(3):1525-39.

Park F. Lentiviral vectors: are they the future of animal transgenesis? Physiol Genomics. 2007 Oct 22;31(2):159-73. Epub 2007 Aug 7. Review.

Punzon I, Criado LM, Serrano A, Serrano F, Bernad A. Highly efficient lentiviral-mediated human cytokine transgenesis on the NOD/scid background. Blood. 2004 Jan 15;103(2):580-2. Epub 2003 Sep 25.

Rodriguez-Antona C, Ingelman-Sundberg M. Cytochrome P450 pharmacogenetics and cancer. Oncogene. 2006 Mar 13;25(11):1679-91. Review.

Ramírez J, Innocenti F, Schuetz EG, Flockhart DA, Relling MV, Santucci R, Ratain MJ. CYP2B6, CYP3A4, and CYP2C19 are responsible for the *in vivo* N-demethylation of meperidine in human liver microsomes. Drug Metab Dispos. 2004 Sep;32(9):930-6.

Rosenbrock H, Hagemeyer CE, Ditter M, Knoth R, Volk B. Expression and localization of the CYP2B subfamily predominantly in neurones of rat brain. J Neurochem. 2001 Jan;76 (2):332-40.

Roy P, Yu LJ, Crespi CL, Waxman DJ. Development of a substrate-activity based approach to identify the major human liver P-450 catalysts of cyclophosphamide and ifosfamide activation based on cDNA-expressed activities and liver microsomal P-450 profiles. Drug Metab Dispos. 1999 Jun;27(6):655-66.

Rubinson DA, Dillon CP, Kwiatkowski AV, Sievers C, Yang L, Kopinja J, Rooney DL, Zhang M, Ihrig MM, McManus MT, Gertler FB, Scott ML, Van Parijs L. A lentivirus-based system to functionally silence genes in primary mammalian cells, stem cells and transgenic mice by RNA interference. Nat Genet. 2003 Mar;33(3):401-6.

Sachdeva G, D'Costa J, Cho JE, Kachapati K, Choudhry V, Arya SK. Chimeric HIV-1 and HIV-2 lentiviral vectors with added safety insurance. J Med Virol. 2007 Feb;79(2):118-26.

Svensson US, Ashton M. Identification of the human cytochrome P450 enzymes involved in the *in vivo* metabolism of artemisinin. Br J Clin Pharmacol. 1999 Oct;48(4):528-35.

Tijsterman M, Plasterk RH. Dicers at RISC; the mechanism of RNAi. Cell. 2004 Apr 2;117(1):1-3. Review.

Tiscornia G, Singer O, Ikawa M, Verma IM. A general method for gene knockdown in mice by using lentiviral vectors expressing small interfering RNA. Proc Natl Acad Sci U S A. 2003 Feb 18;100(4):1844-8.

Tzameli I, Pissios P, Schuetz EG, Moore DD. The xenobiotic compound 1,4-bis[2-(3,5-dichloropyridyloxy)]benzene is an agonist ligand for the nuclear receptor CAR. Mol Cell Biol. 2000 May;20(9):2951-8.

Udomsuk L., Churikawit K., Putalun K., Jarukamjorn K. Impact of Pueraria candollei Root Cultures on Cytochrome P450 2B9 Enzyme and Lipid Peroxidation in Mice Journal of Health Science, 2010, 56(2) 182-187

van Herwaarden, A. E., Wagenaar, E., van der Kruijssen, C. M. M., van Waterschoot, R. A. B., Smit, J. W., Song, J.-Y., van der Valk, M. A., van Tellingen, O., van der Hoorn, J. W. A., Rosing, H., Beijnen, J. H., and Schinkel, A. H. (2007). Knockout of cytochrome P450 3A yields new mouse models for understanding xenobiotic metabolism. *J Clin Invest* **117**.

Wang H, Faucette S, Moore R, Sueyoshi T, Negishi M, LeCluyse E. Human constitutive androstane receptor mediates induction of CYP2B6 gene expression by phenytoin. J Biol Chem. 2004 Jul 9;279(28):29295-301.

Wang H, Tompkins LM. CYP2B6: new insights into a historically overlooked cytochrome P450 isozyme. Curr Drug Metab. 2008 Sep;9(7):598-610. Review.

Ward BA, Gorski JC, Jones DR, Hall SD, Flockhart DA, Desta Z. The cytochrome P450 2B6 (CYP2B6) is the main catalyst of efavirenz primary and secondary

metabolism: implication for HIV/AIDS therapy and utility of efavirenz as a substrate marker of CYP2B6 catalytic activity. J Pharmacol Exp Ther. 2003 Jul;306(1):287-300.

Waxman DJ. Interactions of hepatic cytochromes P-450 with steroid hormones. Regioselectivity and stereospecificity of steroid metabolism and hormonal regulation of rat P-450 enzyme expression. Biochem Pharmacol. 1988 Jan 1;37(1):71-84. Review.

Wei P, Zhang J, Egan-Hafley M, Liang S, Moore DD. The nuclear receptor CAR mediates specific xenobiotic induction of drug metabolism. Nature. 2000 Oct 19;407(6806):920-3.

White IN, De Matteis F, Gibbs AH, Lim CK, Wolf CR, Henderson C, Smith LL. Species differences in the covalent binding of [14C]tamoxifen to liver microsomes and the forms of cytochrome P450 involved. Biochem Pharmacol. 1995 Apr 18;49(8):1035-42.

Wiwi CA, Gupte M, Waxman DJ. Sexually dimorphic P450 gene expression in liver-specific hepatocyte nuclear factor 4alpha-deficient mice. Mol Endocrinol. 2004 Aug;18(8):1975-87. Epub 2004 May 20.

Wolfrum C, Asilmaz E, Luca E, Friedman JM, Stoffel M. Foxa2 regulates lipid metabolism and ketogenesis in the liver during fasting and in diabetes. Nature. 2004 Dec 23;432(7020):1027-32.

Yamano S, Nhamburo PT, Aoyama T, Meyer UA, Inaba T, Kalow W, Gelboin HV, McBride OW, Gonzalez FJ. cDNA cloning and sequence and cDNA-directed expression of human P450 IIB1: identification of a normal and two variant cDNAs derived from the CYP2B locus on chromosome 19 and differential expression of the IIB mRNAs in human liver. Biochemistry. 1989 Sep 5;28(18):7340-8.

Yamazaki H, Inoue K, Hashimoto M, Shimada T. Roles of CYP2A6 and CYP2B6 in nicotine C-oxidation by human liver microsomes. Arch Toxicol. 1999 Mar;73(2):65-70.

Yengi LG, Xiang Q, Pan J, Scatina J, Kao J, Ball SE, Fruncillo R, Ferron G,Roland Wolf C. Quantitation of cytochrome P450 mRNA levels in human skin. Anal Biochem. 2003 May 1;316(1):103-10.

Yoshinari K, Sato T, Okino N, Sugatani J, Miwa M. Expression and induction of cytochromes p450 in rat white adipose tissue. J Pharmacol Exp Ther. 2004 Oct;311(1):147-54. Epub 2004 May 18.

Zhang QY, Dunbar D, Kaminsky LS. Characterization of mouse small intestinal cytochrome P450 expression. Drug Metab Dispos. 2003 Nov;31(11):1346-51.

CHAPTER TWO

LENTIVIRAL-MEDIATED RNAI KNOCKDOWN YIELDS A NOVEL MOUSE MODEL FOR STUDYING CYP2B FUNCTION

Basma Damiri[1], William Baldwin[1,2]

[1] Environmental Toxicology Program, Clemson University, Clemson, SC 29634

[2] Biological Sciences, Clemson University, Clemson SC 29634

Submitted for publication in Toxicological Sciences

2.1 ABSTRACT

There are few *in vivo* knockout models available to study the function of Cyp2 members involved in the metabolism of endogenous and exogenous chemicals. These models may help provide insight into the CYPs responsible for the detoxification and activation of drugs, environmental toxicants, and endobiotics. The aim of this work is to produce a potent Cyp2b-knockdown (KD) mouse for subsequent study of Cyp2b function. We made a quintuple Cyp2b-KD mouse using lentiviral-promoted shRNA homologous to all five murine Cyp2b subfamily members (Cyp2b9, 2b10, 2b13, 2b19, and 2b23). The Cyp2b-KD mice are viable, fertile, and without physiological abnormalities except for an increase in liver weight and abdominal fat deposition. Expression of the three hepatic Cyp2b members, 2b9, 2b10, and 2b13, is significantly repressed as demonstrated by Q-PCR and Western blotting. The CAR activator, TCPOBOP was used to determine if shRNA-mediated Cyp2b10 repression could be outcompeted by Cyp2b10 induction. TCPOBOP-treated Cyp2b-KD mice show 80-90% less Cyp2b protein expression than TCPOBOP-treated WT mice, demonstrating that Cyp induction does not outcompete the repressive function of the shRNA. Furthermore, Cyp2b-KD mice are sensitive to parathion, an organophosphate insecticide primarily metabolized by Cyp2b enzymes, when compared to WT mice, and TCPOBOP-treated Cyp2b-KD mice are poor metabolizers of parathion compared to WT mice. In summary, we designed a shRNA construct that stably repressed the expression and activity of

multiple Cyp2b enzymes. We foresee that this novel Cyp2b-KD mouse model will significantly improve our understanding of the role of Cyp2b enzymes in chemical sensitivity and drug metabolism.

2.2 Introduction

The cytochrome P450s (CYPs) are important in lipid metabolism, including the metabolism of fatty acids, retinoids, eicosanoids, steroids, vitamin D, bilirubin, bile acids, and xenobiotics. The CYPs in families 1-4 are important in the metabolism of xenobiotic chemicals with most of the drug metabolism being performed by CYP families 1-3 (Baldwin *et al.* 2009; Muerhoff *et al.* 1994; Waxman 1988; Waxman *et al.* 1991; Willingham and Keil 2004). The CYP2 family contains several crucial subfamilies involved in detoxification such as CYP2A, 2B, 2C, 2D, and 2E subfamilies.

CYP2B's participate in the metabolism of numerous xenobiotics, including parathion, malathion, diazinon, bupropion, efavirenz, and cyclophosphamide (reviewed in (Hodgson and Rose 2007; Wang and Tompkins 2008)). In some cases CYP2B metabolism leads to chemical activation (Foxenberg *et al.* 2007; Mutch and Williams 2006; Tang *et al.* 2001). The importance of CYP2B proteins as effective monooxygenases for environmental chemicals is illustrated by the fact that phenotyped human microsomes show a correlation between CYP2B6 content and increased production of metabolites of known CYP2B substrates (Hodgson and Rose 2007). It is estimated that up to 12% of the available drugs on the market are metabolized by

CYP2B6 (Wang and Tompkins 2008) although CYP2B6 only makes up about 3-5% of the CYPs in the human liver (Lang *et al.* 2004). However, CYP2B6 content varies as much as 100-fold between individuals (Ekins *et al.* 1998), is sexually dimorphic (Lamba *et al.* 2003), and polymorphic (Lang *et al.* 2004), and these variances probably cause individual differences in the metabolism of these drugs.

Humans have one CYP2B gene, CYP2B6, while mice have five Cyp2b genes, Cyp2b9, Cyp2b10, Cyp2b13, Cyp2b19, and Cyp2b23 (Nelson *et al.* 2004). Cyp2b9, Cyp2b10, and Cyp2b13 are the forms primarily expressed in the liver (Finger *et al.* 2011). CYP2B6 in humans and Cyp2b10 in mice is transcriptionally regulated by the constitutive androstane receptor (CAR), a metabolic and xenobiotic sensing nuclear receptor, (Honkakoski *et al.* 1998; Wang *et al.* 2003; Zhang *et al.* 2002; Kretschmer and Baldwin 2005). Perturbations in CAR activity are known to alter the metabolism and toxicity of bile acids (Uppal *et al.* 2005; Beilke *et al.* 2009), acetaminophen (Zhang *et al.* 2002), and parathion (Mota *et al.* 2010). However, Cyp2b's role in protecting individuals from these endogenous and exogenous chemicals is not fully understood as other detoxification enzymes are also regulated by CAR. Overall, the role of Cyp2b isoforms in mice and CYP2B6 in humans for metabolizing endogenous and exogenous chemicals is often overlooked and poorly understood in part due to the lack of an *in vivo* model (Reschly and Krasowski 2006; Yamada *et al.* 2006; Wang and Tompkins 2008).

Although there are *in vivo* models for studying many drug metabolizing CYPs, including recombinant Cyp2b isoforms, there are few *in vivo* models of CYP function such as CYP-knockout mice. In fact, few of the detoxifying P450s with multiple isoforms have been knocked out. If not for the recent production of the Cyp3a-null mouse (van Herwaarden *et al.* 2007) in part by in chromosomal deletion, there would be no CYP-null mice for P450 subfamilies with multiple isoforms. There are no CYP-null mice for any of the Cyp2 subfamily members critical in detoxification (i.e. Cyp2a, Cyp2b, Cyp2c, and Cyp2d) with the exception of Cyp2e1 (Lee *et al.* 1996), a one-member subfamily. There is also a Cyp2j5-null mouse (Athirakul *et al.* 2008); however, this CYP does not appear to have a significant role in detoxification. Of the 68 functional CYPs in families 1-4, only twelve have been deleted in some forms to our knowledge. The primary reason that Cyp-null mice have rarely been made is because most murine Cyps in subfamilies 2-4 have many individual isoforms that perform redundant functions. For example, the Cyp2b subfamily in mice has five isoforms (Nelson *et al.* 2004). Therefore, knocking out Cyp2b10 may have little effect on the physiology of the mouse because Cyp2b9, Cyp2b13, Cyp2b19, and Cyp2b23 with similar structures and potentially redundant functions are still available. In addition, the cost of making a quintuple knockout has made such inquiries impractical.

Small Interfering RNAs (siRNAs) are short, double-stranded RNA molecules (21-25 nucleotides) that can form complementary sequences with single-stranded mRNAs, and in turn target them for degradation in a process called RNA interference (RNAi)

(Elbashir *et al.*, 2001). This leads to a decrease, but not the absence, of the expression of the corresponding protein. RNAi-mediated gene knockdown has been performed through several techniques at multiple levels and the most successful application of the discovery of RNAi has been to study the gene function in cultured human and mouse cells. The generation of transgenic and knock-out mouse models has been constantly improved, providing researchers with a large number of invaluable animal models. *However,* RNAi has not been used to knockdown whole subfamilies of Cyps, or produce efficient, persistent knockdown mice under the control of a lentiviral promoter that demonstrate the repression of multiple Cyps. Because the Cyp2b murine subfamily members show high homology, the Cyp2b subfamily can be targeted for shRNA-mediated repression. Therefore, we can potentially knockdown all five isoforms with one siRNA construct.

We used siRNA to repress the expression of each member of the murine Cyp2b subfamily. We hypothesized that the whole Cyp2b subfamily can be efficaciously knocked down in mice using lentiviral driven shRNA homologous to each of the five Cyp2b subfamily members and this was tested in the liver of Cyp2b-knockdown (Cyp2b-KD) mice. Further, we tested whether the repression of Cyp2b function caused changes in toxicant metabolism using the pesticide parathion. We envision that the Cyp2b-KD model will provide a new tool for further study of the impact of Cyp2b enzymes on the *in vivo* metabolism of endobiotic and xenobiotic chemicals.

2.3 Materials and Methods

2.3.1 Design of Cyp2b-constructs and generation of shRNA containing lentiviruses.

The five Cyp2b subfamily members were aligned with ClustalW (Fig. 1), and shRNAs were designed based on siRNA Scales (http://gesteland.genetics.utah.edu/siRNA_scales) (Mateeva *et al.* 2007). Constructs of 21-22 base pairs were designed because previous work shows that dsRNA smaller than 23bp do not elicit an anti-viral interferon response that causes the cessation of all protein synthesis rather than elicit specific repression of a gene (Elbashir *et al.* 2001). Three different siRNA constructs (Cyp2b-KD2, Cyp2b-KD3, and scrambled) were chemically synthesized and cloned into the pRNAT-U6.2/Lenti plasmid at their BamH1 and Xho1 sites (Fig. 1). This plasmid also contains coral green fluorescent protein (cGFP) (Genscript, Piscataway, NJ) as a marker for expression.

Lentiviral particles were produced according to the manufacturer's instructions (Invitrogen, Carlsbad, CA). Human embryo kidney (293FT) cells (Invitrogen) were cultured in complete DMEM media containing 10% FBS, 6 mM L-glutamine, 1 mM MEM Sodium Pyruvate, 0.1mM MEM Non-Essentail Amino Acids and 500 µg/ml Geneticin (G418). One day before transfection, $5x10^6$ cells were seeded in 10-cm dishes without G418. Twenty-four hours later the cells were transfected with the pRNAT-U6.2/lenti plasmid from Genscript along with VirapowerTM plasmids and lipofectamineTM 2000 (Invitrogen) following the manufacturer's instructions. The next day, media containing lipofectamine was replaced with complete DMEM media and forty

eight hours later, the viral supernatant was collected, centrifuged, filtered through 0.45µm low protein filter, and concentrated by ultracentrifugation (Burns *et al.* 1993; Ramezani and Hawley 2002). The viral pellets were suspended in complete DMEM media with no antibiotic for perivitelline microinjection. Concentrated and unconcentrated viral stocks were titered and stored at -150 ^{o}C.

Viral concentrations were determined according to the manufacturer's instructions (Invitrogen). HT1080 cells (Invitrogen) seeded in 6-well plate at 200,000 cells/well in complete DMEM media and 1% Penicillin/Streptomycin, were transduced with a serial dilution of the viral stocks, 6 µg/µl polybrene® (Invitrogen), and incubated at 37 ^{o}C overnight in a humidified 5% CO2 incubator. The following day, the media was changed to complete DMEM media and G418 (350 µg/ml) to select the transduced cells. Media was replaced every 3-4 days with fresh media containing G418. Titer was determined by counting the percentage of positive cells (green cells) with an inverted fluorescent microscope after 5-7 days of transduction, or colonies were counted after two weeks of G418 exposure (Sastry *et al.* 2002; Blesch 2004). Lentiviral titers were 1.0, 1.2, 1.5 × 10^{6} Transduction Units (TU) per ml, for Cyp2b-KD2, Cyp2b-KD3, and scrambled, respectively. Concentrated lentiviral titers for Cyp2b-KD2, Cyp2b-KD3, and the scrambled construct were 3×10^{8}, $5\times10^{8,}$ and 1×10^{8} TU, respectively.

2.3.2 Primary hepatocytes transduction.

Primary mouse hepatocytes (Cellzdirect, Pittsboro, NC) from male CD-1 mice plated in 12-well plates (128,000 cell/ well) were transduced with Cyp2b-KD2, Cyp2b-KD3, or scrambled constructs at a multiplicity of infection (MOI) of 5 or 20. Twenty-four hours after transduction, the cells were treated with the CAR activator 1,4-Bis[2-(3,5-dichloropyridyloxy)] benzene (TCPOBOP) (Sigma Aldrich, St. Louis, MO) to induce Cyp2b subfamily members (especially Cyp2b10). Cells were harvested for RNA extraction and Q-PCR 24 hours after TCPOBOP treatment. In addition, the percentage of cells infected based on the presence of green fluorescence using fluorescent microscopy (Zeiss Axiovert 200M, Carl Zeiss International, Gottingen, Germany) was determined so that the drop in Cyp2b expression could be compared to the number of cells transduced.

2.3.3 Perivitelline injection

Donor FVB/NJ (FVB) female mice (The Jackson Laboratory; Bar Harbor, ME) were superovulated and mated to FVB stud males. Donor females showing vaginal plugs were sacrificed. The 1-cell embryos were washed several times in micro drops of M16 medium (Millipore; Billerica, MA) and used in microinjection. Concentrated Cyp2b-KD2 lentivirus (8pl/cell) suspended in DMEM media or PBS at concentrations of approximately 5 $x10^8$ TU were injected into the perivitelline space of fertilized single-cell FVB embryos. The zygotes then were cultured overnight, and transplanted into pseudopregnant CD-1 mice the next morning.

2.3.4 Genotyping

Viral and siRNA integration were detected by PCR analysis and confirmed by sequencing. Total genomic DNA was isolated from mice tail biopsies with the DNeasy® blood and tissue DNA extraction kit following the manufacturer's instructions (Qiagen, Valencia CA). Primers spanning the shRNA were used in PCR to genotype the mice. These primers, pRNAT-U.6/Lenti specific primers and Cyp2b-KD, amplify 956 and 359 bp targets, respectively, within the promoter and shRNA and are available in Supplementary Table 1. Genotyping results were determined from PCR reactions run on 1.6% agarose gels. To confirm the PCR results, the PCR- product was purified using the MinElute® PCR purification kit (Qiagen) and sequenced.

2.3.5 Mice Treatment

All studies were carried out according to NIH guidelines for the humane use of research animals and pre-approved by Clemson University's IACUC. Mice were provided water, and fed *ad libitum* prior to and during treatments. Wild-type (FVB/NJ) mice from The Jackson Laboratory were bred to positive Cyp2b-KD2 mice to maintain the genetic background. Untreated FVB and Cyp2b-KD2 mice were euthanized at 8-12 weeks of age (n = 4-8) to investigate differences in Cyp2b expression. In addition, 8-12 week-old FVB and Cyp2b-KD mice were injected with 3 mg/kg TCPOBOP or received vehicle (corn oil) to investigate Cyp2b expression following treatment with a CAR activator and Cyp2b inducer (Tzameli *et al.* 2000; Wei *et al.* 2000). Mice were weighed prior treatment. Twenty-four hours after treatment, mice were euthanized, livers excised

and weighed, and then cut into three pieces for sample preparation (RNA, protein, histopathology).

2.3.6 Sample preparation.

A portion of the liver was placed in 10% formalin (Fisher Scientific, Pittsburgh, PA) for histology investigations. The rest of the liver was snap frozen, diced, separated into two tubes, and placed in a freezer at -80 ^{o}C for further preparation. Total RNA was extracted from one third of the liver using modified phenol/chloroform extraction technique with TRI-Reagent® according to the manufacturer's instructions followed by DNAse digestion to remove residual genomic DNA (Promega Corporation, Madison WI). RNA concentrations were determined spectrophotometrically at 260/280 nm (Molecular Devices, Ramsey, MN). Reverse transcription was performed to make cDNA using 200 units Moloney Murine Leukemia Virus–Reverse Transcriptase (MMLV-RT), a 10 mM dNTP mixture, and 0.05 mg random hexamers (Promega Corporation, Madison, WI). For cytosol and microsome preparation, the liver was individually homogenized with a Dounce Homogenizer and protein fractions were prepared by differential centrifugation (Van der Hoeven and Coon 1974). Protein concentrations were determined from cytosol and microsomes using the Bio-Rad protein assay according to the manufacturer's instructions (Bio-Rad Laboratories, Hercules, CA).

2.3.7. Quantitative Real-time Polymerase Chain Reaction (Q-PCR).

Quantitative real-time PCR (Q-PCR) was performed using primers for specific isoforms to Cyp2b9, Cyp2b10, and Cyp2b13 subfamily members, and 18S or β-actin as the housekeeping genes (Supplementary Table 1). For primary mouse hepatocytes, cDNA was diluted 1:5 prior to Q-PCR. To generate a standard curve and determine the PCR efficiency of each reaction, a composite sample of cDNA from treated and untreated cells was made with dilutions of 1:1, 1:5: 1:50: and 1:500. For Cyp2b10, a TaqMan probe was used and β-actin was the housekeeping gene; for Cyp2b9, SybrGreen was used and 18S rRNA was the housekeeping gene.

For studies with mice, Cyp2b9, Cyp2b10, Cyp2b13, and CAR were quantified from liver cDNA samples that were diluted 1:10 prior to Q-PCR. The primers used are described in Supplementary Table 1. To generate a standard curve and determine the PCR efficiency of each reaction, a composite sample of cDNA from treated and untreated FVB and Cyp2b-KD mice was made, and dilutions from 1:1 to $1:10^{-6}$ were prepared. Amplifications of the samples and the standard curve were performed in triplicate using a 96-well iQ5™ multicolor Real-Time PCR Detection System (Bio-Rad) with 0.25× SybrGreen (SA Biosciences, Frederick, MD) as the fluorescent double strand-intercalating agent to quantify gene expression as described previously (Hernandez *et al.* 2006; Mota *et al.* 2010). Muller's equation was used to determine relative quantities of each CYP (Muller *et al.* 2002). A minimum of forty cycles was run on all real-time samples to ensure a log based growth curve.

2.3.8 Immunoprecipitations and Western blots.

CAR was immunoprecipitated prior to quantification by Western blotting as described previously (Hernandez *et al.* 2009b). Western blots were also performed to detect and quantify Cyp2b protein levels as described previously using 30 to 50 μg of hepatic microsomal protein. β-actin (Sigma Aldrich, St. Louis, MO) was used as a housekeeper to ensure equal loading of samples (Mota *et al.* 2010). Goat anti-rabbit IgG (Bio-Rad) alkaline-phosphatase coupled secondary antibodies were used for recognizing the Cyp2b primary antibody and goat anti-mouse (Bio-Rad) IgG were used to recognize β-Actin primary antibodies. Bands were visualized with chemiluminescence detection using the Immun-Star AP Chemiluminescent Protein Detection System and quantified with the Chemi Doc XRS HQ using Quantity One 4.6.5 software (Bio-Rad Laboratories).

2.3.9 Parathion metabolism.

Changes in parathion metabolism were examined with 250 μg of microsomes from TCPOBOP-treated FVB and Cyp2b-KD2 mice (Foxenberg *et al.* 2007; Mota *et al.* 2010). Samples were incubated in buffer (0.1M Tris-HCl and 5mM MgCl2 at pH 7.4) and 20 μM parathion at 37°C in the presence of the esterase inhibitors 1mM EDTA and 50 μM iso-OMPA. Reactions were initiated with 1 mM NADPH, and stopped after 60 minutes with 500 μl of methanol/0.1% phosphoric acid. Metabolite concentrations from filtered (0.22 μm PTFE filter; Fisher Scientific) samples were measured by Reverse Phase-HPLC as described previously (Mota *et al.* 2010). Chemical detection was

determined at 275 nm for parathion and paraoxon, and at 310 nm for PNP. The detection limit for paraoxon is 0.0275 µg/ ml, and the detection limit for PNP is 0.0139 µg/ ml.

2.3.10 Histopathology

To evaluate the histopathological effect of Cyp2b repression on Cyp2b-KD mice, liver samples from male and female, corn oil and TC-treated, FVB, and Cyp2b-KD mice (n=3) were fixed in 10% formalin. Samples were processed and stained with hemotoxylin and eosin at Colorado Histo-Prep for blind histopathological evaluation (Fort Collins, CO). Standardized toxicologic pathology criteria and nomenclature for the mouse were used to categorize microscopic tissue changes (Banks 1993; Percy and Barthold 2001). Parameters examined were hepatocellular swelling, necrosis, hypertrophy, hyperplasia, inflammation, bile duct hyperplasia, and mineralization. The individual parameters were scored 0-4 and then summed. There is considered minimal pathology if the mouse liver scored less than 5, mild pathology if the total score is 5-10, moderate pathology if the total score is 10-15, and marked pathology if the total score is 15-20. Total scores for the hepatic histopathology lesions in each mouse were ranked and statistical significance determined by Kruskal–Wallis followed by Dunn's post hoc test.

2.3.11 Zoxazolamine.

Untreated male and female mice from FVB and Cyp2b-KD mice (n = 5-15) were injected with 400 mg/kg zoxazolamine. Paralysis time was measured by placing paralyzed mice on their backs and measuring the time until they were able to consistently

right themselves (Hernandez *et al.* 2007). Mice that did not recover from Zox-induced paralysis within 8 hours were euthanized.

2.3.12 Parathion toxicity.

Both male and female, FVB and Cyp2b-KD mice (n=5-15/treatment) were injected ip with 5 mg/kg/day of parathion and behavioral changes observed over the next 6 hours as described previously (Mota *et al.* 2010). The severity of toxicity was quantified based on these symptoms: 0 = not toxic, 1 = eye leakage, 2 =slow tremors, 3= morbid and 4= death. Mice showing severe toxicity were immediately euthanized.

2.3.13 Statistical analysis.

Results are expressed as mean ± SEM. Tests of significance (GraphPad PRISM 4.0, San Diego, California) were conducted by unpaired Student's t-test, or ANOVA followed by Tukey's post-hoc test when multiple treatments were compared. A p-value < 0.05 is regarded as statistically significant. Differences in the number of mice paralyzed by Zox were determined by the Mann-Whitney rank sum test. Parathion toxicity was determined statistically with behavorial rankings as described previously (Mota *et al.* 2010) using the Kruskal–Wallis nonparametric test for independent variables followed by Dunn's post hoc test.

2.4 Results

2.4.1 Design and determine the efficacy of the Cyp2b shRNA constructs:

ClustalW alignments of the five Cyp2b subfamily members demonstrated that there are five highly homologous areas of the murine Cyp2bs. shRNA constructs that recognize all five Cyp2b subfamily members in mice were designed based on these homologous areas. Three of these sites, designated KD1, KD2, and KD3, respectively (Fig. 2) are potential targets for shRNA based on siRNA scales (Mateeva *et al.* 2007) that indicates these constructs would repress Cyp2b expression greater than 70% in cell culture.

In addition, each construct was compared to several other CYP genes to make sure they were not homologous to other CYPs and cause the repression of their expression. The homologous region of Cyp2a4 is 57% identical to the Cyp2b-KD2 construct; all other Cyps examined showed less than 50% identity to the Cyp2b-KD2 shRNA construct. Homologous regions of Cyp2c29 and Cyp2c37 showed 82% and 73% identity to the Cyp2b-KD3 construct (Additional File 1). All other Cyps examined showed less than 60% identity to the Cyp2b-KD3 shRNA constructs.

The efficacy of Cyp2b-KD2 and KD3 lentiviral shRNA constructs to repress Cyp2b9 and Cyp2b10 expression was tested using primary mouse hepatocytes. The percentage of cells infected based on the presence of green fluorescence using fluorescent microscopy was approximately 80% in KD2 transduced cells at MOI of 5 and about 70%

in KD3 transduced cells at a MOI of 5. Cyp2b-KD2 reduced Cyp2b9 and Cyp2b10 expression 73-98% (Table 1). This suggests that the cells that were infected showed nearly a complete abolishment of these Cyp2b subfamily members. Cyp2b-KD3 was not as efficacious. It reduced Cyp2b10 expression 50% following infection of 70% of the cells; however, KD3 did not repress Cyp2b9 expression relative to cells treated with the scrambled shRNA (Table 1). Because Cyp2b-KD2 is more efficacious, and Cyp2b-KD3 does not reduce Cyp2b9 expression and shows higher homology to other Cyp2 members, transgenic mice were made with the Cyp2b-KD2 construct.

2.4.2 Generation of Transgenic mice

Engineered lentiviral Cyp2b-KD2 particles were microinjected into the perivitelline space of FVB/NJ mouse zygotes. Perivitelline injection of FVBs produced 134 pups of which 100% were positive by PCR genotyping of the tail clippings (Fig. 3). DNA sequencing confirmed the existence of the Cyp2b-KD2 construct in our mice. In addition, newborn mice were screened for GFP under a UV light, and only three mice visually expressed GFP seven days after birth. Several of these mice continued to show fluorescence in the ears, tail, feet, and especially the eyes when adults (Fig. 3). None of the F1 or F2 generation mice tested showed brilliant green skin expression, but some of them expressed green teeth. Five transgenic founders (4 males and 1 female) identified based on genotyping and sequencing results were mated to FVB/NJ mice to obtain F1 progeny. All F0 mice were able to give rise to transgenic offspring. Nearly 86% of our F1 and 49 % of F2 mice are positive after mating positive F1 to FVB/NJ mice. The high

percentage of positive F1 mice indicates that our F0 Cyp2b-KD mice had multiple integrants.

All of the transgenic mice have developed and bred normally. In addition, none of the mice show obvious spontaneous abnormalities except for a putative increase in abdominal fat deposition and a significant increase in liver/body weight ratios (hepatosomatic index) compared to WT mice. Liver index increased 21 to 22% ($p < 0.0001$) in males and females, respectively. Liver enlargement is symptomatic of toxicant exposure and has been observed in other mice with repressed hepatic CYP function such as the P450 oxidoreductase-null (POR-null) mouse (Finn *et al.* 2009).

2.4.3 Efficacy of Cyp2b repression in Cyp2b-KD mice

Q-PCR and Western blots were performed to measure changes in the expression of individual Cyp2b isoforms in wild-type (WT) and Cyp2b-KD mice. Q-PCR of untreated adult WT and Cyp2b-KD mice indicated that most but not all of the hepatic Cyp2b members are repressed in the knockdown mice. The expression of Cyp2b9, Cyp2b10, and Cyp2b13 are repressed in male Cyp2b-KD mice relative to WT mice. In contrast, only Cyp2b10 and Cyp2b13 are repressed in female Cyp2b-KD mice relative to their WT controls (Fig. 4A). Cyp2b9, a female predominant Cyp (Hashita *et al.* 2008) is not repressed in females. Western blots demonstrate that Cyp2b protein expression is also repressed. Two distinct Cyp2b members, thought to be Cyp2b9 and Cyp2b10, are repressed in females (Fig. 4B), indicating that Cyp2b protein expression is reduced in the female Cyp2b-KD mice. Untreated male mice have low Cyp2b expression (Hernandez *et*

al. 2006; Hernandez *et al.* 2009b) and our antibody was not sensitive enough to consistently quantify Cyp2b levels in the FVB or Cyp2b-KD mice. Therefore, we also measured Cyp2b expression in TCPOBOP-treated mice.

The CAR activator, TCPOBOP (Tzameli *et al.* 2000), was used to determine the efficacy of our Cyp2b-KD construct at reducing Cyp2b levels following treatment with a powerful inducer. The primary purpose of this experiment was to determine if TCPOBOP-treatment and the subsequent Cyp2b-induction would outcompete lentiviral-promoted shRNA repression of Cyp2b. None of the hepatic Cyp2b's showed lower transcript expression after TCPOBOP treatment in the Cyp2b-KD mice compared to the WT mice (Fig. 5A). Cyp2b10 and Cyp2b13 showed greater expression in the TCPOBOP-treated female mice than the WT mice by 2.6X, indicating a compensatory mechanism. However, protein levels as determined by Western blots did not confirm the Q-PCR results and actually showed significant decreases in Cyp2b expression (about 5-10X) in the Cyp2b-KD mice compared to the WT mice (Fig. 5B). This demonstrates that TCPOBOP-mediated Cyp2b induction did not outcompete the shRNA's ability to repress Cyp2b protein expression. Therefore, the Cyp2b-KD mouse was still functionally repressing Cyp2b even after the addition of a Cyp2b inducer.

CAR constitutively regulates the expression of Cyp2b10 and Cyp2b13 (Hernandez *et al.* 2009b; Mota *et al.* 2010), and may constitutively regulate the expression of Cyp2b9 in males (Mota *et al.* 2010). Therefore, we hypothesized that CAR

transcript expression may be increased in the Cyp2b-KD mice as a compensatory mechanism that increases CAR's sensitivity to endogenous ligands or its constitutive activity, and in turn increases Cyp2b expression especially Cyp2b10. Q-PCR and Western blotting were performed (Fig. 6), and Q-PCR suggested that CAR may be increased in female Cyp2b-KD mice relative to WT mice, but the data was not statistically significant ($p = 0.061$). Western blots were performed to confirm Q-PCR results and ascertain whether there was a trend suggesting increased CAR in females. CAR protein expression was significant increased (2.9X) in the TC-treated Cyp2b-KD female mice, but not the untreated mice compared to the corresponding WT mice, suggesting that CAR may be involved in a compensatory mechanism that helps Cyp2b-KD mice respond to a chemical insult like TCPBOP (Fig. 6). Overall, this data suggests that increased CAR expression in the TC-treated female mice may provide a compensatory mechanism to increase Cyp2b expression; however, the compensatory mechanism did not overcome the ability of the shRNA construct to repress Cyp2b protein expression in the mice.

2.4.4 Histopathology

Because CAR is critical in hepatic responses to toxicants, we investigated whether Cyp2b-KD mice may show histpathological changes especially after TC-treatment. Summation of the different histopathology parameters examined indicates that only TC-treated Cyp2b-KD female mice responded in an atypical manner (Fig. 7; Additional File 2 contains H&E stained slides). For example, all of the male TC-treated mice and the

female TC-treated FVB mice showed increased histopathology scores primarily because of increased hyperplasia; typical of TC-treated mice (Wei *et al.* 2000). However, TC-treated Cyp2b-KD female mice had significantly decreased histopathology scores. Only eight mice showed a score of 6 or less; this includes all three female TC-treated Cyp2b-KD mice. The other mice with scores of less than 6 were all three male control FVB and two control Cyp2b-KD mice.

2.4.5 Cyp2b-mediated metabolism is compromised in the Cyp2b-KD mice:

The *in vivo* metabolism of parathion was examined in microsomes from TC-treated mice to test whether TC-treated Cyp2b-KD mice demonstrated perturbed metabolism of parathion relative to TC-treated FVB mice. Cyp2b enzymes have a high affinity for parathion and in turn are probably key enzymes in the metabolism of parathion to its toxic form paraoxon (POXON), and its non-toxic form *para*-nitrophenol (PNP) (Foxenberg *et al.* 2008; Foxenberg *et al.* 2007; Mota *et al.* 2010). Parathion metabolism was severely compromised (down 3-7X) in the male and female Cyp2b-KD mice compared to the WT mice (Fig. 8) consistent with the Western blot results demonstrating that TC-treatment cannot overcome the persistent repressive effects of the Cyp2b shRNA.

*2.4.6 Toxicological changes in Cyp2b-KD mice***:**

Zox is a classical CYP substrate used to estimate the functional *in vivo* effects of perturbations in CYP activity, as increased paralysis indicates inhibition or repression of

CYPs and decreased paralysis indicates induction (Hernandez *et al.* 2007; Wei *et al.* 2000). Untreated Cyp2b-KD female mice were extremely sensitive to Zox-treatment as 50% of Cyp2b-KD female mice died 4-5 hours after Zox-treatment and the other 50% were euthanized as they had not recovered from ZOX-induced paralysis after 8-hours (Table 2). In comparison, WT female mice showed little toxicity to Zox-induced paralysis. None of the WT female mice were paralyzed by 400 mg/kg Zox but 3 out of the 5 WT females did show slow eratics movements for 10-15 minutes after injection. Males did not show a significant difference in Zox-paralysis times as few of the WT or CYP2b-KD mice showed significant paralysis although there appeared to be increased "shaking" that lasted hours in the Cyp2b-KD mice.

CAR-null mice show reduced parathion metabolism and increased toxicity (Mota *et al.*, 2010). These mice also have reduced expression of several CYPs including several Cyp2b members (Hernandez et *al.*, *2009*; Mota *et al*., 2010). Since we observed that Cyp2b-KD mice are also poor parathion metabolizers using *in vivo* assays, we examined toxicity induced by parathion *in vivo*. Both Cyp2b-KD males and females showed increased sensitivity to parathion at 5mg/kg compared to WT mice. Initial toxicity was shown by mucous discharge from the eyes and later reduced activity, lethargy, significant morbidity, or death. All of the Cyp2b-KD mice showed toxicity symptoms, and some of the Cyp2b-KD mice showed morbidity. None of the WT mice showed morbidity, a few were lethargic, but almost 50% of the WT mice showed no overt toxicity to parathion. Moreover, WT mice recovered faster than the Cyp2b-KD mice, indicating that Cyp2b's

are key enzymes in the detoxification of parathion, and a lack of metabolic activity towards parathion probably increases the retention of paraoxon and its subsequent toxicity.

2.5 Discussion

Most of the Cyp2b subfamilies in mice have undergoes significant gene duplication events. In contrast, human CYP2B subfamily members often have few or only one gene (Nelson *et al.* 2004). The redundancy of murine Cyp2bs in each subfamily makes targeted mouse gene knockouts impractical and costly because if one Cyp is eliminated, there are still four other Cyp2bs available to carry out potentially redundant functions. To circumvent this limitation, we designed and determined an efficient shRNA construct with the potential to knockdown five isoforms of murine Cyp2b. This construct was used to generate the first persistent quintuple Cyp2b knockout mouse for the subsequent study of Cyp2b functions *in vivo*.

The expression of hepatic Cyp2b isoforms is significantly repressed in the Cyp2b-KD mice. Western blots with liver microsomes demonstrate a near complete abolishment of Cyp2b proteins in the liver of untreated mice, and Q-PCR indicates that all of the hepatic Cyp2b isoforms are repressed in males and all but Cyp2b9 is significantly repressed in females. Furthermore, TCPOBOP-mediated Cyp2b induction did not outcompete the shRNA's ability to repress Cyp2b protein expression demonstrating that the Cyp2b-KD mouse model is functional in the presence of a CAR activator and

powerful Cyp2b inducer. Therefore, we have produced an efficient knockdown of at least the three major hepatic Cyp2b members in mice, including the highly inducible Cyp2b10.

In addition, parathion metabolism was significantly lower in hepatic microsomes from TCPOBOP-induced Cyp2b-KD mice than WT mice. In a previous study, liver microsomes from CAR-null mice that have lower expression of several Cyps including Cyp2b and Cyp3a subfamily members compared to their WT counterparts, metabolize parathion slowly compared to WT mice. Furthermore, CAR-null mice show increased sensitivity to this organophosphate pesticide (Mota *et al.* 2010). Therefore, we examined the role of Cyp2bs in the metabolism of parathion in Cyp2b-KD mice. We observed that parathion metabolism is perturbed in the hepatic microsomes of TCPOBOP-induced Cyp2b-KD mice, and parathion toxicity is greater in Cyp2b-KD mice than WT mice.

Previous studies with rats, chemically-induced liver microsomes, and recombinant human CYPs also indicate a key role for Cyp2b in parathion metabolism, fate, and toxicity (Foxenberg *et al.* 2008; Foxenberg *et al.* 2007; Kim *et al.* 2005; Mota *et al.* 2010; Mutch *et al.* 1999). Parathion toxicity is caused by its bioactivation to the toxic metabolite POXON (Sultatos *et al.* 1984), but we observed reduced POXON production in the Cyp-KD mice. This suggests that toxicity in the Cyp2b-KD mice is due to poor metabolism of parathion to PNP, which is also catalyzed by Cyp2b (Foxenberg *et al.* 2008; Foxenberg *et al.* 2007; Mutch and Williams 2006), extrahepatic metabolism of

parathion, or higher clearance of paraoxon from the liver of Cyp2b-KD mice compared to WT mice because of poor metabolism of parathion and paraoxon. Liver perfusion studies indicate that parathion metabolized to paraoxon may exit the liver as paraoxon and cause toxicity (Sultatos *et al.* 1985). Overall, this study demonstrates that *in vivo* Cyp2b isoforms play a key role in parathion metabolism and toxicity, and is the first study to demonstrate that individuals with compromised Cyp2b are susceptible to the toxic effects of parathion.

ZOX paralysis time is a key indicator of perturbations in Cyp activity *in vivo*. Female Cyp2b-KD mice did not recover from Zox injection indicating poor metabolism and clearance, and indicating a key role of Cyp2b in Zox metabolism. In contrast, male Cyp2b-KD mice did not demonstrate a significant difference in Zox paralysis time. Most Cyp2b's (Cyp2b9, Cyp2b13,and maybe Cyp2b10) are female predominant (Hernandez *et al.* 2006; Hernandez *et al.* 2009a; Wiwi *et al.* 2004), and therefore reducing Cyp2b levels in female mice may cause a more pronounced effect. FVB mice also metabolize Zox better than B6 mice, and a higher dose is needed to cause paralysis (Hernandez *et al.* 2006). A 450 mg/kg dose appeared to high in a previous study (Hernandez *et al.* 2006), and therefore we performed a pilot study and came and decided on 400 mg/kg. However, this dose may have been too low for the FVB male mice as few of them (WT and Cyp2b-KD) were fully paralyzed by Zox.

Furthermore, the Cyp2b-KD mice are viable, fertile, and did not exhibit significantly abnormal phenotypes or physiological abnormalities except TCPOBOP-treated female Cyp2b-KD mice did not respond and show perturbed histopathology parameters, untreated mice showed an increase in liver weight, and a subjective increase was observed in abdominal and renal fat. Liver enlargement has been regarded as a marker of drug associated enzyme induction, and suggests a compensatory mechanism (Amacher *et al.* 2001; Webber *et al.* 1994), probably to adapt to increased concentrations of an endobiotic. Similar increases in hepatostomatic indices have been observed in other transgenic mice with low Cyp activity such as mice that lack key hepatic transcription factors that regulate Cyps. Examples include hepatic POR-null mice (Henderson *et al.* 2003) and HNF4α-null mice (Hayhurst *et al.* 2001) where the liver/body weight ratios probably increased because of the accumulation of lipids.

Interestingly, there also appears to be a molecular compensatory reaction to the repression of Cyp2bs in the Cyp2b-KD mice. For example, Cyp2b9 mRNA expression was not repressed in female Cyp2b-KD mice. Furthermore, no TCPOBOP-treated male mice showed repression of Cyp2b mRNA transcript levels, and female mice actually demonstrate greater expression of Cyp2b10 and Cyp2b13 in Cyp2b-KD mice following TCPOBOP-treatment than WT mice. This suggests that there is some type of compensatory mechanism trying to overcome the repressive effects of the shRNA. CAR basally regulates Cyp2b10 and Cyp2b13, and may in part regulate Cyp2b9 (Hernandez *et al.* 2009b; Mota *et al.* 2010). Therefore, we hypothesized that CAR may be induced in

order to adapt to the lack of Cyp2b members, especially Cyp2b10, in the Cyp2b-KD mice. CAR protein levels are increased in TCPOBOP-treated females, and this may help the mice adapt to lower Cyp2b expression and in turn increase Cyp2b mRNA expression. In addition to CAR, forkhead box protein A2 (FoxA2 also known as hepatic nuclear factor 3β), a female predominant transcription factor, regulates Cyp2b9 (Hashita *et al.* 2008), and therefore this transcription factor may also play a role in the lack of Cyp2b9 repression in untreated and TCPOBOP-treated Cyp2b-KD female mice. Lastly, the compensatory induction of Cyp2b10 in males and females may just be due to increased retention of TCPOBOP caused by the lack of Cyp2b's; leading to greater activation of CAR and in turn higher Cyp2b10 transcript levels.

Overall, even though Cyp2b transcript levels were increased in Cyp2b-KD mice to levels equal to or greater than WT mice following TCPOBOP-treatment, protein expression was still much lower in the Cyp2b-KD mice. It has been suggested that Western blots are more reliable to confirm the efficacy of siRNA (Holmes *et al.* 2010). There are several potential reasons for this including the extracted RNA is nuclear or not available for siRNA degradation, or the 3'mRNA cleavage products resulting from siRNA mediated cleavage accumulate within the cell (Holen *et al.* 2002), but are still large enough fragments that they result in small templates for cDNA synthesis and give rise to a false signal of mRNA detection by Q-PCR (Holmes *et al.* 2010).

The shRNA generated Cyp2b-KD mice demonstrate low expression of hepatic Cyp2b members in untreated and TCPOBOP-treated mice. They also poorly metabolize the Cyp2b substrates Zox and parathion, and in turn are sensitive to these toxicants indicating that Cyp2bs play a key role in protecting individuals from select chemicals. Therefore, Cyp2b-KD mice may be able to act as a sentinel for individuals with low Cyp2b-expression or limited metabolic capacity because of Cyp2b polymorphisms. Further, this model can be built upon to form even better models for human disease, human metabolism, and human genetic polymorphisms by making CYP2B6/7 humanized mice. This study provides a new platform for studying Cyp2b function and especially its role in the metabolism of distinct pharmaceuticals and environmental chemicals.

Acknowledgements: The authors would like to thank Dr. Xianzhong Yu and Mr. Eric Holle for performing the perivitelline injections. This work was supported by NIH grant R15-ES017321, a South Carolina EPSCoR/IDEA CCD project, Clemson University Research Foundation, and Clemson University start-up funds.

2.6 References

Amacher, D. E., Schomaker, S. J., and Burkhardt, J. E. (2001). The relationship among microsomal enzyme induction, liver weight and histological change in beagle dog toxicology studies. *Food Chem Toxicol* **39**, 817-825.

Athirakul, K., Bradbury, J. A., Graves, J. P., DeGraff, L. M., Ma, J., Zhao, Y., Couse, J. F., Quigley, R., Harder, D. R., Zhao, X., Imig, J. D., Pedersen, T. L., Newman, J. W., Hammock, B. D., Conley, A. J., Korach, K. S., Coffman, T. M., and Zeldin, D. C. (2008). Increased blood pressure in mice lacking cytochrome P450 2J5. *FASEB J* **22**, 4096-4108.

Baldwin, W. S., Marko, P. B., and Nelson, D. R. (2009). The Cytochrome P450 (CYP) gene superfamily in *Daphnia pulex*. . *BMC Genomics* **10**, 169.

Banks, W. J. (1993). *Applied Veterinary Histology*. C V Mosby, 3rd edition, St. Louis.

Beilke, L. D., Aleksunes, L. M., Holland, R. D., Besselsen, D. G., Beger, R. D., Klaassen, C. D., and Cherrington, N. J. (2009). Constitutive androstane receptor-mediated changes in bile acid composition contributes to hepatoprotection from lithocholic acid-induced liver injury in mice. *Drug Metab Dispos* **37**, 1035-1045.

Blesch, A. (2004). Lentiviral and MLV based retroviral vectors for ex vivo and *in vivo* gene transfer. *Methods* **33**, 164-172.

Burns, J. C., Friedmann, T., Driever, W., Burrascano, M., and Yee, J. K. (1993). Vesicular stomatitis virus G glycoprotein pseudotyped retroviral vectors: concentration to very high titer and efficient gene transfer into mammalian and nonmammalian cells. *Proc Natl Acad Sci USA* **90**, 8033-8037.

Ekins, S., Vandenbranden, M., Ring, B. J., Gillespie, J. S., Yang, T. J., Gelboin, H. V., and Wrighton, S. A. (1998). Further characterization of the expression in liver and catalytic activity of CYP2B6 *J Pharmacol Exp Ther* **286**, 1253-1259.

Elbashir, S. M., Lendeckel, W., and Tuschl, T. (2001). RNA interference is mediated by 21- and 22-nucleotide RNAs. . *Genes Develop* **15**, 188-200.

Finger, J. H., Smith, C. M., Hayamizu, T. F., McCright, I. J., Eppig, J. T., Kadin, J. A., Richardson, J. E., and Ringwald, M. (2011). The mouse Gene Expression Database (GXD): 2011 update. *Nucleic Acids Res* **39(suppl 1)**, D835-D841.

Finn, R. D., Henderson, C. J., Scott, C. L., and Wolf, C. R. (2009). Unsaturated fatty acid regulation of cytochrome P450 expression via a CAR-dependent pathway. *Biochem J* **417**, 43-54.

Foxenberg, R. J., Knaak, J. B., McGarrigle, B. P., and Olson, J. R. (2008). CYP-specific PBPK-PD models for assess human risk to organophosphorous pesticides. In Society of Toxicology meeting. The Toxicologist Abstract #267, Seattle, WA.

Foxenberg, R. J., McGarrigle, B. P., Knaak, J. B., Kostyniak, P. J., and Olson, J. R. (2007). Human hepatic cytochrome p450-specific metabolism of parathion and chlorpyrifos. *Drug Metab Dispos* **35**, 189-193.

Hashita, T., Sakuma, T., Akada, M., Nakajima, A., Yamahara, H., Ito, S., Takesako, H., and Nemoto, N. (2008). Forkhead box A2-mediated regulation of female-predominant expression of the mouse Cyp2b9 gene. *Drug Metab Dispos* **36**, 1080-1087.

Hayhurst, G. P., Lee, Y. H., Lambert, G., Ward, J. M., and Gonzalez, F. J. (2001). Hepatocyte nuclear factor 4alpha (nuclear receptor 2A1) is essential for maintenance of hepatic gene expression and lipid homeostasis. *Mol Cell Biol* **21**, 1393-1403.

Henderson, C. J., Otto, D. M., Carrie, D., Magnuson, M. A., McLaren, A. W., Rosewell, I., and Wolf, C. R. (2003). Inactivation of the hepatic cytochrome P450 system by conditional deletion of hepatic cytochrome P450 reductase. *J Biol Chem* **278**, 13480-13486.

Hernandez, J. P., Chapman, L. M., Kretschmer, X. C., and Baldwin, W. S. (2006). Gender Specific Induction of Cytochrome P450s in Nonylphenol-Treated FVB/NJ Mice. *Toxicol Appl Pharmacol* **216**, 186-196.

Hernandez, J. P., Huang, W., Chapman, L. M., Chua, S., Moore, D. D., and Baldwin, W. S. (2007). The environmental estrogen, nonylphenol, activates the constitutive androstane receptor (CAR). *Toxicol Sci* **98**, 416-426.

Hernandez, J. P., Mota, L. C., and Baldwin, W. S. (2009a). Activation of CAR and PXR by dietary, environmental and occupational chemicals alters drug metabolism, intermediary metabolism, and cell proliferation. *Curr Pharmacog Personal Med* **7**, 81-105.

Hernandez, J. P., Mota, L. C., Huang, W., Moore, D. D., and Baldwin, W. S. (2009b). Sexually dimorphic regulation and induction of P450s by the constitutive androstane receptor (CAR). *Toxicology* **256**, 53-64.

Hodgson, E., and Rose, R. L. (2007). The importance of cytochrome P450 2B6 in the human metabolism of environmental chemicals. *Pharmacol Ther* **113**, 420-428.

Holen, T., Amarzguioui, M., Wiiger, M. T., Babaie, E., and Prydz, H. (2002). Positional effects of short interfering RNAs targeting the human coagulation trigger tissue factor. *Nucleic Acids Res* **30**, 1757-1766.

Holmes, K., Williams, C. M., Chapman, E. A., and Cross, M. J. (2010). Detection of siRNA induced mRNA silencing by RT-Q-PCR: considerations for experimental design. *BMC Res Notes* **3**, 53.

Honkakoski, P., Zelko, I., Sueyoshi, T., and Negishi, M. (1998). The nuclear orphan-receptor CAR-retinoid X receptor heterodimer activates the phenobarbital-responsive module of the CYP2B gene. *Mol Cell Biol* **18**, 5652-5658.

Kim, D. O., Lee, S. K., Jeon, T. W., Jin, C. H., Hyun, S. H., Kim, E. J., Moon, G. I., Kim, J. A., Lee, E. S., Lee, B. M., Jeong, H. G., and Jeong, T. C. (2005). Role of metabolism in parathion-induced hepatotoxicity and immunotoxicity. *J Toxicol Environ Health A* **68**, 2187-2205.

Kretschmer, X. C., and Baldwin, W. S. (2005). CAR and PXR: Xenosensors of Endocrine Disrupters? *Chem-Biol. Interac* **155**, 111-128.

Lamba, V., Lamba, J., Yasuda, K., Strom, S., Davila, J., Hancock, M. L., Fackenthal, J. D., Rogan, P. K., Ring, B., Wrighton, S. A., and Schuetz, E. G. (2003). Hepatic CYP2B6 expression: gender and ethnic differences and relationship to CYP2B6 genotype and CAR (Constitutive androstane receptor) expression. *J Pharmacol Exp Ther* **307**, 906-922.

Lang, T., Klein, K., Richter, T., Zibat, A., Kerb, R., Eichelbaum, M., Schwab, M., and Zanger, U. M. (2004). Multiple novel nonsynonymous CYP2B6 gene polymorphisms in caucasians: demonstration of phenotypic null alleles. *J Pharmacol Exp Ther* **S11**, 34-43.

Lee, S. S. T., Buters, J. T. M., Pineau, T., Fernandez-Salguero, P., and Gonzalez, F. J. (1996). Role of CYP2E1 in the hepatotoxicity of acetominophen. *J Biol Chem* **271**, 12063-12067.

Mateeva, O., Nechipurenko, Y., Rossil, L., Moore, B., Saetrom, P., Aleksey, Y., Ogurtsov, Y., Atkins, J. F., and Shabalina, S. A. (2007). Comparison of approaches for rational siRNA design leading to a new efficient and transparent method. *Nucleic Acids Res* **35**, e63.

Mota, L. C., Hernandez, J. P., and Baldwin, W. S. (2010). CAR-null mice are sensitive to the toxic effects of parathion: Association with reduced CYP-mediated parathion metabolism. *Drug Metab Dispos* **38**, 1582-1588.

Muerhoff, A. S., Griffin, K. J., and Johnson, E. F. (1994). The peroxisome proliferator-activated receptor mediates the induction of CYP4A6, a cytochrome P450 fatty acid omega-hydroxylase, by clofibric acid. *J Biol Chem* **267**, 19051-19053.

Muller, P. Y., Janovjak, H., Miserez, A. R., and Dobbie, Z. (2002). Processing of gene expression data generated by quantitative real-time RT-PCR. *Biotechniques* **32**, 1372-1379.

Mutch, E., Blain, P. G., and Williams, F. M. (1999). The role of metabolism in determining susceptibility to parathion toxicity in man. *Toxicol Lett* **107**, 177-187.

Mutch, E., and Williams, F. M. (2006). Diazinon, chlorpyrifos and parathion are metabolised by multiple cytochrome P450 in human liver. *Toxicology* **224**, 22-32.

Nelson, D. R., Zeldin, D. C., Hoffman, S. M. G., Maltais, L. J., Wain, H. M., and Nebert, D. W. (2004). Comparison of cytochrome P450 (CYP) genes from the mouse and human genomes, including nomenclature recommendations for genes, pseudogenes and alternative splice variants. . *Pharmacogenetics* **14**, 1-18.

Percy, D. H., and Barthold, S. W. (2001). *Pathology of Laboratory Rodents and Rabbits*. Iowa State University Press, Ames, IA.

Ramezani, A., and Hawley, R. G. (2002). Generation of HIV-1-based lentiviral vector particles *Curr Protoc Mol Biol* **16.22**, 1-15.

Reschly, E. J., and Krasowski, M. D. (2006). Evolution and function of the NR1I nuclear hormone receptor subfamily (VDR, PXR, and CAR) with respect to metabolism of xenobiotics and endogenous compounds. *Curr Drug Metab* **7**, 349-365.

Sastry, L., Johnson, T., Hobson, M. J., Smucker, B., and Cornetta, K. (2002). Titering lentiviral vectors: comparison of DNA, RNA and marker expression methods. *Gene Ther* **9**, 1155-1162.

Sultatos, L. G., Minor, L. D., and Murphy, S. D. (1985). Metabolic activation of phosphorothioate pesticides: role of the liver. *J Pharmacol Exp Ther* **232**, 624-628.

Sultatos, L. G., Shao, M., and Murphy, S. D. (1984). The role of hepatic biotransformation in mediating the acute toxicity of the phosphorothionate insecticide chlorpyrifos. *Toxicol Appl Pharmacol* **73**, 60-68.

Tang, J., Cao, Y., Rose, R. L., Brimfield, A. A., Dai, D., Goldstein, J. A., and Hodgson, E. (2001). Metabolism of chlorpyrifos by human cytochrome P450 isoforms and human, mouse and rat liver microsomes. *Drug Metab Dispos* **29**, 1201-1204.

Tzameli, I., Pissios, P., Schuetz, E. G., and Moore, D. D. (2000). The xenobiotic compound 1,4-bis[2-(3,5-dichloropyridyloxy)]benzene is an agonist ligand for the nuclear receptor CAR. *Mol Cell Biol* **20**, 2951-2958.

Uppal, H., Toma, D., Saini, S. P., Ren, S., Jones, T. J., and Xie, W. (2005). Combined loss of orphan receptors PXR and CAR heightens sensitivity to toxic bile acids in mice. *Hepatology* **41**, 168-176.

Van der Hoeven, T. A., and Coon, M. J. (1974). Preparation and properties of partially purified cytochrome P450 and NADPH-cytochrome P450 reductase from rabbit liver microsomes. *J Biol Chem* **249**, 6302-6310.

van Herwaarden, A. E., Wagenaar, E., van der Kruijssen, C. M. M., van Waterschoot, R. A. B., Smit, J. W., Song, J.-Y., van der Valk, M. A., van Tellingen, O., van der Hoorn, J. W. A., Rosing, H., Beijnen, J. H., and Schinkel, A. H. (2007). Knockout of cytochrome P450 3A yields new mouse models for understanding xenobiotic metabolism. *J Clin Invest* **117**.

Wang, H., Faucette, S., Sueyoshi, T., Moore, R., Ferguson, S., Negishi, M., and LeCluyse, E. L. (2003). A novel distal enhancer module regulated by pregnane X receptor/constitutive androstane receptor is essential for the maximal induction of CYP2B6 gene expression. *J Biol Chem* **278**, 14146-14152.

Wang, H., and Tompkins, L. M. (2008). CYP2B6: New insights into a historically overlooked cytochrome P450 isozyme. *Curr Drug Metab* **9**, 598-610.

Waxman, D. J. (1988). Interactions of hepatic cytochromes P-450 with steroid hormones: Regioselectivity and stereoselectivity of steroid metabolism and hormonal regulation of rat P-450 enzyme expression. *Biochem Pharmcol* **37**, 71-84.

Waxman, D. J., Pampori, N. A., Ram, P. A., Agrawal, A. K., and Shapiro, B. H. (1991). Interpulse interval in circulating growth hormone patterns regulates sexually dimorphic expression of hepatic cytochrome P450. *Proc Natl Acad Sci U S A* **88**, 6868-6872.

Webber, E. M., Wu, J. C., Wang, L., Merlino, G., and Fausto, N. (1994). Overexpression of transforming growth factor-alpha causes liver enlargement and increased hepatocyte proliferation in transgenic mice. . *Am J Pathol* **145**, 398-408.

Wei, P., Zhang, J., Egan-Hafley, M., Liang, S., and Moore, D. D. (2000). The nuclear receptor CAR mediates specific xenobiotic induction of drug metabolism. *Nature* **407**, 920-923.

Willingham, A. T., and Keil, T. (2004). A tissue specific cytochrome P450 required for the structure and function of *Drosophila* sensory organs. *Mech Dev* **121**, 1289-1297.

Wiwi, C. A., Gupte, M., and Waxman, D. J. (2004). Sexually dimorphic P450 gene expression in liver-specific hepatocyte nuclear factor 4α-deficient mice. *Mol Endocrinol* **18**, 1975-1987.

Yamada, H., Ishii, Y., Yamamoto, M., and Oguri, K. (2006). Induction of the hepatic cytochrome P450 2B subfamily by xenobiotics: Research history, evolutionary aspect, relation to tumorigenesis, and mechanism. *Curr Drug Metab* **7**, 397-409.

Zhang, J., Huang, W., Chua, S. S., Wei, P., and Moore, D. D. (2002). Modulation of acetaminophen-induced hepatotoxicity by the xenobiotic receptor CAR. *Science* **298**, 422-424.

Table 2.1: Relative Cyp2b expression in primary hepatocytes transduced with Cyp2b-KD2 and KD3 shRNA compared to hepatocytes transduced with a scrambled construct.

CYP	Scrambled	KD2 (5 MOI)	KD2 (20 MOI)	KD3 (20 MOI)
Cyp2b9	1.0	0.11*	0.02*	1.41
Cyp2b10	1.0	0.27*	0.30*	0.36*

[a]MOI = Multiplicity of Infection

Table 2.2: Zox induced paralysis in Cyp2b-KD mice compared to wild-type mice (WT).

Mouse strain	Male[a]	Female[a]
WT	1/7	0/5
Cyp2b-KD	1/7	15/15*

[a] Data are shown as number of mice showing paralysis /number of mice treated with 400 mg/kg Zox.

An asterisk indicates a significant difference in the percentage of female mice paralyzed by Zox when compared to the corresponding WT mice using Mann-Whitney rank sum test (GraphPad PRISM 4.0).

Figure Legends:

Fig. 2.1: Short hairpin RNA (shRNA) constructs. (A) Simple linear map of the pRNAT U-6.2/lenti vector and the insertion of Cyp2b shRNA constructs. (B) Sequence of full length constructs including sense, loop, and anti-sense Cyp2b shRNA constructs. Underlined areas of the construct are the sense and anti-sense strands that recognize and target CYP mRNA for destruction. Each of the Cyp2b-KD constructs recognizes all five isoforms (genes) of the mouse Cyp2b subfamily (Cyp2b9, Cyp2b10, Cyp2b13, Cyp2b19, Cyp2b23). The scrambled shRNA was used for *in vitro* research and contains the same ATCG percentages as Cyp2b-KD3.

Fig. 2.2: siRNA target areas for mouse Cyp2b genes. There are five areas of the mouse Cyp2b subfamily that are sufficiently conserved so that all of the Cyp2b's could potentially be knocked down by the same siRNA. siRNA Scales estimates a greater than 70% knockdown (shown in parentheses[a]) of Cyp2b expression using three of these siRNAs (shown in gray). shRNA constructs were made to KD2 and KD3 and inserted into the pRNAT-U6.2/lenti vector. NCBI accession numbers are provided next to the name of each Cyp2b gene. Numbers on the right indicate sequence length near the area of homology.

Fig. 2.3: PCR and GFP results for transgenic mice. (A) Gel electrophoresis analysis of mouse genotype using primers that recognize the U6 promoter and an area downstream of the shRNA construct and produce a 956 bp product as described in the Materials and Methods. Mouse 1, 2, and 4 are postive and mouse 3 is negative. Mouse 1: F0-68; 2:F0-38; 3:F1-111; 4:F1-1. (B) Seven-day old pup (F0-68) demonstrating expression of GFP, and (C) GFP expression in this mouse is weakly visible in the eyes, ears, and toes as an adult.

Fig. 2.4: Hepatic Cyp2b expression in WT (FVB) and Cyp2b-KD mice as demonstrated by Q-PCR (A) and Western blots (B). Data is expressed as mean $\pm$ SEM (n = 5-8). Statistical significance was determined by Student's *t test* using the GraphPad Prizm 4.0 software package. An asterisk indicates significant difference with a $p < 0.05$, two asterisks indicate a $p < 0.01$, and three asterisks indicate a $p < 0.001$. WT = wild-type, KD= Cyp2b-KD mice, M= male, F= female. Expression was not quantified in the Western blots because of the low expression of Cyp2b's in the male mice and Cyp2b-KD female mice.

Fig. 2.5: Hepatic Cyp2b expression in WT (FVB) and Cyp2b-KD mice treated with the Cyp2b10 inducer, TCPOBOP. (A) RNA expression of Cyp2b9, Cyp2b10, and Cyp2b13 as measured by Q-PCR (n = 5-8). (B) Protein expression of hepatic Cyp2b subfamily members (n = 3-4). Data is expressed as mean $\pm$ SEM. Statistical significance was determined by Student's *t test* using the GraphPad Prizm 4.0 software package. An asterisk indicates a $p < 0.05$, and two asterisks indicate a $p < 0.01$. WT = wild type, KD= Cyp2b-KD mice, M= male, F= female.

Fig. 2.6: Hepatic expression of CAR in WT and Cyp2b-KD mice treated with TCPOBOP or corn oil (carrier) as measured by Q-PCR (A) or Western blots (B, C). (A) WT mice are shown in white bars and Cyp2b-KD mice are shown in black bars. Statistical significance was determined by ANOVA followed by Tukeys post-hoc test with the GraphPad Prizm 4.0 software package. Western blots in corn oil (B) or TCPOBOP-treated mice (C). Statistical significance of the Western blots was determined by Student's t-test. An asterisk indicates significant difference with a $p < 0.05$.

Fig. 2.7: Histopathology scores of FVB (WT) and Cyp2b-KD (KD) treated with corn oil or TCPOBOP (TC). Histopathology was measured as described in the Materials and Methods using a total histopathology score from several different measures. An asterisk indicates a statistical difference ($p < 0.01$) as determined by Kruskal-Wallis followed by Dunn's multiple comparison test (n = 3).

Fig. 2.8: Microsomal metabolism of parathion. Microsomes from TC-treated WT and Cyp2b-KD mice were exposed to parathion. Quantification of formation of parathion's relatively non-toxic metabolite, p-nitrophenol (PNP) (A), and its toxic metabolite paraoxon (POXON) (B) was measured by HPLC as described in the Materials and Methods. A white bar indicates FVB mice and a black bar indicates Cyp2b-KD mice. Significant differences in the formation of the metabolites between WT and Cyp2b-KD mice were assessed by ANOVA followed by Tukey's multiple comparison test using the GraphPad Prizm 4.0 software package. The letter [a] indicates a significant difference between WT and Cyp2b-KD males ($p < 0.01$), and the letter [b] indicates a significant difference between WT and Cyp2b-KD females ($p < 0.01$).

Fig. 2.9: Increased toxicity of parathion in Cyp2b-KD mice compared to WT mice. (A) WT male mice treated with parathion. (B) Cyp2b-KD male mice treated with parathion, (C) WT female mice treated with parathion. (D) Cyp2b-KD female mice treated with parathion. (E) Overall, differential toxicity to parathion in Cyp2b-KD mice compared to WT mice. A significant increase in toxicity to parathion was observed in Cyp2b-KD mice as determined by the Kruskal–Wallis non-parametric test for independent variables followed by Dunns post hoc test using the GraphPad Prizm 4.0 software package. Severity of toxicity: 0 = not toxic; 1 = eye leakage; 2 = lethargy/tremors; 3 = morbidity; 4 = death ($p < 0.05$). WT= wild type, KD= Cyp2b-KD mice, M=male, F= female.

Figure 2.1

B

shRNA	CONSTRUCT[1]
Scrambled	GGATCCCGACGATTCGAGGCGCAGTGATTTGATATCCGATCACTGCGCCTCGAATCGTCTTTTTTCCAACTCGAG
Cyp2b-KD2	GGATCCCAAGAACACTGAGGTGTACCCCTTGATATCCGGGGGTACACCTCAGTGTTCTTTTTTTTCCAACTCGAG
Cyp2b-KD3	GGATCCCGCAAGACAAATGCGCTTTCCTGTTGATATCCGCAGGAAAGCGCATTTGTCTTGTTTTTTCCAACTCGAG

Figure 2.2

```
Cyp2b member          Cyp2b sequence and homology
KD1 (71%)[a]
Cyp2b9   NM_010000.2    TCCAAAAGGAGATTGATCAGGTGATCGGCTCACACCGGCTACCAACTCTT 1045
Cyp2b13  NM_007813.1    TCCAAAAGGAGATTGATCAGGTGATCGGCTCACACCGGCTACCAACCCTT 1045
Cyp2b23  NM_001081148   TCCAAAAGGAGATTGATCAGGTGATCAGTGCACACCATGTCCCAACCCTT 1020
Cyp2b10  AK028103.1     TCCAAAAGGAGATTGATCAGGTGATCGGCTCACACCGGCTACCAACCCTT 1047
Cyp2b19  AF047529.1     TCCAAAAGGAGATTGATCAGGTGATCGGCTCACACCGGCTACCGACTCTT 1023
                        *************************** *  ******   * ** ** ***
KD2 (83%)[a]
Cyp2b9   NM_010000.2    ACACACTGTTCCGAGGGTACCTGCTCCCCAAGAACACTGAGGTGTACCCC 1195
Cyp2b13  NM_007813.1    ATACCATGTTCCGAGGGTACCTGCTCCCCAAGAACACTGAGGTGTACCCC 1195
Cyp2b23  NM_001081148   ACACAGTGTTCCGAGGATACCTGCTCCCCAAGAACACTGAGGTGTACCCC 1170
Cyp2b10  AK028103.1     ATACCATGTTCCGAGGGTACCTGCTCCCCAAGAACACTGAGGTGTACCCC 1197
Cyp2b19  AF047529.1     ACACACTGTTCCGAGGATACCTGATCCCCAAGAACACTGAGGTGTACCCC 1173
                        * **  ********** ****** **************************
KD3 (73%)[a]
Cyp2b9   NM_010000.2    AAGCTTTTCTGCCCTTCTCCACAGGAAAGCGCATTTGTCTTGGTGAAAGC 1345
Cyp2b13  NM_007813.1    AAGCTTTTCTACCCTTCTCCACAGGAAAGCGCATTTGTCTTGGTGAAAGC 1345
Cyp2b23  NM_001081148   AAGCTTTTCTGCCCTTCTCCACAGGAAAGCGCATTTGTCTTGGCGAAGGC 1320
Cyp2b10  AK028103.1     AAGCTTTTCTGCCCTTCTCAACAGGAAAGCGCATTTGTCTTGGTGAAAGC 1347
Cyp2b19  AF047529.1     AAGCTTTCATGCCCTTCTCCACAGGAAAGCGCATTTGTCTTGGAGAAGGC 1323
                        ******* * ******** ********************** *** **
```

Figure 2.3

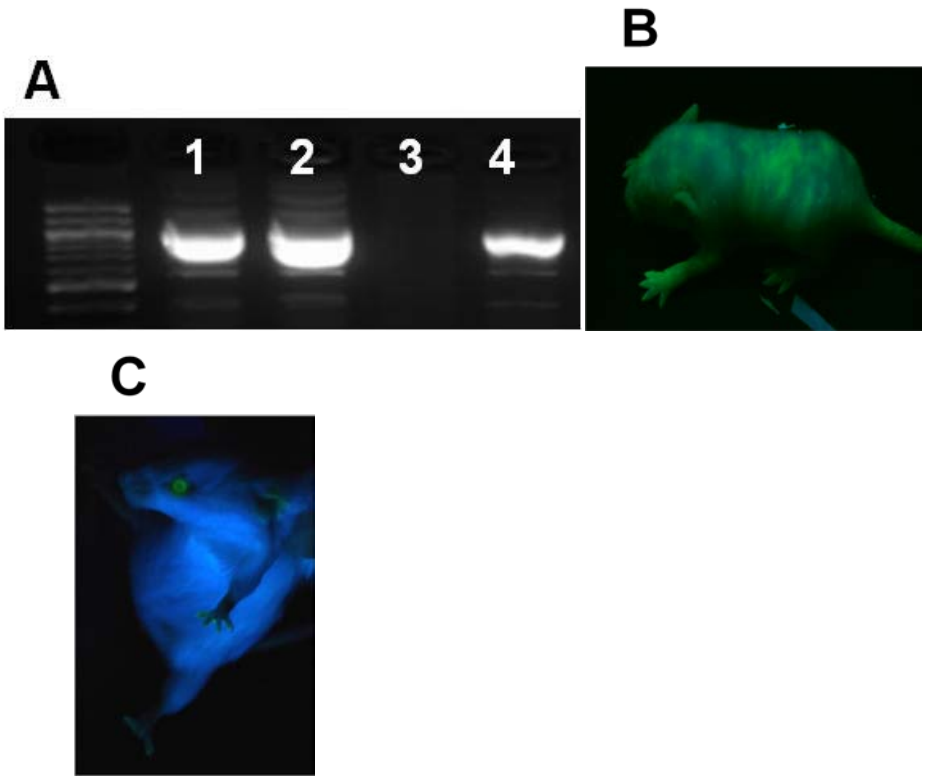

Fig. 2.4

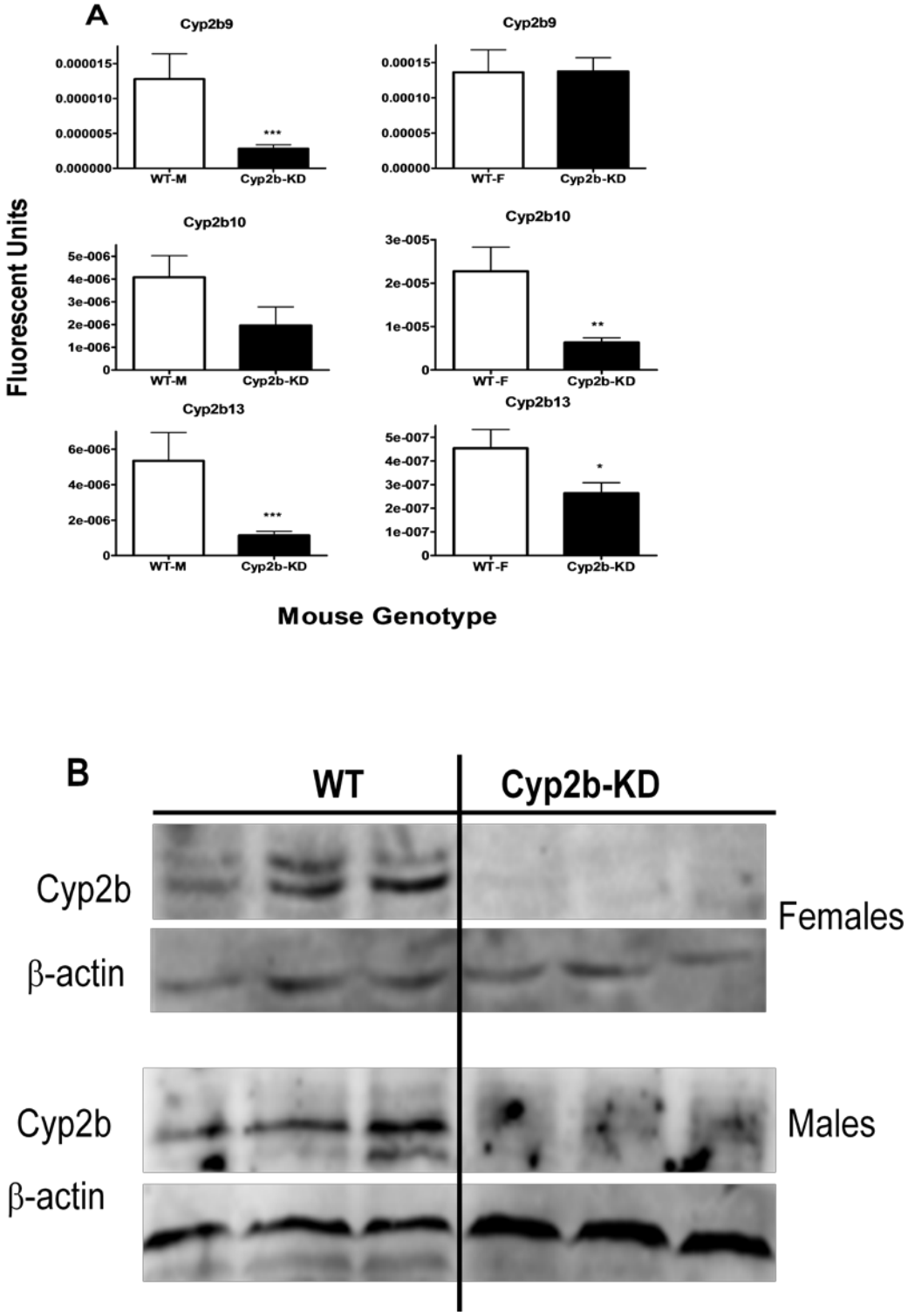
A
Cyp2b9
0.000015
0.000010
0.000005
0.000000
***
WT-M
Cyp2b-KD
Cyp2b9
0.00015
0.00010
0.00005
0.00000
WT-F
Cyp2b-KD
Cyp2b10
5e-006
4e-006
3e-006
2e-006
1e-006
0
WT-M
Cyp2b-KD
Cyp2b10
3e-005
2e-005
1e-005
0
**
WT-F
Cyp2b-KD
Cyp2b13
6e-006
4e-006
2e-006
0
***
WT-M
Cyp2b-KD
Cyp2b13
5e-007
4e-007
3e-007
2e-007
1e-007
0
*
WT-F
Cyp2b-KD
Fluorescent Units
Mouse Genotype
B
WT
Cyp2b-KD
Cyp2b
β-actin
Females
Cyp2b
β-actin
Males

Figure 2.5

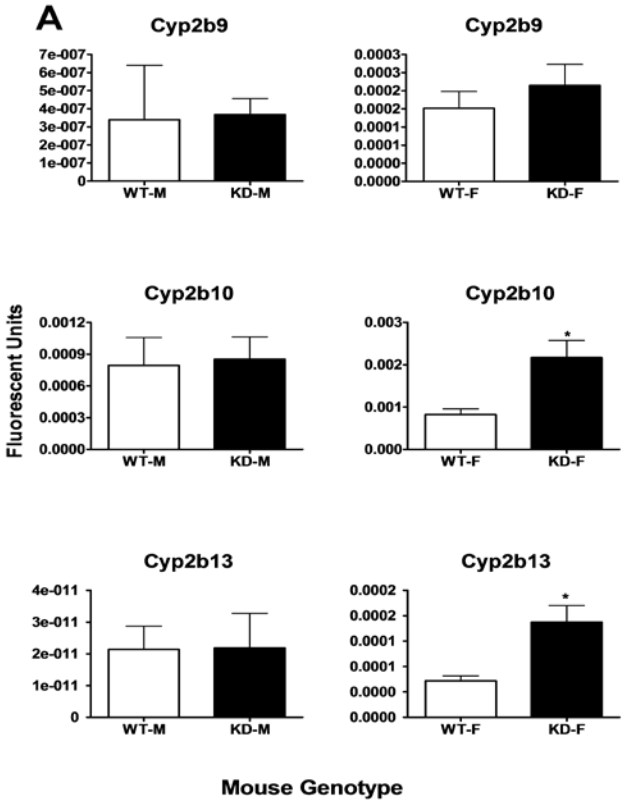
A
Cyp2b9
7e-007
6e-007
5e-007
4e-007
3e-007
2e-007
1e-007
0
WT-M
KD-M
Cyp2b9
0.0003
0.0003
0.0002
0.0002
0.0001
0.0001
0.0000
0.0000
WT-F
KD-F
Cyp2b10
Fluorescent Units
0.0012
0.0009
0.0006
0.0003
0.0000
WT-M
KD-M
Cyp2b10
0.003
0.002
0.001
0.000
*
WT-F
KD-F
Cyp2b13
4e-011
3e-011
2e-011
1e-011
0
WT-M
KD-M
Cyp2b13
0.0002
0.0002
0.0001
0.0001
0.0000
0.0000
*
WT-F
KD-F
Mouse Genotype

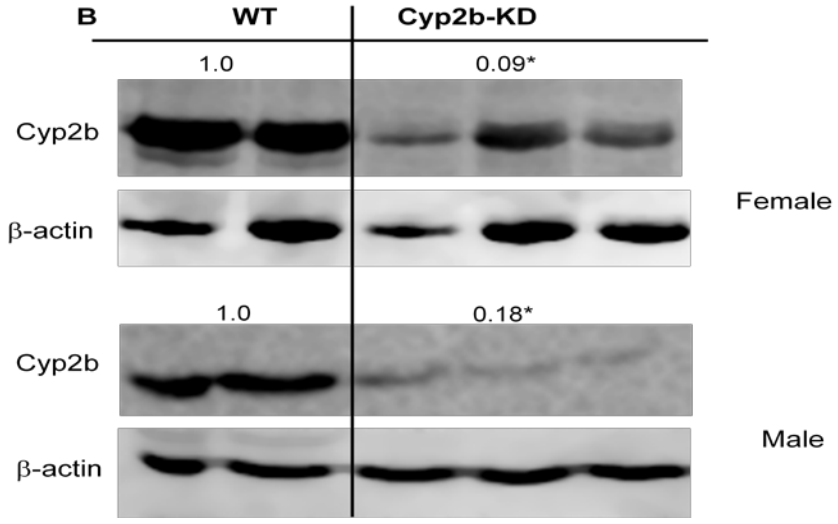
B
WT
Cyp2b-KD
1.0
0.09*
Cyp2b
β-actin
Female
1.0
0.18*
Cyp2b
β-actin
Male

Figure 2.6

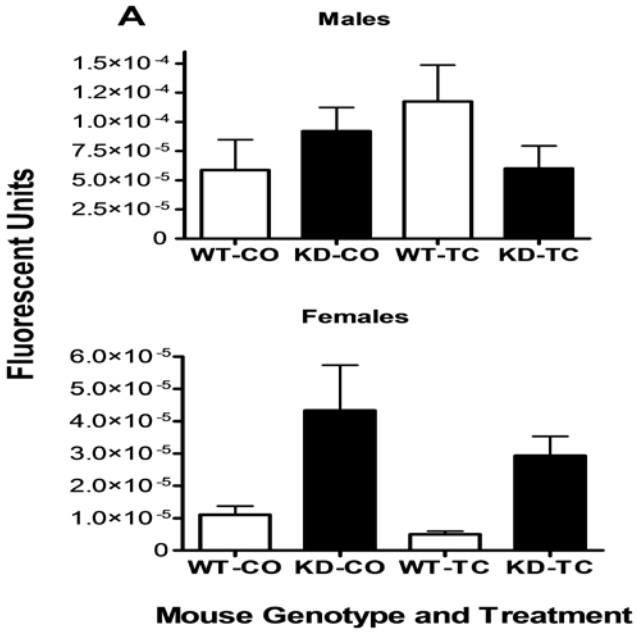
A
Males
1.5×10⁻⁴
1.2×10⁻⁴
1.0×10⁻⁴
7.5×10⁻⁵
5.0×10⁻⁵
2.5×10⁻⁵
0
WT-CO KD-CO WT-TC KD-TC
Females
6.0×10⁻⁵
5.0×10⁻⁵
4.0×10⁻⁵
3.0×10⁻⁵
2.0×10⁻⁵
1.0×10⁻⁵
0
WT-CO KD-CO WT-TC KD-TC
Fluorescent Units
Mouse Genotype and Treatment

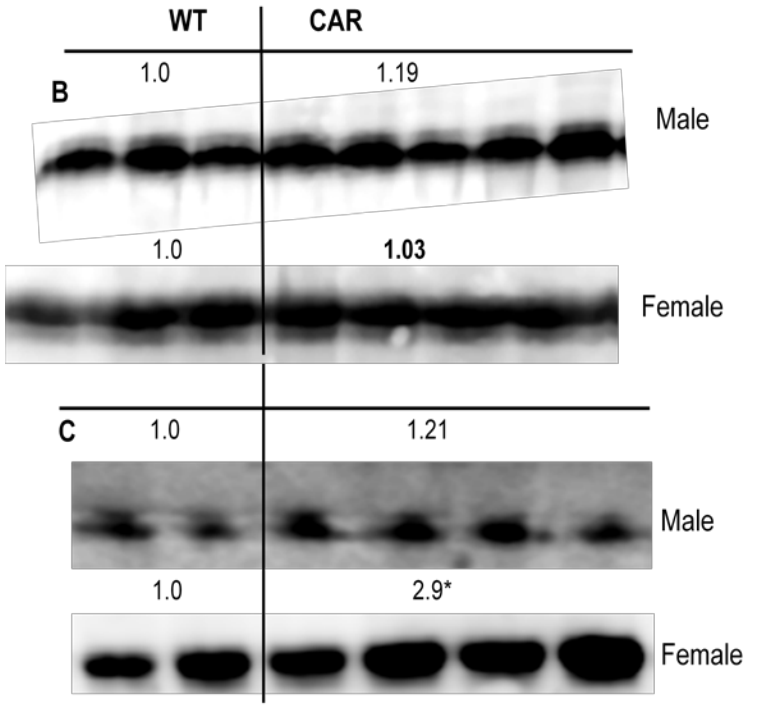
WT
CAR
B
1.0
1.19
Male
1.0
1.03
Female
C
1.0
1.21
Male
1.0
2.9*
Female

9

Figure 2.7

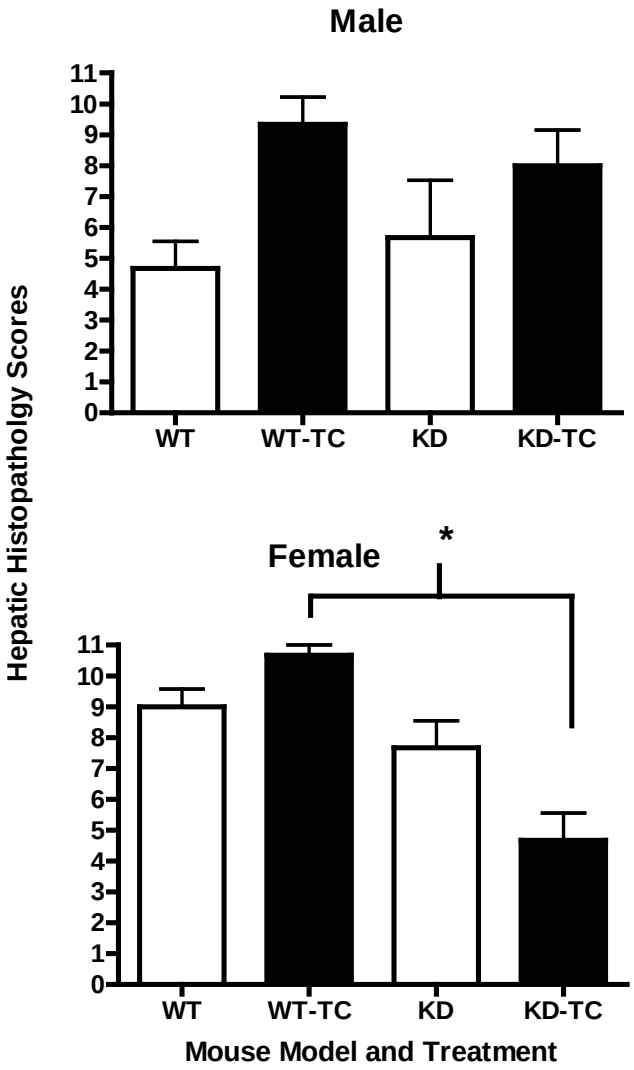

P value < 0.05

Figure 2.8

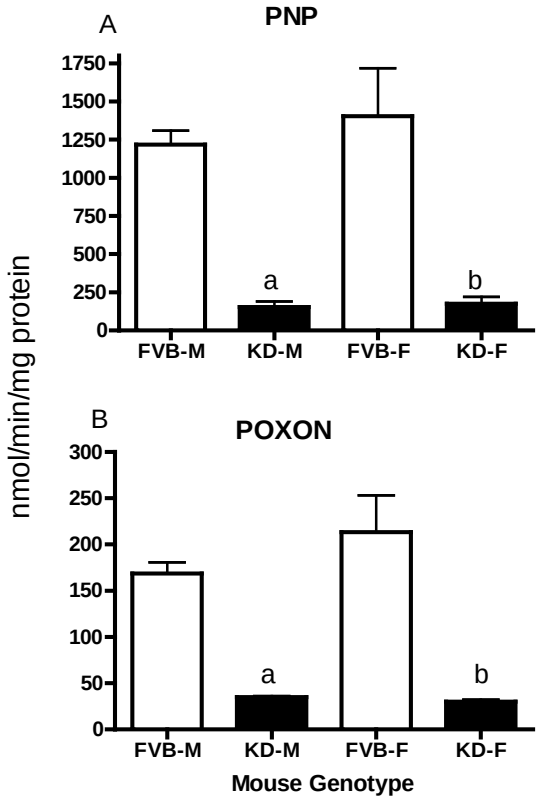

P value <0.01

Figure 2.9

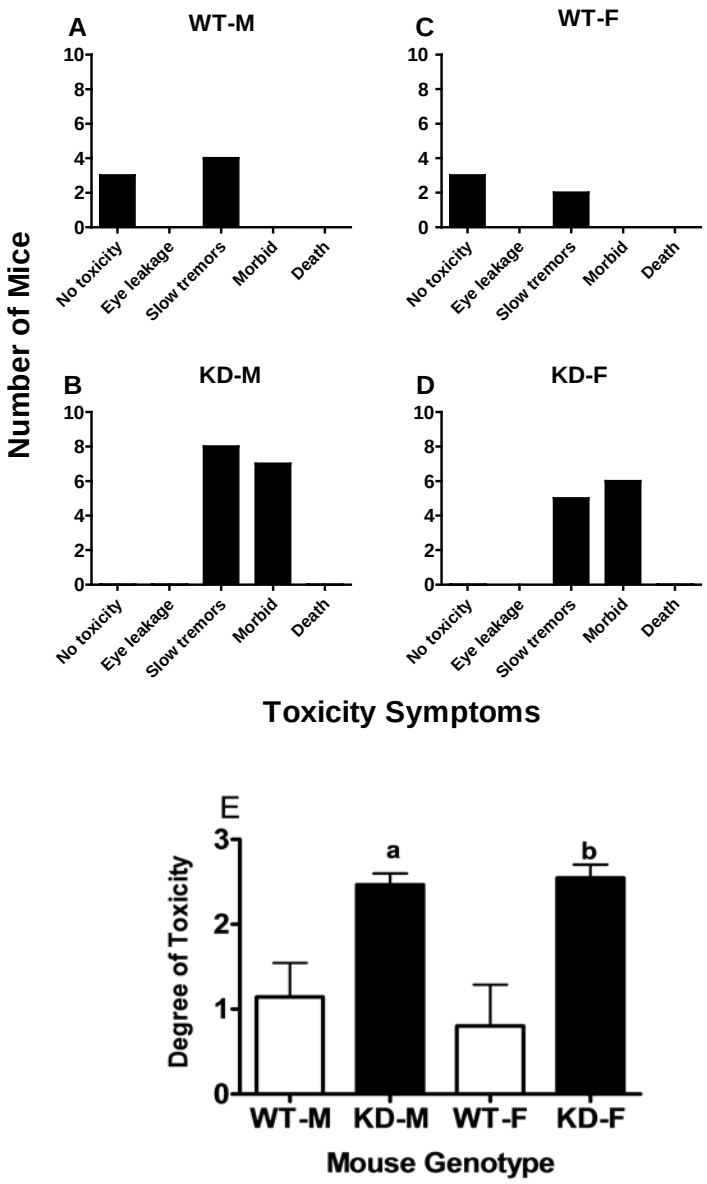

P value < 0.05

Additional Files:

2.3 Supplementary Table 1: PCR primer and probe sequences used for genotyping and Q-PCR.

2.10 Additional File 1: Homology of shRNA constructs designed to knockdown Cyp2b genes to other Cyp2 family genes. (A) The construct is shown in red as part of the Cyp2b10 gene. Homologous regions within the other Cyp genes are below and also in region. The number of identical nucleotides over the total number of nucleotides is provided in (B).

2.11 Additional File 2: Decreased histopathology scores were observed in Cyp2b-KD mice treated with TC compared to mice only receiving the vehicle, corn oil.

2.3 Supplementary Table 1: PCR primer and probe sequences used for genotyping and Q-PCR

Gene	**Forward primer**	**Reverse primer**	**Tm oC**	**AS (bp)**
Cyp2b9	CTGAGACCACAAGCGCCAC	CTTGACCATGAGCAGGACTCC	64.3	71
Cyp2b10	CTGAATCCGCTCCTCCACACTC	TGAGCCAACCTTCAAGGAATAT	61.4	120
Cyp2b13	GAACTGAGACTACCAGCACCACTCCT	TGAGCATGAGCAGGAAACCACT	61.5	72
18s rRNA	ATGGCCGTTCTTAGTTGGTG	ATGCCAGAGTCTCGTTCGTT	61.7	68
18s rRNA	CGCCGCTAGAGGTGAAATTC	CCAGTCGGCATCGTTTATGG	51.0	150
CAR	GGAGCGGCTGTGGAAATATTGCAT	TCCATCTTGTAGCAAAGAGGCCCA	56.5	94
U.6/Lenti	TTATCGTTTCAGACCCACCTCCCAA	TCCCATAAGGTCATGTACTGGGCA	57.0	956
Cyp2b-KD2	GAGGGCCTATTTCCCATGAT	AGGCACAGTCGAGGCTGAT	52.3	359
B-actin	GCTATGTTGCTCTAGACTTCG	CCTCATGGTGCTAGGAGC	52.0	ABS
Cyp2b10	GACTTTGGGATGGGAAAGAG	CCAAACACAATGGAGCAGAT	53.0	136
Cyp2b10 probe	56 FAM/TAGTGGAGGAACTGCGG AAATCCC/3BHQ_1		60.0	

ABS:Human β-actin Part # (4326315E)Applied Biosystem, Foster City, CA
Tm: Annealing Temperature oC
AS bp: amplicon Size (base pair)

2.10 Additional File 1: Homology of shRNA constructs designed to knockdown Cyp2b genes to other Cyp2 family genes. (A) The construct is shown in red as part of the Cyp2b10 gene. Homologous regions within the other Cyp genes are below and also in region. The number of identical nucleotides over the total number of nucleotides is provided in (B).

(A)

KD2

```
Cyp2b10 AK028103.1|            ATACCATGTTCCGAGGGTACCTGCTCCCCAAGAACACTGAGGTGTACCCC 1197
Cyp2c29 NM_007815.3            ACATTAAATTCAGGAAATACCTCATCCCCAAGGGAACTACAGTA-ATAAC
Cyp2c37 NM_010001.2            ACATTAAATTCAGGAACTACTTCATCCCCAAGGGAACAACTGTA-ATAAC
Cyp2a4  NM_000997.2            ACACCAAGTTTCGAGATTTCCTCCTCCCCAAGGGTACTGAAGTATTTCCT
Cyp3a11 NM_007818.3            ATGTTGAACTCAATGGTGTGTATATCCCCAAAGGGTCAACAGTG-ATGAT
Cyp3a41 NM_017396.3            ATGTTGAACTCAATGGTGTGTATATCCCCAAAGGGTCAACAGTG-ATGAT

KD3
Cyp2b10 AK028103.1|            AAGCTTTTCTGCCCTTCTCAACAGGAAAGCGCATTTGTCTTGGTGAAAGC 1347
Cyp2c29 NM_007815.3            ACTACTTCATGCCTTTTTCAACAGGAAAACGGATTTGTGCTGGAGAGGGC
Cyp2c37 NM_010001.2            ACTACTTCATTCCCTTCTCAACAGGGAAACGGATATGTGCAGGAGAGGGC
Cyp2a4  NM_000997.2            ATGCCTTTGTGCCCTTTTCCATTGGAAAACGGTATTGTTCGGAGAAGGAC
Cyp3a11 NM_007818.3            ATGTATATCTGCCCTTTGGGAATGGACCCAGGAACTGCCTTGGCATGAGG
Cyp3a41 NM_017396.3            ATTTATATATGCCCTTTGGAATTGGACCCAGGAACTGCATTGGCATGAGG
```

(B)

KD2

Cyp2c29	10/21
Cyp2c37	9/21
Cyp2a4	13/21
Cyp3a11	6/21
Cyp3a41	6/21

KD3

Cyp2c29	18/22
Cyp2c37	16/22
Cyp2a4	12/22
Cyp3a11	12/22
Cyp3a41	11/22

2.11 Additional File 2: Decreased histopathology scores were observed in Cyp2b-KD mice treated with TC compared to mice only receiving the vehicle, corn oil.

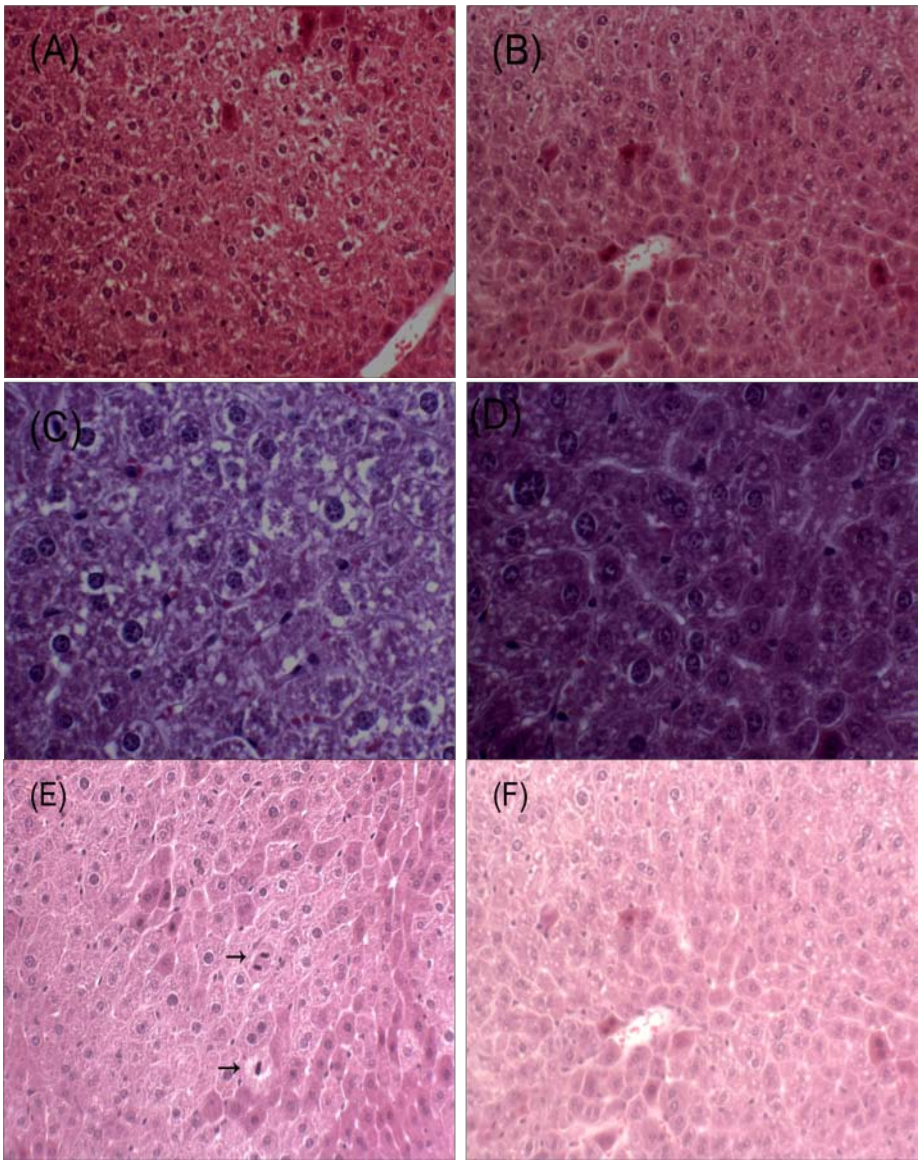

(A) FVB TC -treated female 200X
(B) Cyp2b-Kd TC-treated female 200X
(C) FVB TC -treated female 400X
(D) Cyp2b-Kd TC-treated female 400X
(E) FVB mouse showing Hyperplasia after TC-treatment
(F) Cyp2b-KD mouse showing no hyperplasia after TC-treatment

CHAPTER 3

RNAI REPRESSION OF CYP2B EXPRESSION INCREASES ADIPOSE DEPOSITION AND SERUM LIPIDS

Estimate Publication in American Journal of Physiology Gastrointestinal and Liver Physiology

3.1 Abstract

The Cyp2b subfamily contains five members of which three (Cyp2b9, Cyp2b10, Cyp2b13) are hepatic enzymes involved in xenobiotic detoxification. We made a Cyp2b-knockdown Cyp2b-KD) mouse model using lentiviral-promoted shRNA homologous to all five Cyp2b subfamily members in order to characterize Cyp2b's role in xenobiotic detoxification. Unexpectedly, the 8-12 week old Cyp2b-KD mice showed significant changes in increases in abdominal, inguinal, and renal adipose. Interstingly, associated with changes in fat to body ratios were changes in non-fasting serum triglyceride and VLDL levels with a statistically significant increase in the males. Therefore, wild-type and Cyp2b-knockdown mice were housed for 35 weeks and necropsies performed to test whether these older Cyp2b-KD mice show perturbed lipid utilization. Similar to young Cyp2b-KD mice, 35-week old Cyp2b-KD mice exhibited a significant increase in their body weight caused by a significant increase in fat deposition compared to wild-type (FVB) mice. This was accompanied by increased triglyceride and low density lipoprotein

levels. Subsequent studies were performed with corn oil or the CAR activator and potent Cyp2b-inducer TCPOBOP (TC) dissolved in corn oil as a carrier. Surprisingly, 8-12 week-old Cyp2b-KD mice showed some difficulty acclimating to the corn oil. Significant increases in total serum cholesterol were observed in the corn oil control Cyp2b-KD male and female mice compared to the WT mice, probably because the Cyp2b-KD mice were unable to respond to the unsaturated fatty acids in the corn oil. The increases in non-fasting serum total cholesterol and triglyceride was reversed by TC treatment in Cyp2b-KD male mice but not in Cyp2b-KD female mice as TC treatment caused a significant increase in triglyceride in Cyp2b-KD females. In addition, Cyp2b-KD mice appear to have perturbations in clearing corn oil from the liver as corn oil treatment increased Oil Red O staining indicating accumulation of lipids in the livers of Cyp2b-KD mice compared to WT mice. In conclusion, changes in Cyp2b expression led to perturbation in lipid metabolism in Cyp2b-KD mice. This indicates that Cyp2b is more than a detoxification enzyme, but is also involved in the metabolism of unsaturated fatty acids, as Cyp2b-KD mice have increased fat deposition and show increased serum and liver lipid levels.

3.2 Introduction

Five Cyp2b isoforms have been identified in mouse (Cyp2b9, 2b10, 2b13, 2b19, and 2b23) compared to only one in humans (CYP2B6). CYP2B members participate in the metabolism of endogenous and exogenous compounds. Xenobiotic chemicals metabolized by CYP2B isoforms include parathion, efavirenz, chlorpyrifos, phenobarbital, nonylphenol, some PCBs, and DDT (Lee et al., 1998; Foxenberg et al., 2007; Hodgson and Rose., 2007). Evidence suggests that several endogenous chemicals are also metabolized by CYP2B members including steroid hormones, prostaglandins, and fatty acids (Waxman, 1988; Keeney et al., 1998; Ladd et al., 2003; Du et al., 2005). For example, Cyp2b19 is a potent arachidonic acid epoxygenase primarily found in keratinocytes that is important in 14,15- epoxyeicosatrienoic acid formation, a key factor in epithelial cornification (Keeney et al., 1998).

Cyp2b's are widely expressed. For example, they are expressed in the kidney (Jarukamjorn et al., 2001), small intestine (Zhang et al., 2003), brain (Albores et al., 2001; Rosenbrock et al., 2001; Udomsuk et al., 2010), lungs (Forkert et al., 1986), heart (Isensee et al., 2007), testes, skeletal muscle (Finger et al., 2011); skin (Keeney et al., 1998; Due et al., 2005), adipose (Yoshinari et al., 2004), and prostate (Kumagai et al., 2007). To our knowledge, no studies have established that Cyp2b23 is expressed. However, Cyp2b isoforms are primarily expressed in the liver with Cyp2b9, Cyp2b10, and to a lesser extent Cyp2b13 being the major hepatic CYP2b isoforms (Honkakoski et al., 1998; Wei et al., 2000; Hernandez et al., 2009; Mota et al., 2010).

The hepatic CYPs also show sexual dimorphism as female mice express more cyp2b9 and Cyp2b13 than males (Jarukamjorn et al., 2002; Wiwi et al., 2004; Hernandez et al., 2009; Mota et al., 2010). The sexually dimorphic expression of Cyp2b members is probably regulated by several transcription factors including hepatocyte nuclear factor 4α (HNF-4α), estrogen receptor (ER) and Forkhead box A2 (FoxA2) that regulates Cyp2b9 (Hashita et al., 2008), and the constitutive androstane receptor (CAR) that in part basally regulates Cyp2b9, Cyp2b10, and potentially Cyp2b13 (Hernandez et al., 2009; Mota et al., 2010). Of special interest are CAR (NR1I3) and FoxA2. CAR is a xenobiotic sensor that regulates the induction of Cyp2b10, and several other detoxification genes after exposure to a variety of chemicals, including phenobarbital or 1,4-bis[2-(3,5-dichloropyridyloxy)] benzene (TC) (Honkakoski et al., 1998; Wei et al., 2000; Hernandez et al., 2009). FoxA2, which up-regulates Cyp2b9 (Hashita et al., 2008), has been implicated in sporadic cases of early onset Type II diabetes (Woflrum et al., 2004). FoxA2 is activated by fasting and fatty acids, and inhibited by insulin (Wolfrum et al., 2004). Fatty liver and diabetes activate both of these receptors and increases drug metabolism due in part to increased Cyp2b9 and Cyp2b10 (Wolfrum et al., 2004; Dong et al., 2009).

Recent data indicates that CAR much like FoxA2 is also a metabolic sensor. For example, TC-activation of CAR ameliorated diabetic activity and fatty liver disease in ob/ob mice, and double mutants (ob/ob mice that are also CAR-null) did not respond to

TC-mediated amelioration of diabetes and fatty liver, indicating a role for CAR in inducing β-oxidation (Dong et al., 2009). This provides a link between drug metabolism and energy metabolism. Additionally, the hepatic P450 oxidoreductase-null mouse (hepatic reductase null, POR-null, or HRN), which lacks hepatic CYP activity, shows profound changes in lipid homeostasis and liver size (Finn et al., 2009). This is associated with significantly elevated Cyp2b10, and linked to hepatic triacylglycerol accumulation and increased hepatic unsaturated fatty acids in the HRN mice, indicating a crucial role for CYPs in unsaturated fatty acid metabolism. Furthermore, double HRN/CAR-null mice did not demonstrate Cyp2b10 induction, and linoleic acid, an unsaturated fatty acid, activated CAR in transactivation assays. The authors suggest that increases in Cyp2b10 could be an adaptive response against unsaturated fatty acid toxicity and indicated that this study is the first evidence that P450s, and particularly Cyp2b10, play a major role in controlling unsaturated fatty acid homoeostasis via CAR (Finn et al., 2009).

Recently, we constructed a Cyp2b-knockdown (Cyp2b-KD) mouse model using RNAi technology under the control of a lentiviral promoter, and demonstrated reduced expression of all of the hepatic Cyp2b isoforms. The Cyp2b-KD mice developed normally and were fertile; however, we observed enlarged livers and a putative increase in abdominal fat deposition (Previous Chapter). Therefore, we investigated whether the Cyp2b-KD mouse has increased fat deposition, as well as serum and liver parameters associated with perturbed lipid homeostasis compared to wild-type (WT; FVB) mice. The endogenous role of the Cyp2b subfamily is not known (Yamada.et al, 2006; Reschly et

al., 2006), and this study suggests a role for Cyp2b's in fatty acid metabolism, and therefore they may act as anti-obesity CYPs.

3.3 Materials and Methods

3.3.1 Mice treatment

All studies were carried out according to NIH guidelines for the humane use of research animals and pre-approved by Clemson University's IACUC. Mice were provided water, and fed *ad libitum* prior to and during treatments. Cyp2b-KD mice were constructed as described previously (Previous Chapter), and bred with FVB/NJ (wild-type; WT) mice to maintain the genetic background. Genotyping demonstrated that 86% of the mice were transgenic indicating multiple inserts in the mice and therefore both sibling controls and separate FVB bred lines were used as controls.

In separate experiments, untreated WT and Cyp2b-KD mice at 9 weeks or 35-weeks of age were weighed, blood was collected by heart puncture, and then mice were euthanized. Later WT and Cyp2b-KD mice (9 weeks old), were treated with 3 mg/kg TC or received corn oil as a vehicle control. Treated and corn oil control mice were weighed, blood collected, and then euthanized 24 hours after treatment. During the necropsy, livers were excised and weighed, and then cut into four pieces for sample preparation (RNA, protein, histopathology, and Red Oil O). Abdominal/renal/inguinal fat was collected and weighed in addition to spleen, kidneys, brain, and testes.

3.3.2 Serum Chemistry

Serum was prepared by centrifugation and analyzed at Comparative Pathology Laboratory, Baylor College of Medicine, TX for levels of non-fasting serum; cholesterol, triglyceride, high density lipoporotein (HDL), low density lipoporotein (LDL), very low density lipoprotein (VLDL), albumin, glucose, and phosphorus (n = 4-6).

3.3.3 Sample preparation.

A portion of the liver was placed in formalin for histology investigations and Oil Red O evaluation of liver triglycerides. The rest of the liver was snap frozen, diced, separated into two tubes for RNA or protein sample preparation, and stored at -80^{o}C. Total RNA was extracted with TRI-Reagent® according to the manufacturer's instructions followed by DNAse digestion to remove residual genomic DNA (Promega Corporation, Madison WI). RNA concentrations were determined spectrophotometrically at 260/280 nm (Molecular Devices, Ramsey, MN). Reverse transcription was performed to make cDNA using 200 units Moloney Murine Leukemia Virus–Reverse Transcriptase (MMLV-RT), a 10 mM dNTP mixture, and 0.05 mg random hexamers (Promega Corporation, Madison, WI). Microsomes were prepared by differential centrifugation, and protein concentrations determined with Protein Concentration Reagent (Bio-Rad Laboratories, Hercules, CA).

3.3.4 Quantitative Real-time Polymerase Chain Reaction (Q-PCR).

Quantitative real-time PCR (Q-PCR) was performed as described previously by us and other groups (Muller et al., 2002; Mota et al., 2010), cDNA from liver samples was diluted 1:10 prior to Q-PCR. To generate a standard curve and determine the PCR efficiency of each reaction, a composite sample of cDNA from FVBs and KDs, treated and untreated mice was made and dilutions from 1:1 to $1:10^{-6}$ were prepared. During PCR, samples were denatured at 95°C for 10 s, lowered to the appropriate annealing temperature for 30 s, and extended at 72°C for 20 s. Amplifications of the samples and the standard curve were performed in triplicate using a 96-well MyiQ Real-Time PCR Detection System (Bio-Rad) with 0.25× SybrGreen (SA Biosciences, Frederick, MD) as the fluorescent double strand-intercalating agent to quantify gene expression as described previously using Muller's equation (Muller et al., 2002) to determine relative quantities of each CYP. A minimum of forty cycles was run on all real-time samples to ensure a log based growth curve. 18S was used as he housekeeping gene. The primers and their annealing temperatures are presented in Supplementary Table 1.

3.3.5 Western Blots:

Western blots were performed with 30-50 µg of hepatic microsomal protein as described previously using our rabbit-anti-mouse Cyp2b antibody and a goat anti-rabbit IgG (Bio-Rad) alkaline-phosphatase coupled secondary antibody (Mota et al., 2010). β-actin (Sigma Aldrich, St. Louis, MO) was used as a housekeeper to ensure equal loading of samples. Bands were visualized via chemiluminescent detection (Bio-Rad) and quantified with the Chemi Doc XRS HQ using Quantity One 4.6.5 software (Bio-Rad).

3.3.6 Histopathology and Oil Red O staining

Samples fixed in 10% formalin were processed and stained with hemotoxylin and eosin at Colorado Histo-Prep for blind histopathological evaluation (Fort Collins, CO). Standard toxicology pathology criteria and nomenclature for the mouse were used to categorize microscopic tissue changes (Bank, 1993; Percy and Barthold, 2001; Hernandez et al., 2006; Mota et al., 2010). Individual parameters (hepatocellular swelling, necrosis, hypertrophy, hyperplasia, inflammation, bile duct hyperplasia, mineralization) were scored 0-4 and then summed. Total scores for the hepatic histopathology lesions in each mouse were ranked and statistical significance determined by Kruskal–Wallis followed by Dunn's post hoc test. Tissues samples were also frozen for Oil Red O staining and examination by blind histopathological evaluation by Colorado Histo-Prep (Fort Collins, CO). Results were scored 0-4 for statistical evaluation. Scores of 1 to 4 were recorded based primarily upon the extent of hepatocellular involvement.1 = minimal, 2 = mild, 3 = moderate, 4 = severe

3.4 Results

3.4.1 Fat Deposition in Cyp2b-KD mice

Because we observed what appeared to be a putitive increase in fat in the Cyp2b-KD mice (Chapt 1); at necropsy the body weight of the mice as well as their inguinal, renal, and abdominal fat was combined and measured. In young mice (9 weeks), no significant differences in body weights were observed between KD-mice and their corresponding WT controls. However, the weight of the fat to body weight increased 112% in male and 75.3% in female Cyp2b-KD mice, respectively, compared to the WT controls (Fig. 1).

In contrast to the young mice, a significant increase in body weight of 35-week old Cyp2b-KD female (17.4%) and male (22.3%) mice compared to WT mice was observed (Fig. 1). This was also accompanied by a significant increase in weight in abdominal/inguinal/renal fat (Fig.1) and the fat/body weight ratios of male (73.7%) and female Cyp2b-KD mice (412%). There was a significant increase in weight when comparing young and old mice, however; there was not a significant increase in the weight of fat when comparing the young and old mice. Interestingly, 50% of the aged Cyp2-KD male mice had 3-4 mm of round solid tissue of fat necrosis, but none of the WT mice had fat necrosis.

Liver, kidney, brain, and testis weights were also determined in the young and old mice and these weights were compared to body weight to determine organ to body weight ratio (Supplementary Table 2). Liver weight to body weight ratio (hepatosomatic index) increased 18-26% in the young mice, and increased 26-59% in the older mice. Significant differences in spleen, testes, brain, and kidney weights were also measured between the WT and Cyp2b-KD groups; however, none of these changes remained consistent between the different sexes on ages suggesting that minor physiological perturbation of type II statistical error.

3.4.2 Histopathology:

There are few differences in the histopathology results between the WT and Cyp2b-KD mice. However, all the untreated Cyp2b-KD hepatocytes from the young mice were individualized giving an appearance of slight cytomegally (Fig. 2). No other differences were found. Hepatocytes from 35-week old Cyp2b-KD-male and female mice were more likely to show increased periportal hypertrophy ($p < 0.0001$) as all of the Cyp2b-KD mice showed periportal hypertrophy and none of the WT mice showed periportal hypertrophy. However, the score was one and considered weak or moderate hypertrophy in each individual (Fig. 2). In addition, Oil Red O staining results indicated that no significant fat droplets were observed in the young or older mice Cyp2b-KD mice compared to the WT mice.

3.4.3 Serum lipid levels in young (9 week old) and old (35-week old) mice

To test whether Cyp2b repression caused significant perturbations in serum lipid concentrations and homeostasis; cholesterol, triglycerides, HDL, LDL, and VLDL were measured. Serum triglycerides were significantly higher (39%) in Cyp2b-KD males than WT males and 18.3% higher in Cyp2b-KD females than WT females (Fig. 3), although the increase in serum triglycerides was not significant in females. The increased in serum triglycerides levels were associated with increased VLDL. Cholesterol, HDL, and LDL levels were not perturbed in the 9 week old mice compared to the WT mice (Fig. 3 & 4). Similarly, the 35-week old Cyp2b-KD mice exhibited a significant increase in serum triglycerides (62%) compared to the corresponding WT- mice and this was significant in both males and females (Fig. 3). This was accompanied by increased VLDL in both genders (Fig. 4). In addition, male Cyp2b-KD male mice also showed increased cholesterol and LDL levels at 35-weeks (Fig. 3 & 4). Overall, the age-related changes in serum lipids were more profound in Cyp2b-KD males than Cyp2b-KD females. Hypertriglyceremia is a key biomarker of metabolic disorder and pre-diabetic condition. Therefore, we tested non-fasting blood sugar in both young and old mice. No significant changes in blood sugar were observed in the Cyp2b-KD untreated young and old mice (Supplementary Table 3 & 4).

3.4.4 Changes in CAR, FoxA2, Cpt1a, and Cyp expression:

It is has been demonstrated that CYP2B expression is inducible under some stressful conditions such as fasting or energy restriction (Ding et al., 2006; Rencurel et al., 2005; Rencurel et al., 2006), in addition to xenobiotic activation (Kretschmer and Baldwin, 2005; Wang and Tompkins., 2008). FoxA2 and CAR regulate Cyp2b9 and Cyp2b10 under these nutritional stress conditions (Wolfrum et al., 2004; Dong et al., 2009). Therefore, we examined the expression of FoxA2 and Cpt1a, which is activated by FoxA2 during fasting (Nakamua et al., 2007) but repressed by FoxA2 in coordination with CAR activation (Moreau et al., 2008). Besides that, we examined the expression of CAR, the hepatic Cyp2b members, and several other Cyps reportedly regulated by CAR (Mota et al., 2010). In the young mice, Cyp2b9, Cyp2b10, and Cyp2b13 expression are repressed in the males (Table 1). Female mice show repression of Cyp2b10 and Cyp2b13 but not Cyp2b9 (Table 2), which is in part regulated by FoxA2 (Hashita et al., 2008). However, the FoxA2 biomarker, Cpt1a was not repressed suggesting that the increase in Cyp2b9 in Cyp2b-KD mice was not mediated by FoxA2. The expression of the other Cyps was not perturbed in the 9 week-old or 35-week old mice.

Interestingly, in the older (35-week-old) mice none of the genes investigated showed differences in expression between the WT and Cyp2b-KD mice, including the Cyp2b9, Cyp2b10, and Cyp2b13 genes that are repressed by RNAi. This suggests that some factor is activating the transcription of these genes. Polyunsaturated fatty acids such as linoleic acid have been shown to activate CAR, and monounsaturated fatty acids have

been shown to induce Cyp2b9 and Cyp2b13. Therefore, it is possible that changes in the serum lipid profiles are resulting in changes in Cyp2b expression. However, we did not observe increased lipids in the young or old Cyp2b-KD mice compared to the WT mice. In a previous study, TC-treated Cyp2b-KD mice showed no difference in Cyp2b cDNA expression, but continued to demonstrate a drop in protein expression (Chapter 1). Therefore, Western Blots were performed to test whether Cyp2b protein expression was perturbed in the young and old Cyp2b-KD mice.

3.4.5 Western Blot:

Western blots indicate that Cyp2b protein expression was significantly repressed in male mice. The young mice showed weak to moderate repression and the older mice showed much greater expression (Fig. 5). However, Cyp2b-KD female mice showed no repression of Cyp2b. Cyp2b9 is the primary Cyp2b member in female mouse livers (JAX gene expression; Wiwi et al., 2004; Sutton et al., 2010), suggesting that Cyp2b9 is not being repressed further indicating some compensatory mechanism in females that helps restore Cyp2b9 expression.

3.4.6 The Unsaturated Fats in Corn Oil Increase Serum Lipids in Cyp2b-KD Mice:

Corn oil is a commonly used carrier for chemical treatments as it dissolves lipid soluble chemicals. We treated WT and Cyp2b-KD mice with corn oil or TC dissolved in corn oil for 24 hours, and surprisingly observed a significant increase in total serum

cholesterol in Cyp2b-KD mice compared to their corresponding WT controls (21% males; 40% females). Serum triglyceride and VLDL concentrations were significantly increased in male (53%), but not female Cyp2b-KD mice (21%) (Fig. 6 & 7). In contrast, both males and females exhibited a significant increase in cholesterol (11.1, 16.5%), HDL (17.3, 42.6%), and LDL (42.1, 48.7%). (Fig. 6 &7). Other than phosphorous, no other changes were observed between WT and Cyp2b-KD mice (Supplimentary data 4). Corn oil contains approximately 55% linoleic acid (polyunsaturated), 30% oleic acid (monounsaturated) (85% unsaturated fatty acids), and 15% saturated fatty acids (U.S. Department of Agriculture, Agricultural Research Service. 2007). We hypothesize that the fatty acids in the corn oil perturbed serum lipid concentrations, and the wide range of differences exhibited in lipids measurements in Cyp2b-KD mice compared to WT mice suggests a role for Cyp2bs in lipid metabolism.

Furthermore, the CAR activator and Cyp2b inducer, TC in part, reversed the effects of corn oil on serum lipids. In males, corn oil increased cholesterol, triglycerides, HDL, LDL, and VLDL concentrations, and TC abrogated the effects of corn oil on all of these parameters. The effects of TC in female Cyp2b-KD mice were not as prominent as in males (Fig. 6 & 7). In contrast, TC-treatment led to an increase in serum triglycerides (60%) and VLDL levels (67%) in Cyp2b-KD female mice. It has been demonstrated previously that TC treatment led to a CAR dependent increase in serum TG in mice (Maglich et al., 2009). Therefore, we measured changes in gene expression of CAR and other transcription factors that regulates serum lipids and Cyp2b levels.

3.4.7 Changes in CAR, FoxA2, Cpt1a, and Cyp expression in Corn Oil and TC-treated WT and Cyp2b-KD Mice:

There are no significant differences between the WT and Cyp2b-KD male mice after corn oil or TC-treatment as to the expression of CAR, FoxA2, Cpt1a, and a number of Cyps (Table 3). However, instead of the decreased Cyp2b expression in Cyp2b-KD mice measured in untreated mice (Table 1), corn oil-treated mice showed no significant changes in Cyp2b expression with trends suggesting increased Cyp2b expression (Table 3). Corn oil-treatment caused few significant changes in the Cyp2b-KD female mice compared to the WT mice (Table 4). However once again the Cyp2b isoforms no longer showed a significant drop in expression as they did in untreated animals, and Cyp2b9 was significantly increased in the Cyp2b-KD mice following corn oil-treatment (Table 4). This suggests that corn oil is perturbing liver lipid homeostasis and causing induction of Cyp2b isoforms similar to previous studies that indicate Cyp2b10 mediated induction by linoleic acid (Finn et al., 2009), and Cyp2b9 and Cyp2b13 mediated induction by olive oil (Guillen et al., 2009) which is about 85% monounsaturated fatty acids and primarily comprised of oleic acid (Acin et al., 2007).

TC-treatment was previously shown to protect Cyp2b-KD male mice but not female mice from the increased lipids associated with corn oil (Fig. 6 & 7). However, there were no significant changes in expression between TC-treated WT and TC-treated

Cyp2b-KD mice. Interestingly, male Cyp2b-KD mice did show lower Cyp2b9 and Cyp2b13 after TC-treatment compared to WT mice, as these enzymes are associated with reduced liver lipids (Guillen et al., 2009; Hashita et al., 2008); however the data is not statistically significant. In contrast, the induction of Cyp2b10 and Cyp3a11 is higher in female Cyp2b-KD mice than WT female mice, indicating continued CAR activation in the Cyp2b-KD mice potentially due to an inability to acutely eliminate the TC or the unsaturated fats from the liver after corn oil treatment.

Increased induction of Cyp2b10 and to a lesser extent Cyp3a11 mRNA was shown previously to be associated with increased hepatic triglycerides in the POR-null mouse model lacking all hepatic CYP activity after treatment with a diet rich in sunflower oil, which is approximately 88% unsaturated fatty acids and similar to corn oil primarily linoleic acid and oleic acid (Finn et al., 2009). Therefore, we performed Western blots to test whether Cyp2b levels continued to be repressed in Cyp2b-KD mice following corn oil or TC-treatment. The Western Blots demonstrate that hepatic Cyp2b protein levels continue to be repressed (Fig. 8). TC can increase Cyp2b levels in the Cyp2b-KD mice, but not to the extent that TC can increase Cyp2b in a WT mouse (Fig. 8) demonstrating continued Cyp2b repression following a diet (corn oil) or xenobiotic (TC) insult.

3.4.8 Corn oil treated Cyp2b-KD mice have higher hepatic lipid levels:

Cyp2b-KD mice have perturbation in cleaning hepatic accumulation of corn oil as indicated by Oil Red O (Fig. 9). Cyp2b-KD male mice treaed with corn oil are the only mice exhibited significant increase in hepatostomatic index compared to WT mice (Supplementary Table 5). To determine if the changes in serum lipids are associated with changes in liver steatosis, we performed Oil Red O analysis of hepatic lipids. In addition, because TC appeared to provide some protection from the corn oil-induced increases in lipids in our study and previous studies (Dong et al., 2009), we test whether Oil Red O staining was significantly greater in corn oil treated Cyp2b-KD female mice than corn oil treated WT mice (p value <0.05) (Fig. 9). This indicates that the loss of Cyp2b is causing an increase in hepatic lipid deposition following treatment with unsaturated fatty acids. Therefore, Cyp2bs are probably involved in the metabolism of fatty acids, and specifically hepatic metabolism of unsaturated fatty acids.

3.5 DISCUSSION

There is growing evidence that Cyp2bs could be involved in lipid metabolism and homeostasis. Transcription factors that regulate Cyp2bs such as CAR and FOXA2 are nutrient sensors and involved in energy homeostasis and lipid metabolism (Wolfrum et al., 2004; Finn et al. 2008; Gao et al., 2009). Furthermore, hepatic deletion of POR (HRN mouse) led to a profound time-dependent induction of Cyp2b10 that was associated with increased non-fasting plasma triglyceride and total cholesterol levels (Finn et al., 2008). In this manuscript, we demonstrate that Cyp2b-KD mice have increased fat deposition,

increased serum lipids, and in comparison to WT mice are unable to eliminate unsaturated fatty acids.

Although Cyp2b-KD mice were fertile and developed normally, they exhibit significantly abnormal phenotypic changes associated with decreased Cyp2bs at basal expression. Young Cyp2b-KD mice have enlarged livers, and they maintain an increased load of abdominal body fat associated with hypertriglycemia, key symptoms of metabolic disorders, although Cyp2b-KD young mice were not overweight. These changes were more profound in Cyp2b-KD male mice than female mice in untreated mice. Most but not all (56-79%) of the hepatic Cyp2b members were repressed in the knockdown mice at early age. The expression of the three Cyp2bs tested, Cyp2b9, Cyp2b10, and Cyp2b13, in Cyp2b-KD males and Cyp2b10 and Cyp2b13 in Cyp2b-KD females were repressed relative to WT mice. Cyp2b9, a female predominant Cyp2b regulated by FoxA2 (Hashita et al. 2008) was not repressed in females. These finding suggest that Cyp2b-KD young mice that lack Cyp2bs (mainly Cyp2b10 and 2b13) were not able to utilize the increased serum triglyceride which led to an accumulation of central fat.

Regulation of CYP2B expression is markedly influenced by not only various endogenous and exogenous compounds, but also age, sex, and nutritional status (Udomsuck et al., 2009). Therefore, to determine possible changes associated with stressors, we challenged Cyp2b-KD mice by aging or injecting them with corn oil. It has been demonstrated that expression of Cyp2bs decreases during aging and males express

less Cyp2bs than females (Lam et al., 2010). Therefore, to determine possible age-dependent physiological changes in Cyp2b-KD mice, both male and female Cyp2b-KD mice were housed for 35-weeks. In contrast to younger Cyp2b-KD mice, both old male and female Cyp2b-KD mice were obese. Similar to young Cyp2b-KD mice, both old Cyp2b-KD male and female mice exhibited increased fat weight associated with a significant increase in serum triglyceride and cholesterol in males but triglycerides in females. The increased serum lipids in old Cyp2b-KD male mice was associated with increased expression of Cyp2b9 and 2b13 as was demonstrated by Q-PCR instead of decreased expression. Overall, as the mice aged, the Cyp2b-KD mice showed increased fat deposition relative to body weight and greater perturbations in serum lipid levels. We hypothesize that the profound changes in serum lipids in older males could be as a result of the lower expression of Cyp2bs in males compared to female mice.

Obesity, increased abdominal fat deposition, and increased triglycerides are all key symptoms of prediabetic and strongly associated with metabolic disorder. Many diabetic/obesity models did not show much difference than WT mice unless challenged with a high fat diet. We (inadvertently) challenged our Cyp2b-KD mice with one dose of corn oil (100 ul ip). Both Cyp2b-KD male and female mice appear to show perturbations in clearing the injected corn oil, which is 99% triglyceride (85% unsaturated fats and 15% saturated fats). During fasting and low blood sugar, triglycerides are converted into free fatty acids that bind to albumin, which in turn transports the fatty acids to organs such as the muscles and liver for oxidation. The normal levels of serum glucose in

untreated Cyp2b-KD young mice indicate that both mice are not diabetic. However, Cyp2b-KD female mice treated with corn oil revealed a significant decrease in serum glucose levels (p value 0.02) associated with increases in Cyp2b levels, serum lipids , serum albumin (Supplementary File 3&4), a free fatty acid carrier, and greater triglycerides (Oil Red O staining) in the liver. These changes are also common during fasting conditions.

It has been demonstrated that fatty liver and diabetes activate CAR and FoxA2 and increase drug metabolism due in part to increased Cyp2b9 and Cyp2b10 (Wolfrum et al., 2004; Dong et al., 2009). POR null mice also show induction of Cyp2b10 in association with increased fatty liver due to the lack of CYPs and the inability to metabolize and eliminate fatty acids (Finn et al., 2009). In addition, in humans non-alcoholic fatty liver disease (NAFLD) progression increases CYP2B6 and CYP2C9 mRNA and protein levels (Chtioui et al., 2007). The increased hepatic lipids of NAFLD is associated with increased plasma fatty acids released from adipose stores or dietary sources (Chtioui et al., 2007). Cyp2bs are regulated by the metabolic transcription factors CAR and FoxA2, as well as other transcription factors such as STAT5b and HNF4a that in part cause their sexually dimorphic expression (Wiwi et al., 2004, Hashita et al., 2008, Dong et al., 2009). In normal conditions or under metabolic stress, CAR and FoxA2, which are transcription factors important in the expression of hepatic genes involved in glucose, cholesterol, and fatty acid metabolism, exhibit constitutive transactivation activity apparently by being continuously bound to a variety of fatty acids (Jump et al.,

2005) that affect the expression of Cyp2bs such as Cyp2b13 (Wortham et al., 2003; Holloway et al., 2008).

CAR activation modulates hepatic metabolism by lowering lipids and glucose levels and by compromising liver adaptation to hyperlipidemia (Dong et al., 2009). However, others have shown that CAR activation by TC led to increased serum triglycerides in mice fed high fat diet (Maglich and Moore, 2009). Interestingly, our studies show that CAR activation by TC reversed serum hyperlipidemia in male but not female Cyp2b-KD mice while the TC-induced reversal in male mice is probably due to the regulation of multiple genes, it is interesting to speculate that Cyp2bs may play a crucial role. As for females, CAR expression is greater in Cyp2b-KD female mice treated with TC (Chapter 1) and in turn Cyp2b10 induction is greater in TC-treated Cyp2b-KD mice than WT mice (Table 4). This increased activity is associated with decreased hepatic triglycerides, but increased serum lipids. Overall, increased expression of Cyp2b mRNA as mice age or are exposed to corn oil suggests CAR or FoxA2 activation as a compensatory mechanism to lower serum and liver lipids. .

Hepatic lipid accumulation as was indicated by Oil red O staining results was not correlated with changes in both liver/body weight ratio and the change in serum total cholesterol and triglyceride in all treatments. However, most of the hepatocytes in all corn oil and TC treatments showed mild to moderate swelling where the cytoplasm of the hepatocytes showed glycogenosis or showed low to moderate numbers of discrete-to-

coalescing, smooth surfaced microvacuoles consistent with an incipient hepatic lipidosis indicating depuration of the unsaturated fatty acids. The only significant increased in liver index was observed in corn oil treaed males where the hepatocells showed dysplasia.

Taken together, our data suggest an influence of Cyp2b isoforms on regulation of serum lipid and hepatic lipids. Coupled with recent data demonstrating unsaturated fatty acid activation of CAR, Cyp2b10 induction, and fatty liver in HRN mice fed excess unsaturated fatty acids in sunflower oil (Finn et al., 2009), as well as a different study demonstrating Cyp2b9 and Cyp2b13 induction by olive oil (Guillen et al., 2009); we propose that hepatic Cyp2b's are increased in response to unsaturated fatty acids and are important in the regulation of unsaturated fatty acids. Although Cyp2bs are expressed in the small amounts in the uninduced liver, there is significant evidence for lipid metabolism and homeostasis in addition to their role in xenobiotic metabolism.

3.6 References

Acín S, Navarro MA, Perona JS, Surra JC, Guillen N, Arnal C, Sarría AJ, Arbonés-Mainar JM, Carnicer R, Ruiz-Gutiérrez V, Osada J. Microarray analysis of hepatic genes differentially expressed in the presence of the unsaponifiable fraction of olive oil in apolipoprotein E-deficient mice. Br J Nutr. 2007 Apr;97(4):628-38.

Albores A, Ortega-Mantilla G, Sierra-Santoyo A, Cebrián ME, Muñoz-Sánchez JL, Calderón-Salinas JV, Manno M. Cytochrome P450 2B (CYP2B)-mediated activation of methyl-parathion in rat brain extracts. Toxicol Lett. 2001 Oct 15;124(1-3):1-10.

Banks, W. J. (1993). Applied Veterinary Histology. C V Mosby, 3rd edition, St. Louis.

Chtioui H, Semela D, Ledermann M, Zimmermann A, Dufour JF. Expression and activity of the cytochrome P450 2E1 in patients with nonalcoholic steatosis and steatohepatitis. Liver Int. 2007 Aug;27(6):764-71.

Ding X, Kaminsky LS. Human extrahepatic cytochromes P450: function in xenobiotic metabolism and tissue-selective chemical toxicity in the respiratory and gastrointestinal tracts. Annu Rev Pharmacol Toxicol. 2003;43:149-73. Review.

Dong B, Saha PK, Huang W, Chen W, Abu-Elheiga LA, Wakil SJ, Stevens RD, Ilkayeva O, Newgard CB, Chan L, Moore DD. Activation of nuclear receptor CAR ameliorates diabetes and fatty liver disease. Proc Natl Acad Sci U S A. 2009 Nov 3;106(44):18831-6.

Du L, Yermalitsky V, Ladd PA, Capdevila JH, Mernaugh R, Keeney DS. Evidence that cytochrome P450 CYP2B19 is the major source of epoxyeicosatrienoic acids in mouse skin. Arch Biochem Biophys. 2005 Mar 1;435(1):125-33.

Finger JH, Smith CM, Hayamizu TF, McCright IJ, Eppig JT, Kadin JA, Richardson JE, Ringwald M. The mouse Gene Expression Database (GXD): 2011 update. Nucleic Acids Res. 2011 Jan;39(Database issue):D835-41.

Finn RD, Henderson CJ, Scott CL, Wolf CR. Unsaturated fatty acid regulation of cytochrome P450 expression via a CAR-dependent pathway. Biochem J. 2009 Jan 1;417(1):43-54.

Forkert PG, Vessey ML, Elce JS, Park SS, Gelboin HV, Cole SP. Localization of phenobarbital- and 3-methylcholanthrene-inducible cytochromes P-450 in mouse lung with monoclonal antibodies. Res Commun Chem Pathol Pharmacol. 1986 Aug;53(2):147-57.

Foxenberg RJ, McGarrigle BP, Knaak JB, Kostyniak PJ, Olson JR. Human hepatic cytochrome p450-specific metabolism of parathion and chlorpyrifos. Drug Metab Dispos. 2007 Feb;35(2):189-93.

Gao J, He J, Zhai Y, Wada T, Xie W. The constitutive androstane receptor is an anti-obesity nuclear receptor that improves insulin sensitivity. J Biol Chem. 2009 Sep 18;284(38):25984-92.

Guillen N, Acín S, Surra JC, Arnal C, Godino J, García-Granados A, Muniesa P, Ruiz-Gutiérrez V, Osada J. Apolipoprotein E determines the hepatic transcriptional profile of dietary maslinic acid in mice. J Nutr Biochem. 2009 Nov;20(11):882-93.

Hashita T, Sakuma T, Akada M, Nakajima A, Yamahara H, Ito S, Takesako H, Nemoto N. Forkhead box A2-mediated regulation of female-predominant expression of the mouse Cyp2b9 gene. Drug Metab Dispos. 2008 Jun;36(6):1080-7.

Hernandez JP, Chapman LM, Kretschmer XC, Baldwin WS. Gender-specific induction of cytochrome P450s in nonylphenol-treated FVB/NJ mice. Toxicol Appl Pharmacol. 2006 Oct 15;216(2):186-96.

Hernandez JP, Huang W, Chapman LM, Chua S, Moore DD, Baldwin WS. The environmental estrogen, nonylphenol, activates the constitutive androstane receptor. Toxicol Sci. 2007 Aug;98(2):416-26.

Hernandez JP, Mota LC, Huang W, Moore DD, Baldwin WS. Sexually dimorphic regulation and induction of P450s by the constitutive androstane receptor (CAR). Toxicology. 2009 Feb 4;256(1-2):53-64.

Hodgson E, Rose RL. The importance of cytochrome P450 2B6 in the human metabolism of environmental chemicals. Pharmacol Ther. 2007 Feb;113(2):420-8. Epub 2006 Oct 24. Review.

Holloway MG, Miles GD, Dombkowski AA, Waxman DJ. Liver-specific hepatocyte nuclear factor-4alpha deficiency: greater impact on gene expression in male than in female mouse liver. Mol Endocrinol. 2008 May;22(5):1274-86.

Honkakoski P, Zelko I, Sueyoshi T, Negishi M. The nuclear orphan receptor CAR-retinoid X receptor heterodimer activates the phenobarbital-responsive enhancer module of the CYP2B gene. Mol Cell Biol. 1998 Oct;18(10):5652-8.

Isensee J, Witt H, Pregla R, Hetzer R, Regitz-Zagrosek V, Noppinger PR. Sexually dimorphic gene expression in the heart of mice and men. J Mol Med (Berl). 2008 Jan;86(1):61-74. Epub 2007 Jul 24. Review.

Jarukamjorn K, Sakuma T, Nemoto N. Sexual dimorphic expression of mouse hepatic CYP2B: alterations during development or after hypophysectomy. Biochem Pharmacol. 2002 Jun 1;63(11):2037-41.

Jump DB, Botolin D, Wang Y, Xu J, Christian B, Demeure O. Fatty acid regulation of hepatic gene transcription. J Nutr. 2005 Nov;135(11):2503-6. Review.

Keeney DS, Skinner C, Wei S, Friedberg T, Waterman MR. A keratinocyte-specific epoxygenase, CYP2B12, metabolizes arachidonic acid with unusual selectivity, producing a single major epoxyeicosatrienoic acid. J Biol Chem. 1998 Apr 10;273(15):9279-84.

Kretschmer XC, Baldwin WS. CAR and PXR: xenosensors of endocrine disrupters? Chem Biol Interact. 2005 Aug 15;155(3):111-28. Review.

Kumagai J, Fujimura T, Takahashi S, Urano T, Ogushi T, Horie-Inoue K, Ouchi Y,Kitamura T, Muramatsu M, Blumberg B, Inoue S. Cytochrome P450 2B6 is a growth-inhibitory and prognostic factor for prostate cancer. Prostate. 2007 Jul 1;67(10):1029-37.

Ladd PA, Du L, Capdevila JH, Mernaugh R, Keeney DS. Epoxyeicosatrienoic acids activate transglutaminases in situ and induce cornification of epidermal keratinocytes. J Biol Chem. 2003 ;278(37):35184-92.

Lam JL, Jiang Y, Zhang T, Zhang EY, Smith BJ. Expression and functional analysis of hepatic cytochromes P450, nuclear receptors, and membrane transporters in 10-and 25-week-old db/db mice. Drug Metab Dispos. 2010Dec;38(12):2252-8.

Lee PC, Marquardt M, Lech JJ. Metabolism of nonylphenol by rat and human microsomes. Toxicol Lett. 1998 Oct 15;99(2):117-26.

Maglich JM, Lobe DC, Moore JT. The nuclear receptor CAR (NR1I3) regulates serum triglyceride levels under conditions of metabolic stress. J Lipid Res. 2009 Mar;50(3):439-45. Epub 2008 Oct 21.

Moreau A, Vilarem MJ, Maurel P, Pascussi JM. Xenoreceptors CAR and PXR activation and consequences on lipid metabolism, glucose homeostasis, and inflammatory response. Mol Pharm. 2008 Jan-Feb;5(1):35-41.

Mota LC, Hernandez JP, Baldwin WS. Constitutive androgen receptor-null mice are sensitive to the toxic effects of parathion: association with reduced cytochrome p450-mediated parathion metabolism. Drug Metab Dispos. 2010 Sep;38(9):1582-8.

Muller, P. Y., Janovjak, H., Miserez, A. R., and Dobbie, Z. (2002). Processing of gene expression data generated by quantitative real-time RT-PCR. Biotechniques 32, 1372-1379.

Nakamura K, Moore R, Negishi M, Sueyoshi T. Nuclear pregnane X receptor cross-talk with FoxA2 to mediate drug-induced regulation of lipid metabolism in fasting mouse liver. J Biol Chem. 2007 Mar 30;282(13):9768-76.

Percy, D. H., and Barthold, S. W. (2001). Pathology of Laboratory Rodents and Rabbits. Iowa State University Press, Ames, IA.

Reschly EJ, Krasowski MD. Evolution and function of the NR1I nuclear hormone receptor subfamily (VDR, PXR, and CAR) with respect to metabolism of xenobiotics and endogenous compounds. Curr Drug Metab. 2006 May;7(4):349-65. Review.

Rencurel F, Stenhouse A, Hawley SA, Friedberg T, Hardie DG, Sutherland C, Wolf CR. AMP-activated protein kinase mediates phenobarbital induction of CYP2B gene expression in hepatocytes and a newly derived human hepatoma cell line. J Biol Chem. 2005 Feb 11;280(6):4367-73.

Rencurel F, Foretz M, Kaufmann MR, Stroka D, Looser R, Leclerc I, da SilvaXavier G, Rutter GA, Viollet B, Meyer UA. Stimulation of AMP-activated protein kinase is essential for the induction of drug metabolizing enzymes by phenobarbital in human and mouse liver. Mol Pharmacol. 2006 Dec;70(6):1925-34.

Rosenbrock H, Hagemeyer CE, Ditter M, Knoth R, Volk B. Expression and localization of the CYP2B subfamily predominantly in neurones of rat brain. J Neurochem. 2001 Jan;76 (2):332-40.

Sutton CW, Sutherland M, Shnyder S, Patterson LH. Improved preparation and detection of cytochrome P450 isoforms using MS methods. Proteomics. 2010 Jan;10(2):327-31.

U.S. Department of Agriculture, Agricultural Research Service. 2007. USDA National Nutrient Database for Standard Reference, Release 20. Nutrient Data Laboratory Home Page, listed under "Oil, corn, industrial and retail, all purpose salad or cooking

Wang H, Tompkins LM. CYP2B6: new insights into a historically overlooked cytochrome P450 isozyme. Curr Drug Metab. 2008 Sep;9(7):598-610. Review.

Waxman DJ. Interactions of hepatic cytochromes P-450 with steroid hormones. Regioselectivity and stereospecificity of steroid metabolism and hormonal regulation of rat P-450 enzyme expression. Biochem Pharmacol. 1988 Jan 1;37(1):71-84. Review.

Wei P, Zhang J, Egan-Hafley M, Liang S, Moore DD. The nuclear receptor CAR mediates specific xenobiotic induction of drug metabolism. Nature. 2000 Oct 19;407(6806):920-3.

Wiwi CA, Gupte M, Waxman DJ. Sexually dimorphic P450 gene expression in liver-specific hepatocyte nuclear factor 4alpha-deficient mice. Mol Endocrinol. 2004 Aug;18(8):1975-87. Epub 2004 May 20.

Wolfrum C, Asilmaz E, Luca E, Friedman JM, Stoffel M. Foxa2 regulates lipid metabolism and ketogenesis in the liver during fasting and in diabetes. Nature. 2004 Dec 23;432(7020):1027-32.

Wortham M, Czerwinski M, He L, Parkinson A, Wan YJ. Expression of constitutive androstane receptor, hepatic nuclear factor 4 alpha, and P450 oxidoreductase genes determines interindividual variability in basal expression and activity of a broad scope of xenobiotic metabolism genes in the human liver. Drug Metab Dispos. 2007 Sep;35(9):1700-10.

Yamada H, Ishii Y, Yamamoto M, Oguri K. Induction of the hepatic cytochrome P450 2B subfamily by xenobiotics: research history, evolutionary aspect, relation to tumorigenesis, and mechanism. Curr Drug Metab. 2006 May;7(4):397-409. Review.

Yoshinari K, Sato T, Okino N, Sugatani J, Miwa M. Expression and induction of cytochromes p450 in rat white adipose tissue. J Pharmacol Exp Ther. 2004 Oct;311(1):147-54. Epub 2004 May 18.

Zhang QY, Dunbar D, Kaminsky LS. Characterization of mouse small intestinal cytochrome P450 expression. Drug Metab Dispos. 2003 Nov;31(11):1346-51.

Table 3.1: Q-PCR for Cyps and transcription factors in male mice

Males	Untreated (9) weeks		Old 35-weeks	
	WT	**KD**	WT	KD
Cyp2b9	1.0 ± 0.28	0.29 [a**] ± 0.31	1.0 ± 0.43	8.76 ± 0.33
Cyp2b10	1.0 ± 0.31	0.33 ± 0.08	1.0 ± 0.26	2.12 ± 0.47
Cyp2b13	1.0 ± 0.30	0.21 [a***] ± 0.03	1.0 ± 0.26	8.75 ± 0.62
Cyp2a4	1.0 ± 0.19	0.48 [a*] ± 0.12	1.0 ± 0.53	0.20 ± 0.03
Cyp2c29	1.0 ± 0.32	1.19 ± 0.41	1.0 ± 0.28	1.79 ± 0.5
Cyp3a11	1.0 ± 0.18	1.43 ± 0.64	1.0 ± 0.11	1.49 ± 0.48
CAR	1.0 ± 0.18	0.89 ± 0.24	1.0 ± 0.22	1.44 ± 0.54
FoxA2	1.0 ± 0.23	0.60 ± 0.12	1.0 ± 0.23	0.83 ± 0.21
CPT1A	1.0 ± 0.32	0.85 ± 0.29	1.0 ± 0.32	0.65± 0.41

a:WT vs KD * P value <0.05 , **< 0.01, *** < 0.001

Table 3.2: Q-PCR for Cyps and transcription factors in female mice

Females	Untreated (8-12) weeks		Old 35-weeks	
	WT	**KD**	**WT**	**KD**
Cyp2b9	1.0 ± 0.18	1.33 ± 0.24	1.0 ± 0.30	0.98 ± 0.18
Cyp2b10	1.0 ± 0.29	0.33[a*] ± 0.09	1.0 ± 0.24	0.61 ± 0.11
Cyp2b13	1.0 ± 0.07	0.46 [a*] ± 0.09	1.0 ± 0.49	3.11 ± 1.12
Cyp2a4	1.0 ± 0.03	0.81 ± 0.15	1.0 ± 0.53	1.10 ± 0.15
Cyp2c29	1.0 ± 0.29	1.05 ± 0.34	1.0 ± 0.27	0.74 ± 0.12
Cyp3a11	1.0 ± 0.29	1.03 ± 0.22	1.0 ± 0.79	1.17 ± 0.25
CAR	1.0 ± 0.30	0.30 ± 0.0.09	1.0 ± 0.27	0.85 ± 0.09
FoxA2	1.0 ± 0.21	0.42 ± 0.03	1.0 ± 0.36	1.34 ± 0.55
CPT1A	1.0 ± 0.16	0.85 ± 0.23	1.0 ± 0.31	0.84 ± 0.15

a:WT vs KD * P value <0.05 , **< 0.01, *** < 0.001

Table 3.3: Q-PCR measured expression of Cyps, CAR and FoxA2 in corn oil- and TC-treated male mice.

Males	Treated (8-12) weeks			
	WT-CO	**KD-CO**	**WT -TC**	**KD-TC**
Cyp2b9	1.0 ± 0.92	19.0 ± 7.05	91.1 ± 29.8	13.8 ± 6.61
Cyp2b10	1.0 ± 0.37	6.31 ± 2.33	514 ± 171	552 [d*] ± 138
Cyp2b13	1.0 ± 0.98	3.37 ± 2.53	5.34 ± 4.52	0.136 ± 0.068
Cyp2a4	1.0 ± 0.20	1.19 ± 0.42	1.5 ± 0.65	0.37± 0.11
Cyp2c29	1.0 ± 0.54	0.043 ± 0.023	13.4 ± 5.1	21.7 ± 8.5
Cyp3a11	1.0 ± 0.42	0.46 ± 0.15	2.9 ± 1.36	2.88 ± 0.45
CAR	1.0 ± 0.47	1.74 ± 0.39	4.41 ± 1.74	1.34 ± 0.46
FoxA2	1.0 ± 0.51	5.79 ± 2.2	9.67 ± 7.03	2.60 ± 0.77
CPT1A	1.0 ± 0.34	1.33 ± 0.32	0.59 ± 0.16	1.84 ± 0.55

a:WT-CO vs KD-CO * P value <0.05 , **< 0.01, *** < 0.001
b: WT-TC vs KD-TC
c: WT-CO vs WT-TC
d: KD-CO vs KD-TC

Table 3.4: Q-PCR measured expression of Cyps, CAR, and FoxA2 in corn oil- and TC-treated female mice.

Females	Treated (8-12) weeks			
	WT-CO	**KD-CO**	**WT -TC**	**KD-TC**
Cyp2b9	1.0 ± 0.05	2.23 [a**] ± 0.35	0.07 ± 0.02	0.13 [d***] ± 0.03
Cyp2b10	1.0 ± 0.03	2.14 ± 0.7	51.0 ± 8.39 [c**]	135, [d***] ± 25.2
Cyp2b13	1.0 ± 0.28	2.31 ± 0.59	0.59 ± 0.08	1.74 ± 0.27
Cyp2a4	1.0 ± 0.38	0.96 ± 0.22	1.54 ± 0.34	1.05 ± 0.41
Cyp2c29	1.0 ± 0.10	4.63 ± 1.56	45.8 ± 9.93	126.0 ±32.9
Cyp3a11	1.0 ± 0.22	1.74 ± 0.49	7.19 ± 2.08 [c***]	20.6,[d***] ± 1.83
CAR	1.0 ± 0.24	3.1 ± 1.03	0.46 ± 0.08	2.66 ± 0.55
FoxA2	1.0 ± 0.40	4.2 ± 1.17	0.53 ± 0.23	3.0 ± 0.75
CPT1A	1.0 ± 0.19	3.9 ± 0.99	0.41 ± 0.23	1.3 ± 0.28

a:WT-CO vs KD-CO * P value <0.05 , **< 0.01, *** < 0.001
b: WT-TC vs KD-TC
c: WT-CO vs WT-TC
d: KD-CO vs KD-TC

Figure legend

Fig. 3.1: Increased fat deposition and body weight of Cyp2b-KD mice. Untreated young and old Cyp2b-KD mice show significant increased fat deposition in (A) female, (B) male mice compared with wild-type (FVB) mice. Old Cyp2b-KD mice show increased body weight in (C) females and (D) males compared with wild-type (FVB) mice. Significant differences between WT and Cyp2b-KD mice were assessed by ANOVA followed by Tukey's multiple comparison tests using the GraphPad Prizm 4.0 software package. An asterisk indicates a significant difference with a $p < 0.05$, two asterisks indicate a $p < 0.01$, and three asterisks indicate a $p < 0.001$.The letter [a] indicates a significant difference between young WT and young Cyp2b-KD mice, the letter [b] indicates a significant difference between old WT and old Cyp2b-KD mice, the letter [c] indicates significant differences between young WT and old WT mice, and the letter [d] indicates significant difference between young Cyp2b-KD and young Cyp2b-KD mice. WT= wild-type, KD= Cyp2b-KD mice, M = male, F= female, Y = Young, O =Old

Fig. 3.2: Liver Histopathology in untreated young and old mice. Mouse liver fragments were stained using hematoxylin and eosin stain from male mice (A) FVB -young, (B) Cyp2b-KD–young male, (C) FVB-old male, (D) Cyp2b-KD – old male, and female mice (E) FVB-young, (F)- Cyp2b-KD-young female, (G) FVB-old female, and (H) Cyp2b-KD-old female. Minimal hypertrophy (score of 1) of hepatocytes

in the periportal area of both Cyp2b-KD old male and female mice was observed but not in WT mice.

Fig. 3.3: Non-fasting serum lipid profile for untreated young (Y; 9 weeks) and old (O; 35 weeks). Serum cholesterol level in (A) females (B) in males indicated significant increase in cholesterol only in Cyp2b-KD males compared to wild-type mice. Serum triglyceride levels in (C) female and (D) male mice indicated significant increase levels in both young and old Cyp2b-KD mice. Significant differences between WT and Cyp2b-KD mice were assessed by ANOVA followed by Tukey's multiple comparison tests using the GraphPad Prizm 4.0 software package. An asterisk indicates significant difference with a $p < 0.05$, two asterisks indicate a $p < 0.01$, and three asterisks indicate a $p < 0.001$. The letter [a] indicates a significant difference between young WT and young Cyp2b-KD, the letter [b] indicates a significant difference between old WT and old Cyp2b-KD, the letter [c] indicates significant differences between young WT and old WT mice, and the letter [d] indicates significant difference between young Cyp2b-KD and young Cyp2b-KD. WT = wild-type, KD= Cyp2b-KD mice, M = male, F= female, Y = Young, O = old.

Fig. 3.4: Lipoprotein profiles for untreated young (Y; 9 weeks) and old (O: 35 weeks) mice. (A) HDL in females (B) HDL in males (C) LDL in females (D) LDL in males (E) VLDL in females and (F) VLDL in males indicated significant increase

in LDL in old Cyp2b-KD male mice compared to both WT old mice and young Cyp2b-KD mice. VLDL significantly increased in both young and old Cyp2b-KD males. Significant differences between WT and Cyp2b-KD mice were assessed by ANOVA followed by Tukey's multiple comparison tests using the GraphPad Prizm 4.0 software package. An asterisk indicates significant difference with a $p < 0.05$, two asterisks indicate a $p < 0.01$, and three asterisks indicate a $p < 0.001$. The letter [a] indicates a significant difference between young WT and young Cyp2b-KD, the letter [b] indicates a significant difference between old WT and old Cyp2b-KD, the letter [c] indicates significant differences between young WT and old WT mice, and the letter [d] indicates significant difference between young Cyp2b-KD and young Cyp2b-KD. WT = wild-type, KD= Cyp2b-KD mice, M = male, F= female, Y = Young, O = Old.

Fig. 3.5: Hepatic Cyp2b expression in WT (FVB) and Cyp2b-KD mice as demonstrated by Western blots of young and old mice.

Fig. 3.6: Non-fasting serum cholesterol and TG in WT and Cyp2b-KD mice after treatment with corn oil or TCPOBOP. Corn oil treatment significantly increased cholesterol levels in both Cyp2b-KD (A) female and (B) male mice compared to their wild-type mice and serum triglyceride levels were significantly increased in (C) TC treated female (D) corn oil treated male mice. Significant differences between WT and Cyp2b-KD mice were assessed by ANOVA followed by Tukey's

multiple comparison tests using the GraphPad Prizm 4.0 software package. An asterisk indicates significant difference with a $p < 0.05$, two asterisks indicate a $p < 0.01$, and three asterisks indicate a $p < 0.001$. The letter [a] indicates a significant difference between WT treatd with corn oil and Cyp2b-KD treated with corn oil, the letter [b] indicates a significant difference between WT treated with TC and Cyp2b-KD treated with TC, the letter [c] indicates significant differences between WT treated with corn oil and old WT treated with TC, and the letter [d] indicates significant difference between Cyp2b-KD treated with corn oil and Cyp2b-KD treated with TC. WT = wild-type, KD= Cyp2b-KD mice, M = male, F= female, CO = corn oil, TC= TCPOBOP.

Fig. 3.7: Lipoprotein profiles in WT and Cyp2b-KD mice after corn oil and TCPOBOP treatments. Corn oil treatment significantly increased levels of HDL in (A) Cyp2b-KD females (B) Cyp2b-KD males, LDL levels in (C) Cyp2b-KD females (D) Cyp2b-KD males, and VLDL levels in (F) Cyp2b-KD males. Significant differences between WT and Cyp2b-KD mice were assessed by ANOVA followed by Tukey's multiple comparison tests using the GraphPad Prizm 4.0 software package. An asterisk indicates significant difference with a $p < 0.05$, two asterisks indicate a $p < 0.01$, and three asterisks indicate a $p < 0.001$. The letter [a] indicates a significant difference between WT treatd with corn oil and Cyp2b-KD treated with corn oil, the letter [b] indicates a significant difference between WT treated with TC and Cyp2b-KD treated with TC, the letter [c] indicates significant

differences between WT treated with corn oil and old WT treated with TC, and the letter [d] indicates significant difference between Cyp2b-KD treated with corn oil and Cyp2b-KD treated with TC. WT = wild-type, KD= Cyp2b-KD mice, M = male, F= female, CO = Corn oil, TC= TCPOBOP.

Fig. 3.8: Hepatic Cyp2b expression in WT (FVB) and Cyp2b-KD mice treated with corn oil and TCPOBOP as demonstrated by Western blots (A) female (B**)** male mice demonstrated increased expression of Cyp2b9 and Cyp2b10. Statistical significance was determined by Student's *t test*. An asterisk indicates significant difference with a $p < 0.05$ WT= wild-type, KD= Cyp2b-KD mice, M=male, F= female. CO = Corn oil, TC = TCOPBOP.

Fig. 3.9: Increased Oil Red O staining in the hepatocytes of Cyp2b-KD mice treated with corn oil or TCPOBOP. Corn oil significantly increased Oil Red O staining in livers of corn oil-treated Cyp2b-KD mice compared to WT mice. (A) Liver from an untreated WT female mouse. (B) Liver from a corn oil-treated WT female mouse. (C) Liver from a corn-oil treated Cyp2b-KD female mouse. The average extent of Cyp2b-KD mice treated with CO or TC hepatocellular involvement in Oil Red O staining compared to their corresponding WT is shown in (D). [a] indicates a significant difference between WT and Cyp2b-KD treated with corn oil. An asterisk indicates significant difference with a $p < 0.05$ WT= wild-type, KD= Cyp2b-KD mice, M=male, F= female. CO = Corn oil, TC = TCOPBOP.

Figure 3.1

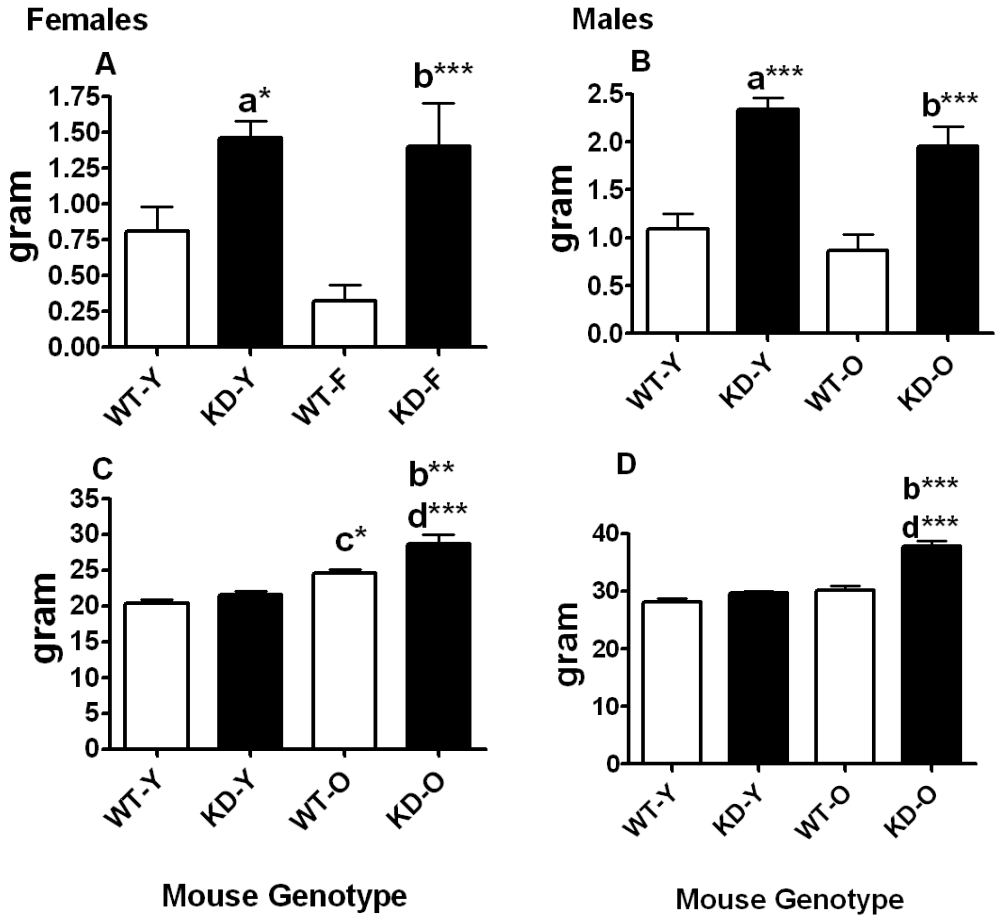
Females
A
a*
b***
gram
1.75
1.50
1.25
1.00
0.75
0.50
0.25
0.00
WT-Y
KD-Y
WT-F
KD-F
Males
B
a***
b***
gram
2.5
2.0
1.5
1.0
0.5
0.0
WT-Y
KD-Y
WT-O
KD-O
C
b**
d***
c*
gram
35
30
25
20
15
10
5
0
WT-Y
KD-Y
WT-O
KD-O
Mouse Genotype
D
b***
d***
gram
40
30
20
10
0
WT-Y
KD-Y
WT-O
KD-O
Mouse Genotype

Figure 3.2

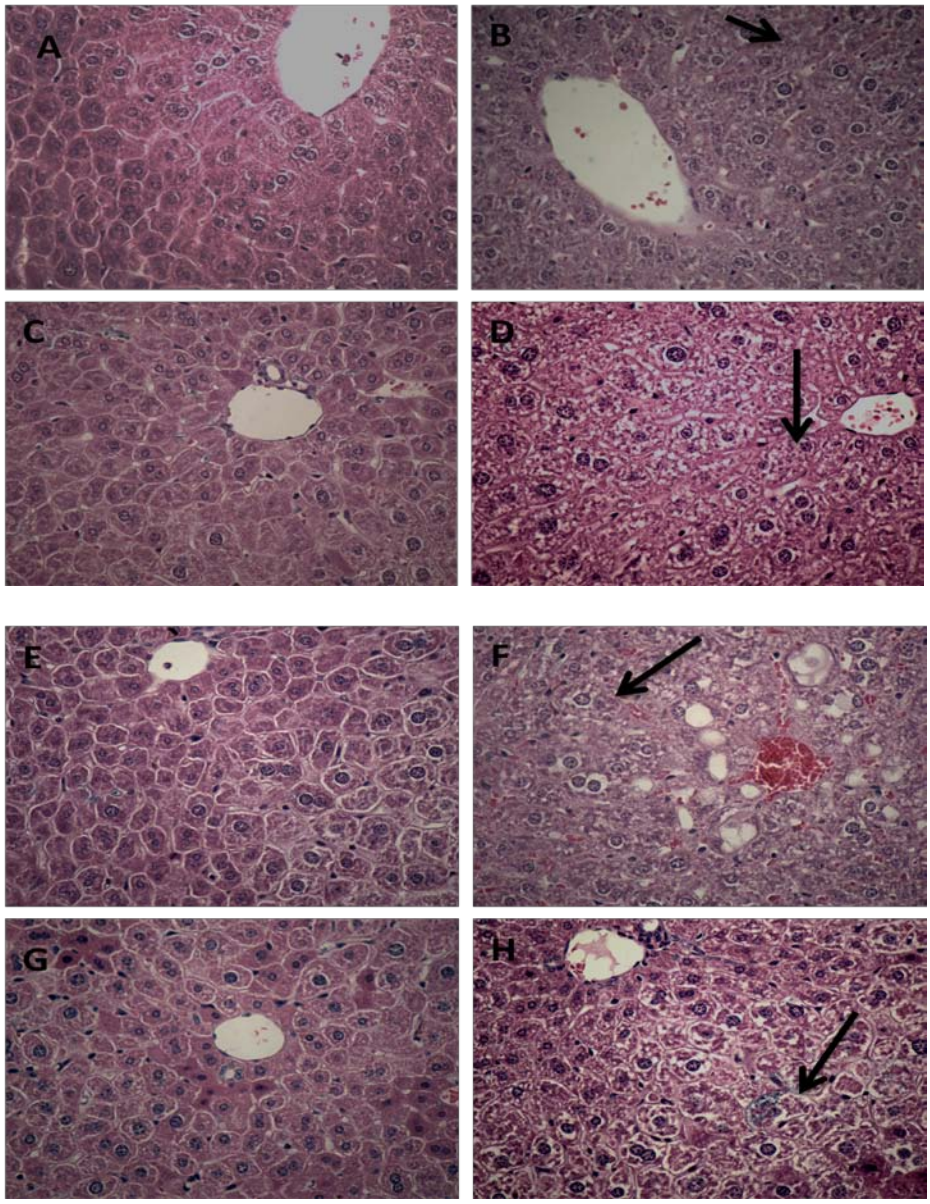

(A) **WT-Young male**
(B) **Cyp2b-KD-Young male**
(C) **WT-Old male**
(D) **Cyp2b-KD-Old male**
(E) **WT-Young female**
(F) **Cyp2b-KD-Young female**
(G) **WT-Old female**
(H) **Cyp2b-KD-Old female**

Figure 3.3

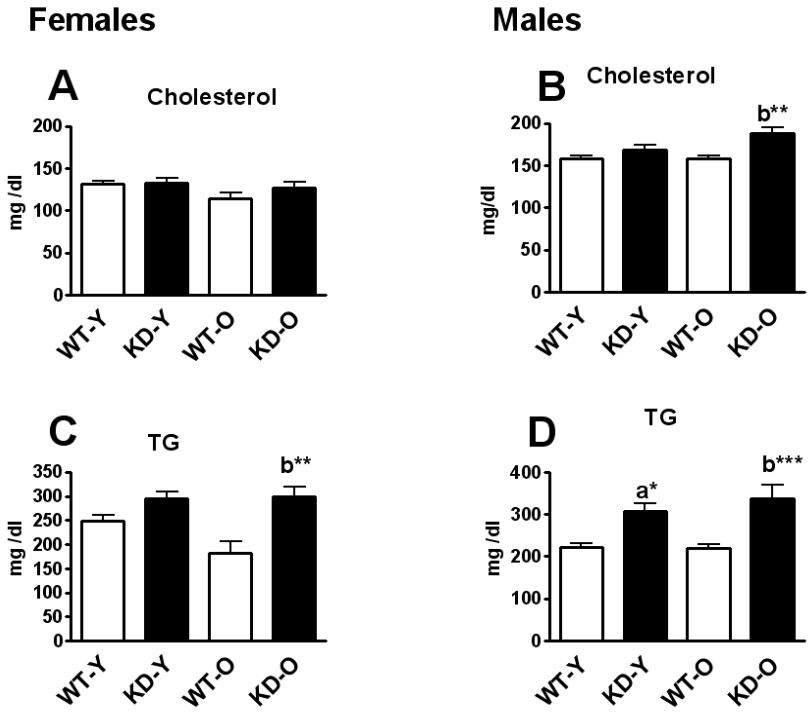
Females
Males
A
Cholesterol
mg /dl
200
150
100
50
0
WT-Y
KD-Y
WT-O
KD-O
B
Cholesterol
b**
mg/dl
C
TG
b**
mg /dl
350
300
250
200
150
100
50
D
TG
a*
b***
400

Figure 3.4

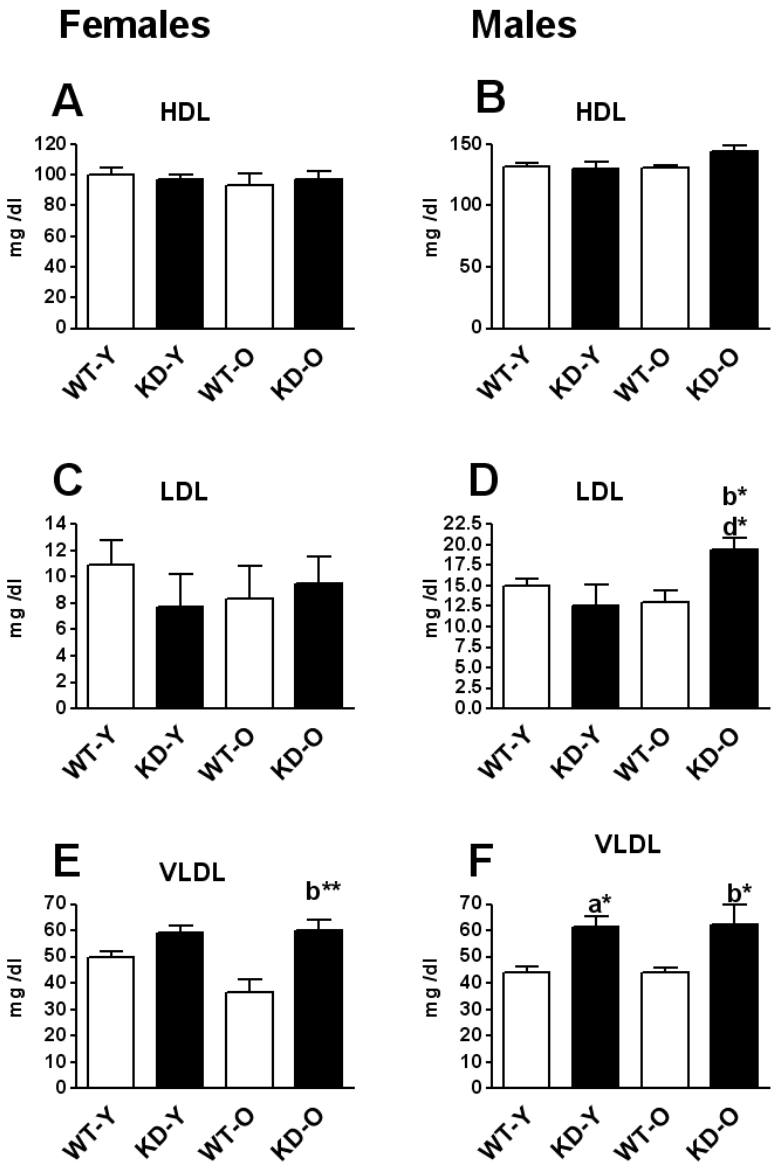
Females
Males
A
HDL
B
HDL
C
LDL
D
LDL
b*
d*
E
VLDL
b**
F
VLDL
a*
b*
mg /dl
WT-Y
KD-Y
WT-O
KD-O

Figure 3.5

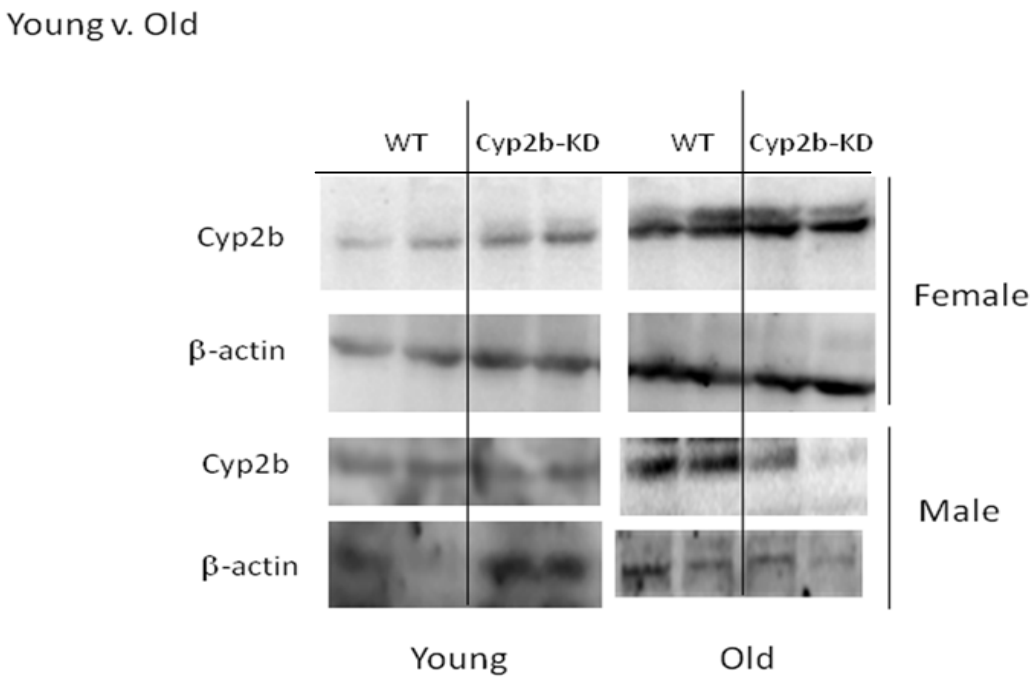
Young v. Old
WT
Cyp2b-KD
WT
Cyp2b-KD
Cyp2b
β-actin
Female
Cyp2b
β-actin
Male
Young
Old

Figure3.6

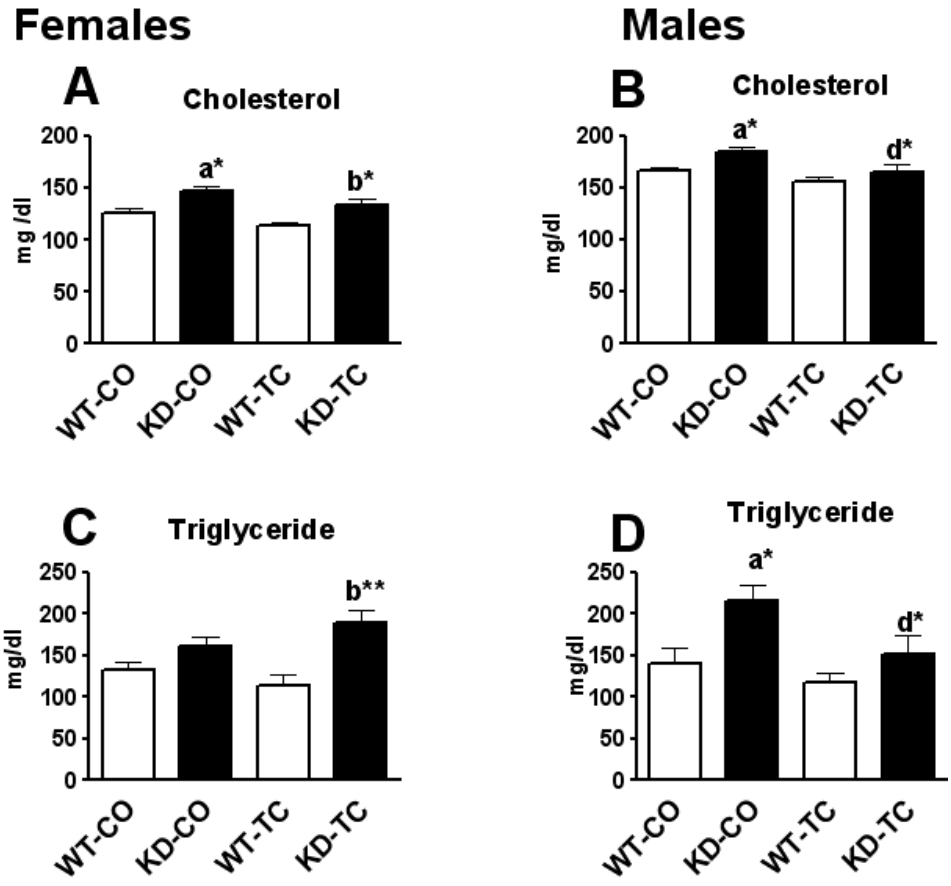
Females
Males
A
Cholesterol
B
Cholesterol
mg /dl
mg/dl
200
150
100
50
0
a*
b*
a*
d*
WT-CO
KD-CO
WT-TC
KD-TC
C
Triglyceride
D
Triglyceride
mg/dl
250
200
150
100
50
0
b**
a*
d*

Figure 3.7

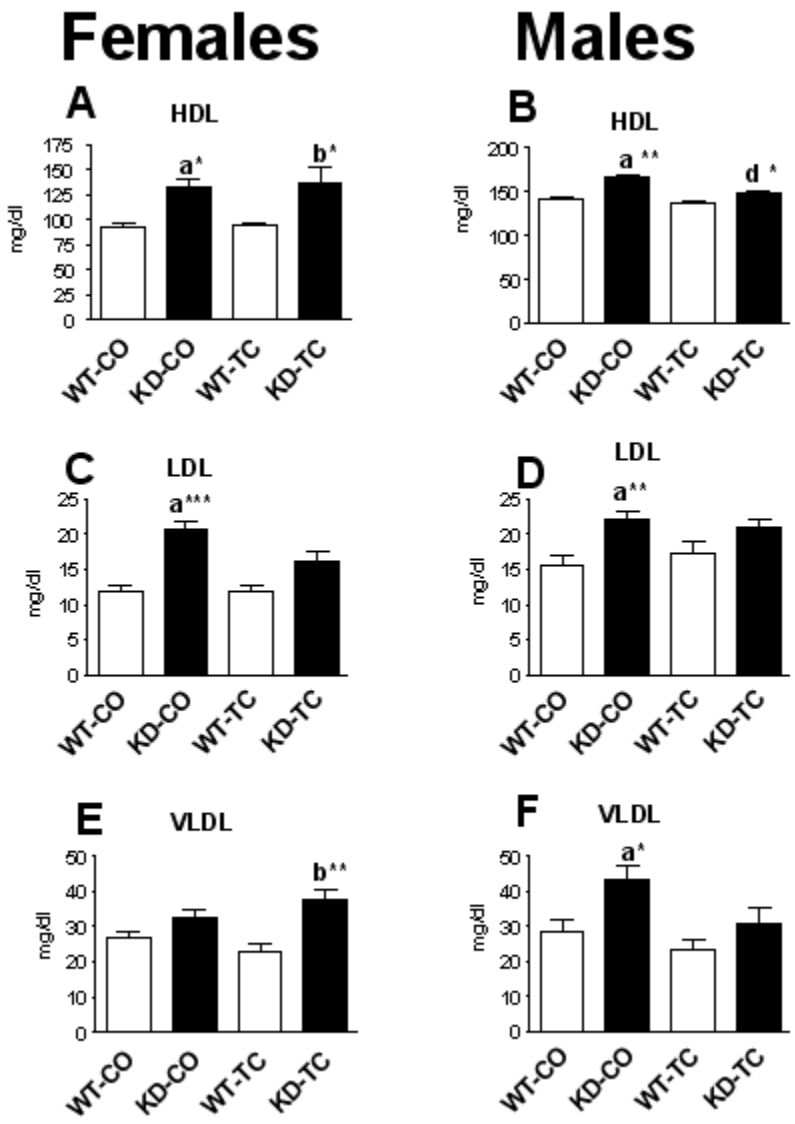
Females
Males
A
HDL
mg/dl
a*
b*
WT-CO
KD-CO
WT-TC
KD-TC
B
HDL
mg/dl
a **
d *
C
LDL
a***
D
LDL
a**
E
VLDL
b**
F
VLDL
a*

Figure3.8:

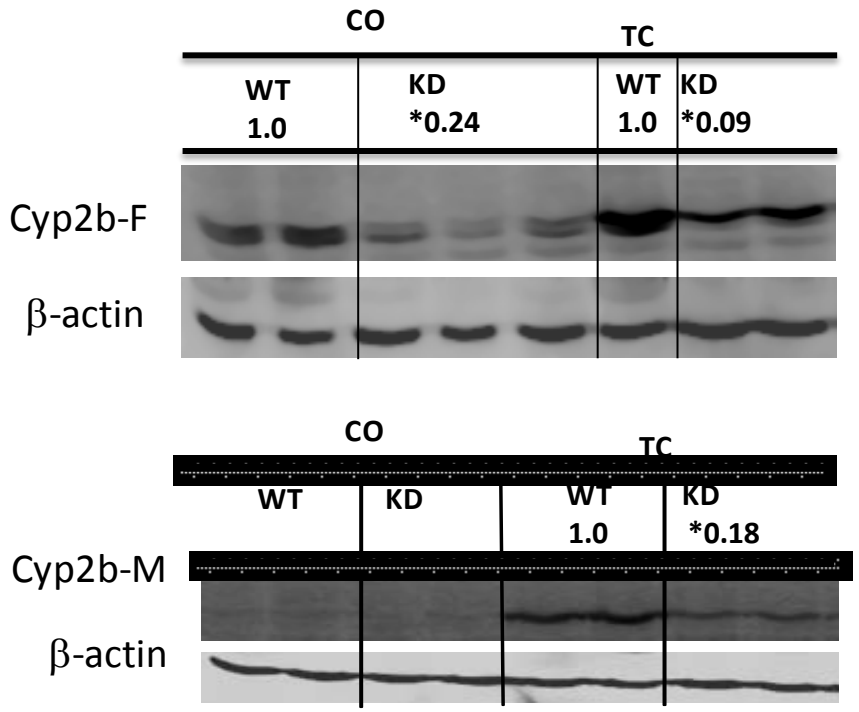
CO
TC
WT
1.0
KD
*0.24
WT
1.0
KD
*0.09
Cyp2b-F
β-actin
CO
TC
WT
KD
WT
1.0
KD
*0.18
Cyp2b-M
β-actin

Figure3.9
(A)

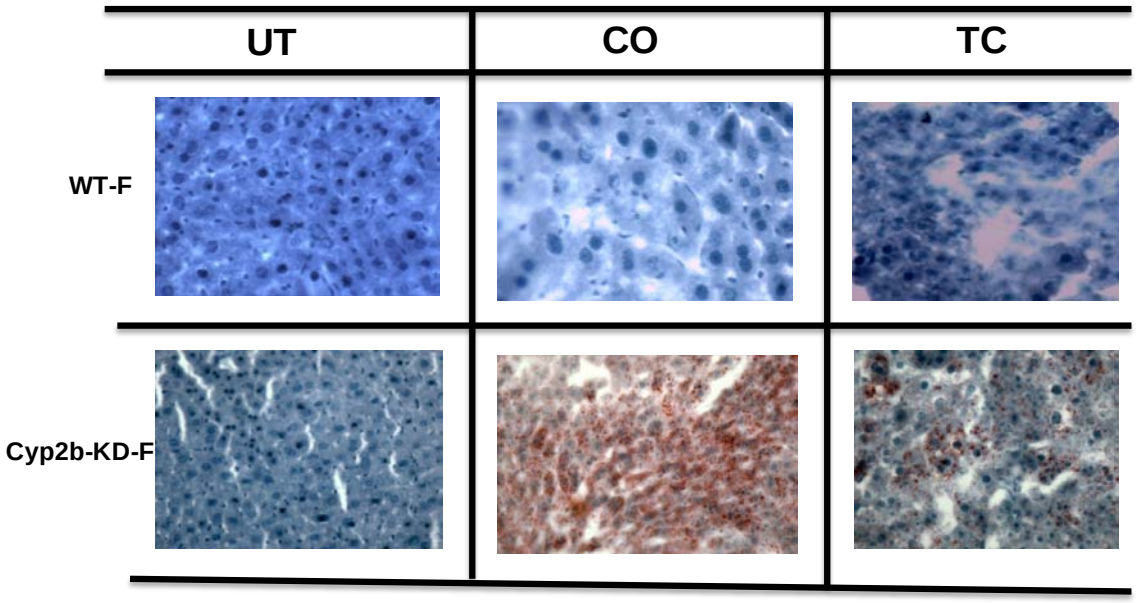

(B)

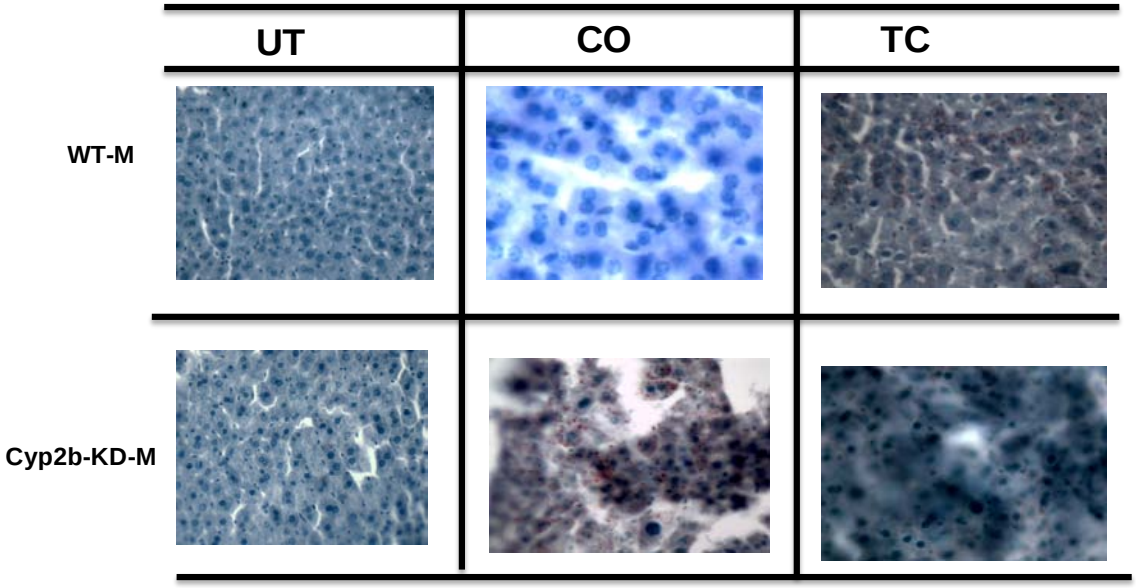

(C)

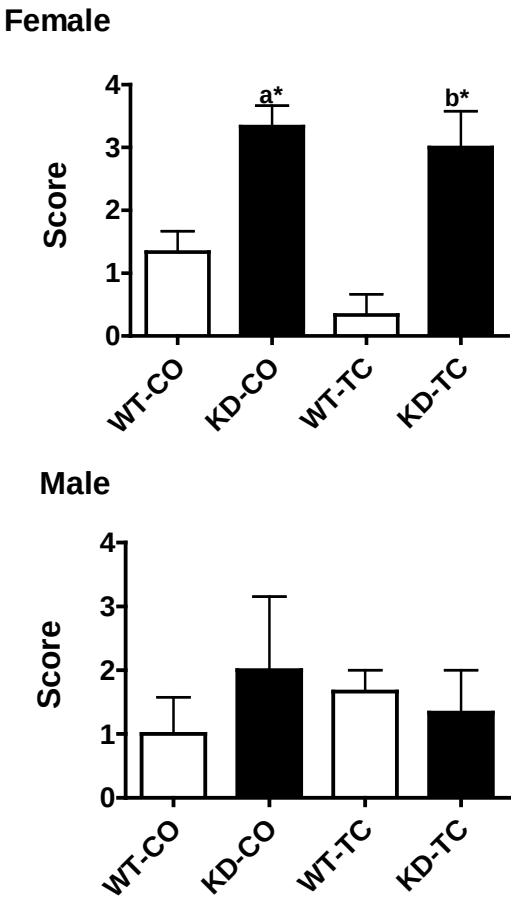

(A): Oil Red O results for females

(B): Oil Red O results for males

(C): Hepatic lipid accumulation scores

3.5 Additional Files

Supplementary Table 1: PCR primer and probe sequences used in Q-PCR

Gene	Forward primer	Reverse primer	T_m (°C)	Reference
CAR	GGAGCGGCTGTGGAAATATTGCAT	TCCATCTTGTAGCAAAGAGGCCCA	56.5	Thismanuscript
CPT1 A	TTGATCAAGTGCCGGACGAGT	GTCCATCATGGCCAGCACAAAGTT	55.5	This manuscript
Cyp2a4	AGCAGGCTACCTTCGACTGG	GCTGCTGAAGGCTATGCCAT	63.6	(Wiwi et al. (2004)
Cyp2b9	CTGAGACCACAAGCGCCAC	CTTGACCATGAGCAGGACTCC	64.3	(Wiwi et al. (2004)
Cyp2b10	CTGAATCCGCTCCTCCACACTC	TGAGCCAACCTTCAAGGAATAT	61.4	(Hernandezet al., 2006)
Cyp2b13	GAACTGAGACTACCAGCACCACTCCT	TGAGCATGAGCAGGAAACCACT	61.5	(Wiwi et al. (2004)
Cyp2c29	GGCCTCAAAGCCCTACTGTCA	AACGCCAAAACCTTTAATC	53.6	(Luo et al. (1998)
Cyp3a11	CTTTCCTTCACCCTGCATTCC	CTCATCCTGCAGTTTTTTCTGGAT	64.2	(Wiwi et al. (2004)
FoxA2	TCAACGACTGCTTTCTCAAGGTGC	TTCTCGAACATGTTGCCCGAGTCT	57.8	(Wiwi et al. (2004)
18s rRNA	CGCCGCTAGAGGTGAAATTC	CCAGTCGGCATCGTTTATGG	51	(Hernandezet al., 2006)

Tm: Annealing Temperature oC

AS bp: amplicon Size (base pair)

3.6 Supplementary Table 2: Organ weights and organ to body weight ratios of Young (9-week old) and older (35-week-old) WT and Cyp2b-KD mice. Statistical analysis was performed by Student's t-test. P-values are shown.

A: Organ weights of 9–week- old male mice

Males	Organ weight (g) ± SEM		% of differences	P value
	WT	Cyp2b-KD		
Liver	1.29 ± 0.06	1.76 ± 0.05	+ 36.4	<0.0001
Fat	1.09 ± 0.16	2.33 ± 0.12	+ 13.8	<0.0001
Kidneys	0.47 ± 0.02	0.52 ± 0.01	+ 6.3	0.1
Spleen	0.089 ± 0.00	0.11± 0.006	+ 24.2	0.3
Brain	0.419 ± 0.017	0.405± 0.034	+ 3.3	0.7
testes	0.20 ± 0.008	0.27 ± 0.015	+ 35	0.0002
Body weight (g)	28.14 ± 0.67	27.29 ± 0.05	-3.1	0.37

n=5-6

B: Organ weights of 9-week-old female mice

Females	Organ weight (g) ± SEM		% of differences	P value
	WT	Cyp2b-KD		
Liver	1.37 ± 0.03	1.45 ± 0.037	+ 5.8	<0.0001
Fat	0.81 ± 0.19	1.47 ± 0.11	+ 81.5	0.0004
Kidneys	0.31 ± 0.01	0.38 ± 0.01	+ 6.0	0.6
Spleen	0.108 ± 0.006	0.114 ± 0.005	+ 10.3	0.4
Brain	0.417 ± 0.001	0.43 ±.017	+1.2	0.3
Body weight (g)	20.42 ± 0.50	20.42 ± 0.17	0	0.998

n=5-8

C: Organ weights of 35-week-old male mice

Males	Organ weight (g) ± SEM		% of differences	P value
	WT	Cyp2b-KD		
Liver	0.94 ± 0.04	1.81± 0.04	+ 92.5	<0.0001
Fat	0.87 ± 0.17	1.85 ± 0.17	+ 112.6	0.0007
Kidneys	0.58 ± 0.02	0.62 ± 0.01	+ 6.9	0.086
Spleen	0.084 ± 0.004	0.097 ± 0.003	+15.5	0.017
Brain	0.43 ± 0.007	0.44 ± 0.016	+ 2.3	0.46
testes	0.21 ± 0.006	0.24 ± 0.009	+ 14.3	0.04
Body weight (g)	30.24 ± 073	36.98 ± 0.87	+22.3	<0.0001

n=9-10

D: Organ weights of 35-week-old female mice

Aged Females	Organ weight (g) ± SEM		% of differences	P value
	WT	Cyp2b-KD		
Liver	0.99 ± 0.11	1.44 ± 0.05	+ 45.5	<0.0032
Fat	0.32 ± 0.11	1.69 ± 0.55	+ 428	0.0075
Kidneys	0.41 ± 0.02	0.43 ± 0.019	+ 4.9	0.308
Spleen	0.092 ± 0.005	0.10 ± 0.006	+8.7	0.29
Brain	0.46 ± 0.009	0.44 ± 0.013	- 4.4	0.23
Body weight (g)	24.63 ± 0.44	28.91 ± 1.34	+ 17.4	0.0096

n=9-11

E: organ weight to body weight ratio of 9-week-old male mice

Young Males	% Organ/body weight ± SEM		% of difference	P value
	WT	Cyp2b-KD		
Liver	5.18 ± 0.001	6.13 ± 0.001	+18.3	0.0002
Fat	3.15 ± 0.004	6.68 ± 0.003	+112.1	0.0003
Kidneys	1.69 ± 0.0004	1.59 ± 0.0004	- 6.3	0.92
Spleen	0. 32 ± 0.0000	0. 37 ± 0.0001	+15.2	0.46
Brain	1.51± 0.0006	1.34 ± 0.0004	-9.3	0.2
Testes	0. 55 ± 0.0003	0. 89 ± 0.0006	+ 61.8	<0.0001

n=10-12

F: Organ weight to body weight ratio of 9-week-old female mice

Young Females	% (Organ/body weight) ± SEM		% of difference	P value
	WT	Cyp2b-KD		
Liver	5.34 ± 0.003	6.71 ± 0.001	+ 25.6	<0.0001
Fat	3.25 ± 0.005	5.64 ± 0.003	+ 73.5	0.0004
Kidneys	1.49 ± 0.0002	1.48 ± 0.0005	- 0.7	0.92
Spleen	0. 40 ± 0.0003	0.48 ± 0001	+19.2	0.03
Brain	1.62 ± 0.001	1.83 ± 0.0006	+ 11.4	0.21

n=8-12

G: Organ weight to body weight ratio of 35-week-old male mice

Aged Males		% (Organ/body weight) ± SEM		
	WT	Cyp2b-KD	% of differences	P value
Liver	3.09 ± 0.0012	4.90 ± 0.0012	+ 58.6	<0.0001
Fat	2.85 ± 0.005	4.95 ± 0.0034	+73.7	0.005
Kidneys	1.89 ± 0.0005	1.68 ± 0.0006	+12.5	0.01
Spleen	0. 28 ± 0.0001	0. 26 ± 0.0000	-7.7	0.2
Brain	1.43 ± 0.0004	1.21 ± 0.0005	-18.2	0.07
testes	0. 62 ± 0.0008	0. 65 ± 0.0004	+ 4.8	0.39

n=9-10

H: organ weight to body weight ratio of 35-week-old female mice

Aged Females	% (Organ/body weight) ± SEM		% of differences	P value
	WT	Cyp2b-KD		
Liver	4.04 ± 0.005	5.04 ± 0.0021	+ 24.7	<0.009
Fat	1.29 ± 0.004	5.31± 0.0150	+ 411.6	0.003
Kidneys	1.66 ± 0.0009	1.51± 0.0006	- 9.0	0.2
Spleen	0. 38 ± 0.0002	0. 35 ± 0.0002	- 8.6	0.4
Brain	1.85 ± 0.0004	1.53 ± 0.0007	- 20.9	0.007

n=9-11

3.7 Supplementary Table 3: Blood chemistry profiles in young and old Cyp2b-KD mice compared to WT mice.

Gender	Blood Test	Young (9) weeks		Old 35-weeks	
		WT	**KD**	**WT**	**KD**
Female	**Albumin**	2.9 ± 0.03	2.93 ± 0.07	2.90 ± 0.04	2.8 ± 0.06
	Phosphorus	8.89 ± 0.81	8.1 ± 0.75	6.85 ± 0.52	9.43 ± 0.49
	Glucose	279.7 ±27.8	288.0 ± 10.4	235.7 ± 12.3	205.3 ± 10.1
Male	**Albumin**	2.6 ± 0.03	2.84 ± 0.02	2.83 ± 0.02	2.6 ± 0.05
	Phosphorus	7.58 ± 0.36	8.97 ± 0.42	6.84 ± 0.3	8.1 ± 0.41**
	Glucose	313.4 ± 14.3	284.6 ± 10.3	297.3 ± 26.8	284.6 ± 10.4

a:WT-CO vs KD-CO * P value <0.05 , **< 0.01, *** < 0.001
b: WT-TC vs KD-TC
c: WT-CO vs WT-TC
d: KD-CO vs KD-TC
n = 4- 6

3.8 Supplementary Table 4: Blood chemistry profiles in corn oil- and TC-treated Cyp2b-KD mice compared to WT mice.

Gender	Blood Test	Treated (8-12) weeks			
		WT-CO	**KD-CO**	**WT-TC**	**KD-TC**
Female	**Albumin**	2.8 ± 0.02	3.25[a]*** ± 0.05	2.9 ± 0.11	3.25 [b] *± 0.06
	Phosphorus	11.65 ± 1.35	8.88 [a] * ± 0.21	8.33 ± 1.0	9.78 ± 1.01
	Glucose	268.5 ± 5.5	204.8 ±14.8	226.0 ± 27.0	227.3 ± 23.7
Male	**Albumin**	2.66 ± 0.06	2.89 [a] * ± 0.08	2.75 ± 0.05	2.93 ± 0.11
	Phosphorus	6.55 ± 0.36	9.99 [a] ** ± 0.69	6.95 ± 0.48	9.9 [b] ** ± 0.37
	Glucose	253.0 ± 10.4	257.0 ± 36.0	253.7 ± 10.4	214.3 ± 43.0

a:WT-CO vs KD-CO * P value <0.05 , **< 0.01, *** < 0.001
b: WT-TC vs KD-TC
c: WT-CO vs WT-TC
d: KD-CO vs KD-TC
n = 4 -6

3.9 Supplementary Table 5: Liver weight to body weight for treated corn oil and TC (9-week-old) male and female mice

Treatment	% (liver/body weight) ± SEM		% of differences	P value
	WT	KD		
CO-Female	5.00 ± 0.0031	5.11 ± 0.0025	+ 2.2	0.28
TC-Female	5.90 ± 0.0014	6.20 ± 0.0033	+ 5.1	0.49
CO-Male	4.38 ± 0.0034	4.92 ± 0.0065	+ 11.2	0.0013
TC-Male	5.17 ± 0.0027	5.47 ± 0.0015	+ 5.8	0.36

n = 4-5

CHAPTER FOUR

DISCUSSION

In this study, we made a Cyp2b-knockdown mouse using lentiviral-promoted shRNA homologous to all five Cyp2b subfamily members in FVB/NJ mouse to characterize Cyp2b's role in xenobiotic detoxification. We focused in assessing the *in vivo* function of Cyp2bs in the toxicity from pesticides (i.e. parathion) and drugs (i.e. zoxazolamine). In addition, we in partially phenotyped and characterized Cyp2b-KD model and assessed changes associated with the lack of Cyp2bs. We focused on role that Cyp2bs play in lipid metabolism. Our data suggest that Cyp2b is more than a detoxification enzyme, but is also involved in the metabolism of unsaturated fatty acids. Cyp2b-KD model will provide a new tool for further study of the impact of Cyp2b enzymes on the *in vivo* metabolism of endobiotic and xenobiotic chemicals.

The discovery of RNA interference (RNAi) has had a great impact on toxicology and CYP-mediated metabolism and drug discovery. Small interference RNA (siRNA) has emerged as a powerful tool to down regulate the expression of specific genes (Wiznerowicz et al., 2006). Knockout mouse models have become the experimental model of choice for the study of human genetics, physiology, metabolism and disease (Barbaric et al., 2007). The Cyp2b subfamily in mouse species contains five members (Cyp2b9, Cyp2b10, Cyp2b13, Cyp2b19, and Cyp2b23) of which three (Cyp2b9, Cyp2b10, Cyp2b13) are hepatic enzymes. The multiple murine Cyp2b isoforms and the

redundancy of these isoforms in each subfamily made targeted mouse gene knockouts impractical and costly. To circumvent these limitations, we designed and determined an efficient shRNA construct with the potential to knockdown five isoforms of murine Cyp2b (Chapter1). This construct was used to generate the first persistent quintuple Cyp2b knockout mouse for the subsequent study of Cyp2b functions *in vivo* (Chapter 1).

We demonstrated that Cyp2b isoforms play a key role in parathion and Zoxazolamine metabolism and toxicity (Chapter 1). In addition, we in partially phenotyped and characterized the Cyp2b-KD model and assessed changes associated with the lack of Cyp2bs and we focused in lipid metabolism (Chapter 2). Our data suggests that Cyp2b is more than a detoxification enzyme, but is also involved in the metabolism of unsaturated fatty acids as Cyp2b-KD mice have increased fat deposition and show increased serum and liver lipid levels. This study is the first step in demonstrating the *in vivo* function of Cyp2b. The next step is to perform more *in vivo* studies to determine the Cyp2b function and to fully characterize Cyp2b-KD model. These studies will increase our knowledge of the human sensitivity to toxicant and drugs and will aid to the understanding of the xenobiotic metabolism. Cyp2b-KD mice may be able to act as a sentinel for individuals with low Cyp2b-expression or limited metabolic capacity because of Cyp2b polymorphisms. Significances of Cyp2b-KD mouse model, suggested future research, and directions are described below.

Overall results and the purpose of the research

4.1 Objective 1

Several siRNA constructs that recognize all five Cyp2b subfamily members in FVB/NJ mouse, typically without significant overlap with human CYPs were designed and build in a lentiviral vector. These constructs were tested *in vivo* using primary mouse hepatocytes to choose the potent construct that will knockdown major hepatic Cyp2bs (Cyp2b9, Cyp2b10, and Cyp2b13).

4.2 Objective 2

Using a highly concentrated lentivirus preparation, we generated the first persistent quintuple Cyp2b knockout mouse by perivitelline injection for the subsequent study of Cyp2b functions *in vivo*. Our work demonstrated that the expression of the three hepatic Cyp2bs tested (Cyp2b9, Cyp2b10, and Cyp2b13) isoforms is significantly repressed in male but Cyp2b9 in female Cyp2b-KD mice. Furthermore, TCPOBOP-mediated Cyp2b induction did not outcompete the shRNA's ability to repress Cyp2b protein expression demonstrating that the Cyp2b-KD mouse model is functional in the presence of a CAR activator and powerful Cyp2b inducer. Therefore, we have produced an efficient Cyp2b knockdown of at least the three major hepatic Cyp2b members in mice, including the highly inducible Cyp2b10 that is responsible for different xenobiotic metabolism.

4.3 Objective 3

In this study, we in part characterized Cyp2b-KD mice to determine the phenotypes associated with low Cyp2bs induction. This study demonstrates that *in vivo* Cyp2b isoforms play a key role in parathion and Zoxazolamine metabolism and toxicity. It is the first study to demonstrate that individuals with compromised Cyp2b are susceptible to the toxic effects of parathion. We also observed that parathion metabolism is perturbed in the hepatic microsomes of TCPOBOP-induced Cyp2b-KD mice as parathion metabolism was significantly lower in these microsomes than WT mice. Our *in vivo* and *in vitro* data agreed with previous studies (Mutch et al. 1999; Kim et al. 2005; Foxenberg et al. 2007; Mota et al. 2010).

Zoxazolamine paralysis time is a key indicator of perturbations in Cyp activity *in vivo*. Interestingly, more pronounced Zox toxicity effect was observed on Cyp2b-KD female mice than male mice. In contrast to males, female Cyp2b-KD mice showed poor metabolism and clearance for Zox as they did not recover indicating a key role of Cyp2b in Zox metabolism. Sex differences in the induction of Cyp2bs could be a critical factor for Zox toxicity differences. In addition, it appears to be a molecular compensatory reaction to the repression of Cyp2bs in the Cyp2b-KD mice. For example, Cyp2b9 mRNA expression was not repressed in female Cyp2b-KD young and old mice. Since most Cyp2b's (Cyp2b9, Cyp2b13, and may be Cyp2b10) are female predominant (Hernandez et al. 2006; Hernandez et al. 2009; Wiwi et al. 2004), reducing Cyp2b levels

in female mice may cause a more pronounced effect. In addition, Cyp2b-KD young males did not exhibit significant Cyp2b10 repression like the females.

We also in part characterized Cyp2bs function in lipid metabolism. We showed that Cyp2b-KD mice are viable, fertile, and did not exhibit significantly abnormal phenotypes or physiological abnormalities. However, both young and old Cyp2b-KD mice showed an increase in liver weight, and a subjective increase was observed in abdominal and renal fat in both male and female mice indicating that our Cyp2b-KD mice exhibit the same phenotypes.

The increased in fat weight in Cyp2b-KD mice was associated with an increase in serum lipids. Different than young mice, Cyp2b-KD old mice exhibit increased body weight and increased Cyp2bs induction. This suggests that there is some type of compensatory mechanism trying to overcome the repressive effects of the shRNA and to adapt the increased serum lipids and the increased weight. These data also demonstrated the importance of Cyp2bs in lipid metabolism and as anti obesity enzymes.

Lentiviral vector-mediated transgene expression can be maintained for long periods of time (Park, 2007). Lentiviral integration is thought to allow for longer and more stable transgene expression. To determine if our siRNA-Cyp2b transgene in the old mice is stable and the phenotypes observed are due to the lack of Cyp2bs, Western bolts for old mice were performed. Old Cyp2b-KD male mice exhibited low expression of

Cyp2bs comparing to old WT- mice indicating that our transgenic siRNA is still functional over the 35 weeks.

Nutritional stressor such as unsaturated fatty acids in the injected corn oil caused dramatic increase in serum lipids, changes in liver histopathology, increased accumulation of hepatic lipids, and activated molecular compensatory mechanisms (increased Cyp2bs induction mediated by increased CAR and FoxA2) as an attempt to adapt to and clear the unsaturated fatty acids. These findings suggested that there is significant evidence for Cyp2bs specific involvement in lipid metabolism and homeostasis. These data are consistent with other ther studies. The hepatic P450 oxidoreductase-null mouse (hepatic reductase null, POR-null, or HRN), which lacks hepatic CYP activity, shows profound changes in lipid homeostasis, increased liver size. This was associated with significantly elevated Cyp2b10, and linked to hepatic triacylglycerol accumulation and increased hepatic unsaturated fatty acids simalr to our cyp2b-KD female mice. Furthermore, double HRN/CAR-null mice did not demonstrate Cyp2b10 induction, and linoleic acid, an unsaturated fatty acid, activated CAR in transactivation assays. The authors suggest that increases in Cyp2b10 via CAR activation could be an adaptive response against unsaturated fatty acid toxicity and indicated that this study is the first evidence that P450s, and particularly Cyp2b10, play a major role in controlling unsaturated fatty acid homoeostasis via CAR (Finn et al., 2009). However, further studies to investigate the function of Cyp2bs as energy P450 are needed.

4.5 Significance and future considerations

The production of Cyp2b-KD mouse model provides many benefits for toxicologist, investigators, and pharmaceutical companies. This study provides a new platform for studying Cyp2b function, especially its role in the metabolism of distinct pharmaceuticals and environmental chemicals as well as its role as energy related P450. Cyp2b-KD mice may be able to act as a sentinel for individuals with low Cyp2b expression or limited metabolic capacity because of Cyp2b polymorphisms. The lack of Cyp2B in some individuals could have a protective effect against the toxicity of certain compounds such as organophosphates that can be metabolized to more toxic metabolite by Cyp2bs. Cyp2b-KD animals could be used to determine if these enzymes play protective roles in these individuals. Cyp2b polymorphism and dimorphism can have a pronounced effect of the metabolism of different xenobiotics and xenobiotics. Scientist can study the role of Cyp2bs in the metabolism, activation, detoxification, elimination, and homeostasis of xenobiotics and different compounds such as industrial chemicals, pharmaceutical, and pesticides in an *in vivo* system.

Cyp2b-KD model could be used for future studies to test chemicals and drugs with potential clinical implication to investigate the fate, the metabolism, the clearance, and the effects of these drugs. Scientist can study the role of Cyp2bs in drug-drug interaction in an *in vivo* system. Impact of low Cyp2bs induction and drug drugh interaction could have a great impact on our understanding to drug toxicity.

Scientist can study the function of Cyp2bs in metabolizing endogenous compounds an *in vivo* system. For instance, we can determine if Cyp2bs are involved in steroids hormone or bile acid homeostasis. Cyp2b-KD mice exhibited changes in lipid metabolism and increased serum lipids such as increased cholesterol in males by aging and by dietary unsaturated acids. This increase may lead to difference in steroids synthesis and metabolism which may also lead to changes in several biological activities such as reproduction. It has been demonstrated previously that Changes in Cyp2B expression under stress conditions such as fasting and energy restriction may suggest the involvement of CYP2B6 in pathways of energy metabolism, homeostasis, and the metabolism of endobiotics (Wang and Tompkins, 2008). These pathways could be harmful or protective pathways. Cyp2b-KD mice may provide a good model to identify direct evidence for such involvement.

Cyp2b-KD model can be built upon to form even better models for human disease, human metabolism, and human genetic polymorphisms by making CYP2B6/7 humanized mice. In addition, polymorphic humanized mice can be made to study slow metabolism or gene-environment interactions, and toxic responses mediated by P450s as they would occur in humans. Further use of this technology to produce other P450 knockdown mouse models of other subfamilies will enhance toxicology and our ability to study Cytochrome P450 function.

In this study, we have taken the first steps towards developing a potent Cyp2b-knockdown (KD) mouse for subsequent study of Cyp2b function. To enhance our understanding for the effect of the loss of Cyp2b on xenobiotic metabolism and elimination and on physiological function, especially those pertaining to endobiotic metabolism and elimination, more work is needed. This includes but not limited to:

1- Microarray test: This test will enable us to measure changes in the expression levels of large numbers of genes in Cyp2b-KD mice at basal or induced level.

2- Challenge the mice with different types of diet especially, high fat diet to tested if Cyp2bs are anti-obesity enzymes and are involved in the utilization and deposition of fatty acids in the body. Cyp2b-KD mice demonstrated high serum lipids, triglyceride, and enlarged liver at early age and showed increased body weight and greater perturbations in serum lipid levels in elderly age. Obesity and increased serum triglyceride are key biomarkers of pre-diabetic and metabolic syndrome and strongly associated with hypertension and type II diabetes all of which increase risk of heart diseases. Obesity, diabetes, and heart diseases are growing problems in the United States and much of the world. Controlling obesity could significantly enhance the worldwide health. Cyp2b-KD mouse may able to act as a pre-diabetic/ metabolic syndrome/or obesity model and thus, it could enable us understanding the molecular mechanisms of obesity and diabetes. This may improve our ability to develop new therapeutics as well as better understand the genetic and environmental basis for these diseases. However, many diabetic/obesity models did

not show much difference than WT mice unless challenged with a high fat diet (Maglich and Moore, 2009). To determine whether Cyp2b-KD mice are able to properly metabolize and utilize a high fat diet, Cyp2b-KD mice need to be challenged with different nutritional stressors. This could be clear from the fact that injected corn oil also acted as a nutritional stressor to this model and Cyp2b-KD mice acted as in fasting-conditions under the corn oil stressing effect. Fasting is one of the obligations for millions of people, both sexes and in different ages, in different religions and cultures especially in the Middle East and Asia. It can be long enough (e.g. 11-15 hours daily for 30 days) to cause changes in energy metabolism and ultimately, in Cyp2B and other Cyps induction. There is a high prevalence of diabetes mellitus, obesity, hypertension in the Middle East and cardiovascular disease is a major health problem (Motlagh et al., 2009). Cyp2b-KD model can be used to further understanding of potential risks of fasting associated with low Cyp2bs levels (polymorphisms). Furthermore, additional studies can be performed to determine if TCPOBOP-treatment can alleviate some of the symptoms of obesity and help reducing fat deposition. This can help in finding more specific drugs that could alleviate serum lipids. Besides that, Cyp2b-KD mice exhibit enlarged liver, non alcoholic fatty liver (NAFL), when they were treated with corn oil. Further studies could be done to determine the histopathological changes of NAFL in Cyp2b-KD mice using different drugs.

3- Distributed metabolic regulation in Cyp2b-KD can also be studied using glucose tolerance test and insulin tolerance test. Blood glucose level alters insulin

expression and serum hepatic lipids levels which in turn affect other transcription factors such as CAR and FoxA2. This will ultimately change Cyp2bs regulation.

4- How down regulation of Cyp2bs will affect immune system and immune response? It has been demonstrated that LPS significantly down regulates the induction of Cyp2b10 and Cypp2b9 even in the presence of phenobarbital (Li-Masters and Morgan, 2001). To study the physiological changes and modulation of gene expression in Cyp2b-KD mice during inflammation, Cyp2b-KD mice need to be challenged by lipopoly saccharide (LPS).

- Cyp2b-KD mice showed significant phonotypical changes by nutritional stressors, which led to hepatic steatosis. Hepatic inflammation, steatohepatitis, can develop because of hepatic steatosis (Angulo, 2002).
- Cyp2b is also involved in arachadonic acid metabolism (Keeney et al., 1998), therefore, skin development may be affected, and immune system may be weaker in Cyp2b-KD mice. Only two Cyp2b-KD female mice were used in breeding and both developed skin inflammation and lost their toes after they were used in breeding for 3 times. None of other Cyp2b-KD females showed similar symptoms. This could be an indicator of changes in the immune system due to a stressor (pregnancy).

4.6 Summary

The endogenous role of the Cyp2bs is poorly understood (Reschly and Krasowski, 2006; Yamada et al., 2006), probably in part due to a lack of an *in vivo* model to study

Cyp2b function. A Cyp2b-KD transgenic mouse model has been developed using siRNA that recognizes the five Cyp2bs subfamily members in FVB/NJ mice. Our data demonstrated that Cyp2bs have specific involvement in lipid metabolism and homeostasis besides their role in xenobiotic metabolism. Cyp2-KD mouse model will provide a powerful model to study the *in vivo* function of Cyp2bs.

4.7 References

Angulo P. Nonalcoholic fatty liver disease. N Engl J Med. 2002 Apr 18;346(16):1221-31. Review.

Barbaric I, Miller G, Dear TN. Appearances can be deceiving: phenotypes of knockout mice. Brief Funct Genomic Proteomic. 2007 Jun;6(2):91-103.

Finn RD, Henderson CJ, Scott CL, Wolf CR. Unsaturated fatty acid regulation of cytochrome P450 expression via a CAR-dependent pathway. Biochem J. 2009 Jan 1;417(1):43-54.

Foxenberg RJ, McGarrigle BP, Knaak JB, Kostyniak PJ, Olson JR. Human hepatic cytochrome p450-specific metabolism of parathion and chlorpyrifos. Drug Metab

Hernandez JP, Chapman LM, Kretschmer XC, Baldwin WS. Gender-specific induction of cytochrome P450s in nonylphenol-treated FVB/NJ mice. Toxicol Appl Pharmacol. 2006 Oct 15;216(2):186-96.

Hernandez JP, Mota LC, Huang W, Moore DD, Baldwin WS. Sexually dimorphic regulation and induction of P450s by the constitutive androstane receptor (CAR). Toxicology. 2009 Feb 4;256(1-2):53-64.

Keeney DS, Skinner C, Wei S, Friedberg T, Waterman MR. A keratinocyte-specific epoxygenase, CYP2B12, metabolizes arachidonic acid with unusual selectivity, producing a single major epoxyeicosatrienoic acid. J Biol Chem. 1998 Apr 10;273(15):9279-84.

Li-Masters T, Morgan ET. Effects of bacterial lipopolysaccharide onphenobarbital-induced CYP2B expression in mice. Drug Metab Dispos. 2001 Mar;29(3):252-7.

Mota LC, Hernandez JP, Baldwin WS. Constitutive androgen receptor-null mice are sensitive to the toxic effects of parathion: association with reduced cytochrome p450-mediated parathion metabolism. Drug Metab Dispos. 2010 Sep;38(9):1582-8.

Maglich JM, Lobe DC, Moore JT. The nuclear receptor CAR (NR1I3) regulates serum triglyceride levels under conditions of metabolic stress. J Lipid Res. 2009 Mar;50(3):439-45.

Motlagh B, O'Donnell M, Yusuf S. Prevalence of cardiovascular risk factors in the Middle East: a systematic review. Eur J Cardiovasc Prev Rehabil. 2009 Jun;16(3):268-80. Review.

Mutch E, Blain PG, Williams FM. The role of metabolism in determining susceptibility to parathion toxicity in man. Toxicol Lett. 1999 Jun 30;107(1-3):177-87.

Park F. Lentiviral vectors: are they the future of animal transgenesis? Physiol Genomics. 2007 Oct 22;31(2):159-73. Epub 2007 Aug 7. Review.

Wiwi CA, Gupte M, Waxman DJ. Sexually dimorphic P450 gene expression in liver-specific hepatocyte nuclear factor 4alpha-deficient mice. Mol Endocrinol. 2004 Aug;18(8):1975-87. Epub 2004 May 20.

Wiznerowicz M, Szulc J, Trono D. Tuning silence: conditional systems for RNA interference. Nat Methods. 2006 Sep;3(9):682-8. Review.

Reschly EJ, Krasowski MD. Evolution and function of the NR1I nuclear hormone receptor subfamily (VDR, PXR, and CAR) with respect to metabolism of xenobiotics and endogenous compounds. Curr Drug Metab. 2006 May;7(4):349-65. Review.

Yamada H, Ishii Y, Yamamoto M, Oguri K. Induction of the hepatic cytochrome P450 2B subfamily by xenobiotics: research history, evolutionary aspect, relation to tumorigenesis, and mechanism. Curr Drug Metab. 2006 May;7(4):397-409. Review.